Pilot-Scale Silicone Process for Low-Cost Carbon Dioxide Capture

GE GRC: D. Hancu, B. Wood, S. Genovese, T. Westendorf, R. Perry, I. Spiry, R. Farnum, S. Singh, P. Wilson, W. Chen, J. McDermott, M. Doherty, M. Rainka, B. Miebach, S. Buddle

DUNS Number: 086188401

DE-FE0013755

Project Grant Period: 1/1/2014 to 4/30/2017

Executive Summary

GE Global Research has developed, over the last eight years, a platform of cost effective CO_2 capture technologies based on a non-aqueous aminosilicone solvent (GAP-1_m). As demonstrated in a previously funded DOE project (DE-FE0007502), the GAP-1_m solvent has increased CO_2 working capacity, lowered volatility and corrosivity relative to the benchmark aqueous amine technology. The current report describes the cooperative program between GE Global Research (GE GRC), and the National Carbon Capture Center (NCCC) to design, construct, and operate a pilot-scale process using GAP-1_m solvent to demonstrate its performance at 0.5 MW_e.

(i) Performance of the GAP-1_m solvent was demonstrated in a 0.5 MW_e pilot with real flue gas for over 900 hours of operation using two alternative desorption designs: a Continuous Stirred Tank Reactor (CSTR), and a Steam Stripper Column (SSC). The CSTR is a one-stage separation unit with reduced space requirements, and capital cost. The alternative is a multi-stage separation column, with improved desorption efficiency. Testing the two desorber options allowed us to identify the most cost effective, and space efficient desorber solution.

(ii) *CSTR Campaign:* The CSTR desorber unit was designed, fabricated and integrated with the pilot solvent test unit (PSTU), replacing the PSTU Steam Stripper Column at NCCC. Solvent management and waste water special procedures were implemented to accommodate operation of the non-aqueous solvent in the PSTU.
Performance of the GAP-1_m solvent with the CSTR was demonstrated for over 500 hours while varying temperature of the desorption (230 – 265 ^oF), solvent circulation rate (GAP-1_m : CO_2 (molar) = 1.5 – 4), and flue gas flow rates (0.2 – 0.5 MW_e). Solvent carry-over in the CO_2 product was minimized by maintaining water content below 5 wt.%, and desorption pressure at 7 psig. CO_2 capture efficiency achieved was 95% at 0.25 MW_e (GAP-1_m : CO_2 = 4 (molar), 230 ^oF desorption), and 65% at 0.5 MW_e (GAP-1_m : CO_2 (molar) = 1.5, 248 ^oF). Solvent loss was dominated by thermal degradation of the rich solvent.

(iii) *Steam Stripper Column Campaign:* Higher expected cost of the solvent vs. aqueous amines makes solvent management a top priority to maintain the low cost for the process. During the testing of the GAP-1_m solvent with the CSTR, thermal degradation of the rich solvent was found to be the main mechanism in solvent loss. Small amounts of water in the working solution were found to be an effective way to enable steam stripping, thereby lowering desorption temperature, and hence reducing thermal degradation. Steam stripping also increased working capacity by 30% due to a more efficient desorption. The concept was first tested in a glass stripping column (lab scale,

GE GRC), optimized in a continuous bench scale system (2 kW_e, GE GRC), and demonstrated in a 0.5 MW_e PSTU at NCCC. No special system modifications were required to the PSTU to accommodate the testing of the non-aqueous GAP-1 solvent with the regenerator column. SSC was found to be more robust towards solvent entrainment (H_2O < 35 wt.%). 90 – 95% CO_2 capture efficiency was achieved under stoichiometric conditions at 0.5 MW_e (235 °F desorption, 2 psig and 19 wt. % H_2O). Both CO_2 capture efficiency and specific duty reached optimum conditions at 18 wt.% H_2O. Low amine degradation (< 0.05 wt.%/day) was recorded over 350 hours of operation. Controlled water addition to GAP-1_m solvent decreased the desorption temperature, thermal degradation, and improved the CO_2 working capacity due to more efficient absorption and desorption processes. Under these conditions, the GAP-1_m solvent exhibited a 25% increased working capacity, and 10% reduction in specific steam duty vs. MEA, at 10 °F lower desorption temperature.

(iv) *Techno-economic Analysis:* The pilot-scale PSTU engineering data were used to update the capture system process models, and the techno-economic analysis was performed for a 550 MW coal fired power plant. The 1st year CO_2 removal cost for the aminosilicone-based carbon-capture process was evaluated at \$48/ton CO_2 using the steam stripper column. This is a 20% reduction compared to MEA, primarily due to lower overall capital cost. CO_2 cost using the CSTR desorber is dominated by the economics of the solvent make-up. The steam stripper desorber is the preferred unit operation due to a more efficient desorption, and reduced solvent make-up rate. Further reduction in CO_2 capture cost is expected by lowering the manufacturing cost of the solvent, implementing flowsheet optimization and/or implementing the next generation aminosilicone solvent with improved stability and increased CO_2 working capacity.

Table of Contents

4.4.4. MEA vs. Aminosilicone (CSTR and SSC) at 0.5 MW_e

4.5. SSC Campaign: Summary

5.0 Techno-economic analysis

6.0 Summary

1. Projective Objectives and Timeline

The primary objective of the cooperative agreement between GE Global Research, National Carbon Capture Center (NCCC) and Department of Energy was to design, construct, and operate a pilot-scale process using a novel aminosilicone-based CO_2 capture solvent (GAP-1_m/TEG). **Figure 1** and **Figure 2** describe the overall objectives of the program, and program timeline, respectively.

Performance of the GAP-1_m/TEG solvent was demonstrated in a 0.5 MW_e pilot with real flue gas for over 900 hours of operation using two alternative desorption designs: a Continuous Stirred Tank Reactor (CSTR), and a Steam Stripper Column (SSC). The CSTR desorber was designed, fabricated and integrated with the pilot solvent test unit (PSTU), replacing the PSTU Steam Stripper Column at NCCC. During the testing of the GAP-1_m/TEG solvent with the CSTR, thermal degradation of the rich solvent was found to be the main mechanism in solvent loss. Small amounts of water in the working solution were found to be an effective way to enable steam stripping, lower desorption temperature, and hence reduce thermal degradation. The concept was first tested in a glass stripping column (GE GRC), optimized in a continuous bench scale system (2 kW_e, GE GRC), and demonstrated in a 0.5 MW_e pilot (NCCC). No special system modifications were required to the PSTU to accommodate the testing of the non-aqueous GAP-1_m/TEG solvent with the regenerator column.

Data obtained from the system included solvent stability, effects of flue gas contaminants, and recommended operating conditions for both CSTR and SSC desorbers. The pilot-scale engineering data was used to update the capture system process models in collaboration with Carbon Capture Simulation Initiative (CCSI) and West Virginia University. The updated models were used to complete the techno-economic analysis and to develop a scale-up strategy to evaluate the progress in meeting the DOE goal of CO_2 capture cost from coal-fired power plants at less than \$40/tonne of CO_2.

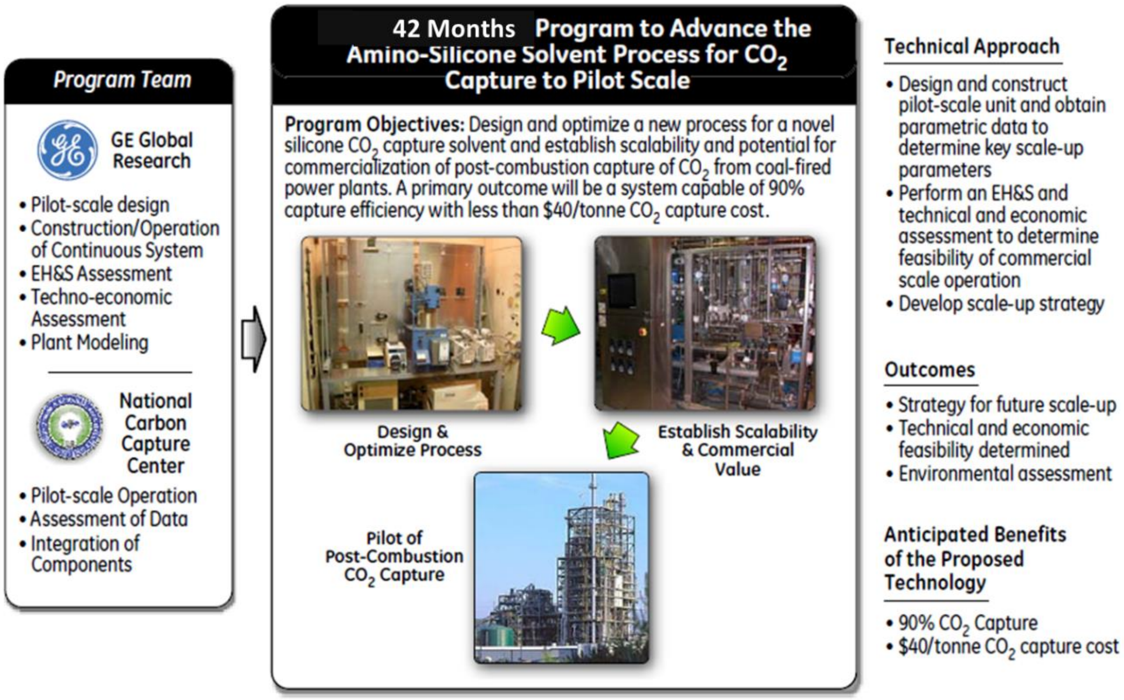

Program Team

GE Global Research

- Pilot-scale design
- Construction/Operation of Continuous System
- EH&S Assessment
- Techno-economic Assessment
- Plant Modeling

National Carbon Capture Center

- Pilot-scale Operation
- Assessment of Data
- Integration of Components

42 Months Program to Advance the Amino-Silicone Solvent Process for CO_2 Capture to Pilot Scale

Program Objectives: Design and optimize a new process for a novel silicone CO_2 capture solvent and establish scalability and potential for commercialization of post-combustion capture of CO_2 from coal-fired power plants. A primary outcome will be a system capable of 90% capture efficiency with less than $40/tonne CO_2 capture cost.

Technical Approach

- Design and construct pilot-scale unit and obtain parametric data to determine key scale-up parameters
- Perform an EH&S and technical and economic assessment to determine feasibility of commercial scale operation
- Develop scale-up strategy

Outcomes

- Strategy for future scale-up
- Technical and economic feasibility determined
- Environmental assessment

Anticipated Benefits of the Proposed Technology

- 90% CO_2 Capture
- $40/tonne CO_2 capture cost

Figure 1. Pilot-Scale Silicone Process for Low-Cost Carbon Dioxide Capture: Project Objectives

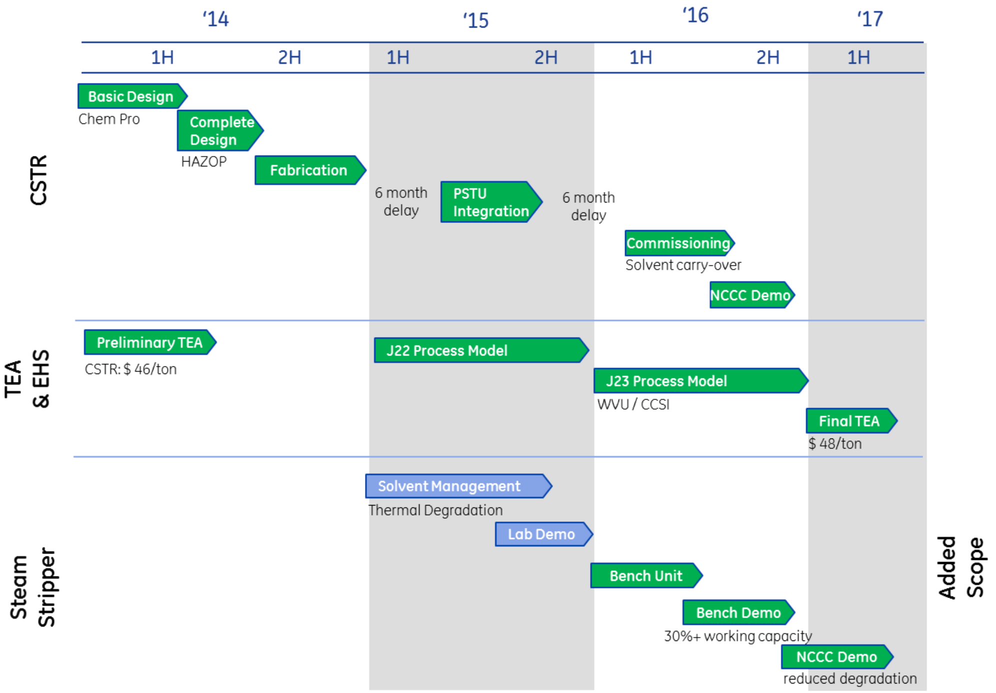

Figure 2. Pilot-Scale Silicone Process for Low-Cost Carbon Dioxide Capture: Overall Timeline

2. GE Aminosilicone Technology

The proposed technology is to use an aminosilicone-based solvent for CO_2-capture from the flue gas of a pulverized coal power plant. In previous GE Global Research work, as part of a prior DOE project (DE-NT0005310) an aminosilicone solvent was identified that demonstrates superior performance for CO_2 capture. This material consists of an aminosilicone oligomer known as GAP (3-aminopropyl end-capped polydimethylsiloxanes [PDMS]). It was found that the best performance was GAP-1 (1,5-Bis(3-aminopropyl 1,1,3,3,5,5-hexamethyl trisiloxane)), GAP-1 structure is shown in **Figure 3**.

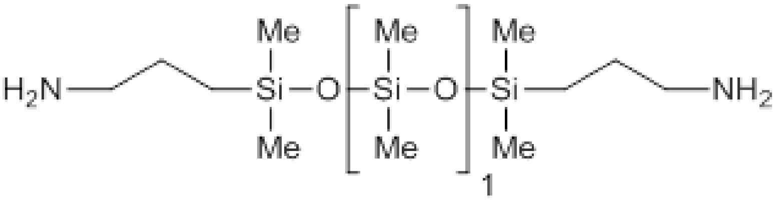

Figure 3. GAP-1 (1,5-Bis(3-aminopropyl) 1,1,3,3,5,5-hexamethyl trisiloxane).

GAP-1 readily reacts with CO_2 to form a carbamate (**Figure 4).**

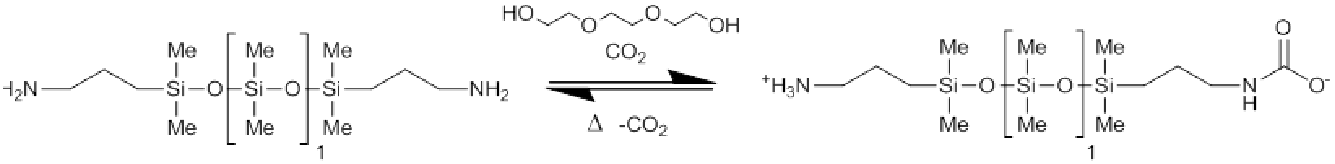

Figure 4. GAP-1 material reacting with CO_2

The GAP-1 synthesized for this project is actually a statistical mixture of GAP molecules with x values of 0 to 3, and will be distinguished from pure GAP-1 by the subscript “m” (GAP-1_m). GAP-1_m consists of 40 wt% GAP-0, 33 wt% GAP-1, 19% GAP-2, and 8% GAP-3, as determined by ^{1}H NMR, with the average molecular weight being that of GAP-1. At elevated temperatures CO_2 is reversibly desorbed from GAP-1_m, permitting reuse of the CO_2 capture solvent. However, the viscosity of GAP-1_m increases significantly upon absorption of CO_2, and can solidify at high CO_2 loadings. In order to mitigate these issues, it was found that a suitable CO_2 capture solvent could be produced by diluting GAP-1_m in a co-solvent. Using triethylene glycol (TEG) as a co-solvent, a CO_2 capture solvent comprised of 60% (by wt) GAP-1_m with 40% TEG demonstrated improved thermal stability and volatility relative to MEA with a similar capacity for CO_2. The use of a co-solvent ensures that the viscosity of the aminosilicone-based solvent is acceptable even at high CO_2 loadings, and inhibits solidification of the aminosilicone.

GAP-1_m/TEG exhibits a number of desirable properties as a CO_2 capture solvent when compared to MEA. **Figure 5** shows the vapor pressure of both MEA and GAP-1_m. As shown, both GAP-1_m and TEG are significantly less volatile than MEA. This lower volatility simplifies CO_2 desorption and potentially reduces the solvent loss in both clean flue gas and CO_2 streams.

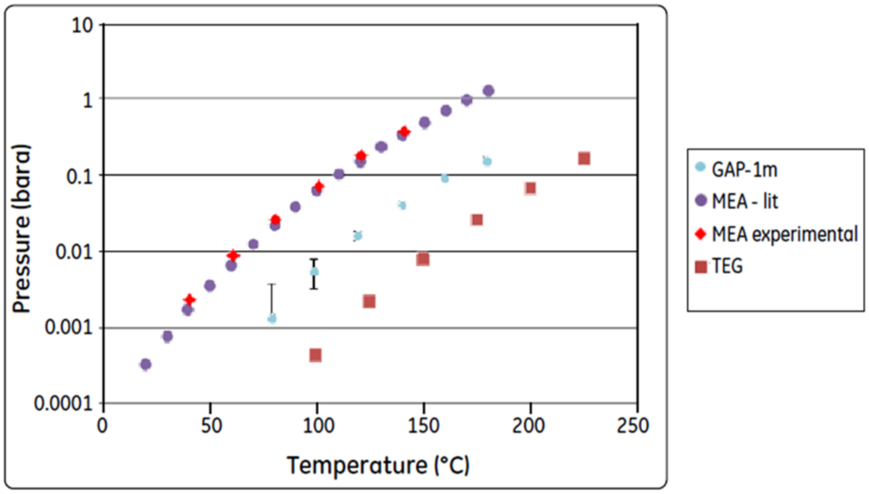

Figure 5. **Vapor Pressure**: MEA vs. GAP-1_m/TEG solvent

Thermal stability tests were performed in prior DOE funded projects, in which GAP-1_m (lean solvent) was heated at temperatures from 120 to 160°C for over 80 days, in the presence of air. **Figure 6** shows the results when compared to MEA. At 120 °C, it was observed by GC that there was no detectable degradation of the material. At 150 °C, lean aminosilicone solvent exhibits one order of magnitude lower thermal degradation rate than MEA.

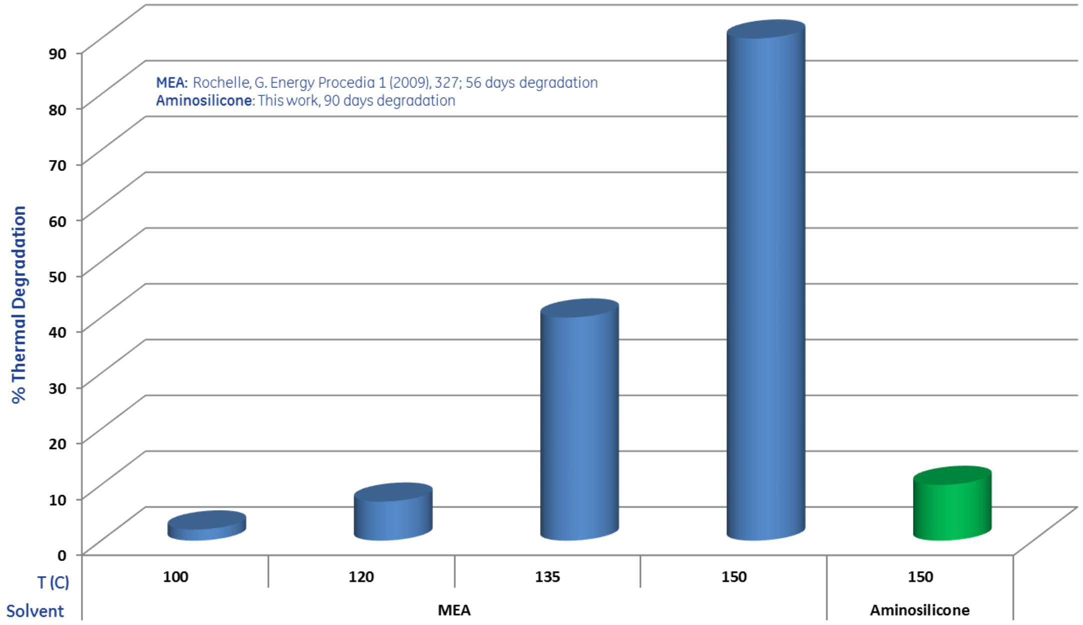

Figure 6. **Thermal Degradation:** MEA vs. GAP-1_m/TEG solvent (lean)

More recent studies were completed looking at the effects of water and CO_2 on thermal degradation. It was found that high concentration of CO_2 results in elevated thermal degradation rates. This is shown in **Figure 7**. Solvent that is fully loaded with CO_2 (the blue curves), shows a higher rate of thermal degradation over a range of temperatures, than the partially loaded samples (the green curves). Additionally, it was determined that the addition of water (at 5-10 wt%) decreased the rate of thermal degradation for both the 100% - loaded solvent and the 25% - loaded solvent.

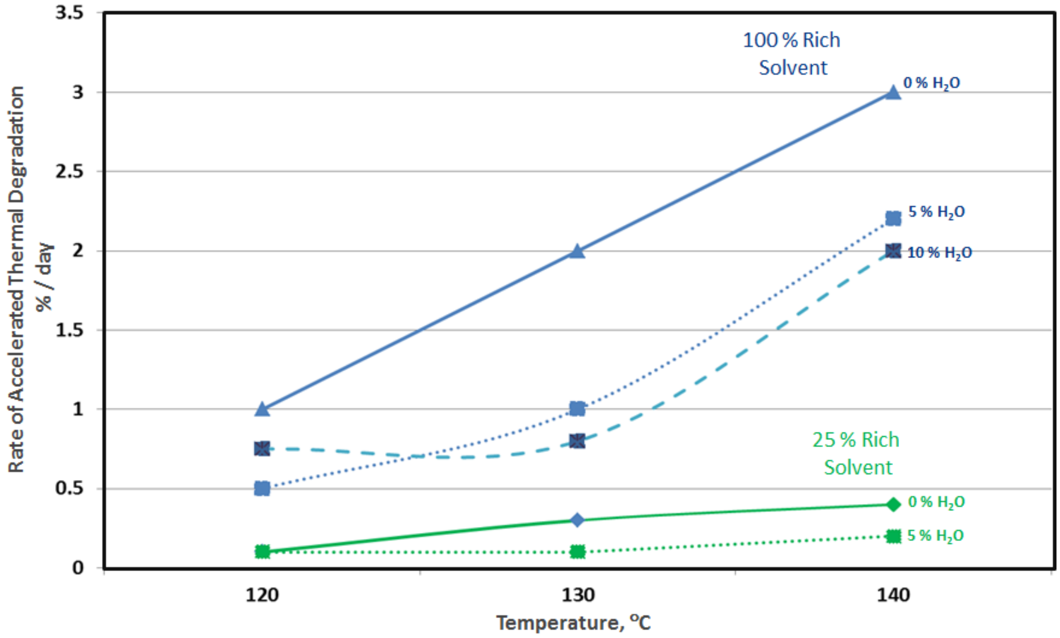

Figure 7. **Thermal Degradation:** GAP-1_m/TEG solvent (rich)
Rate of thermal degradation as a function of temperature, percent CO_2 loading, and water loading (2 kW bench scale process)

In order to better understand why CO_2 would promote thermal degradation, and why water would inhibit it, various analytical techniques were used to determine the products of thermal degradation. The route for thermal degradation identified is shown in **Figure 8**.

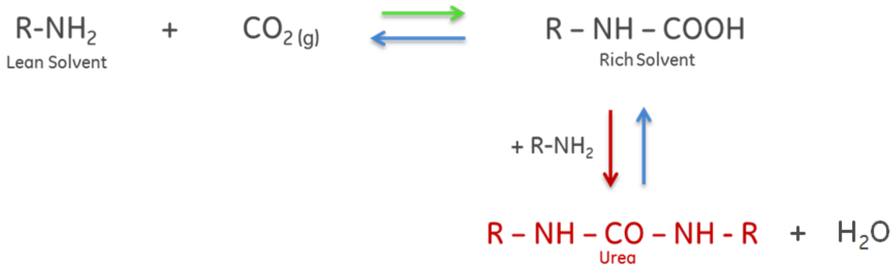

Figure 8. **Thermal Degradation of GAP-1_m/TEG solvent (rich):** Proposed Mechanism

Lean aminosilicone solvent can react with CO_2 to form a carbamate (CO_2-rich solvent). The carbamate molecule can then react with a CO_2-lean molecule in a side reaction to form urea and water, where two amine groups are inactive in the urea form. Increasing the concentration of CO_2-rich solvent pushes the equilibrium of the side reaction to favor the formation of urea, therefore increasing the rate of thermal degradation of the solvent. However, water is also a product of the side reaction. So adding water to the solvent should help push the equilibrium of the side reaction back to favoring the non-urea form. In summary, we found that the rate of thermal degradation of the rich solvent is proportional to temperature, CO_2 content of the solvent leaving the desorber and inversely proportional to water content (eq. [1]).

$$Rate\ of\ thermal\ degradation \sim \frac{T \times \%CO_{2,lean}}{\%\, H_2O} \qquad [1]$$

Finally, corrosivity studies conducted in our bench-scale system [DE-FE0007502] have shown that GAP-1_m/TEG is significantly less corrosive than MEA under the absorber and rich/lean heat exchanger conditions, decreasing capital costs by using less expensive materials of construction. **Figure 9** gives the corrosion rates in the bench-scale system.

Figure 10 shows the CO_2 capture process that was developed to take advantages of the unique properties of the aminosilicone solvent (increased CO_2 capacity, lower volatility and lower corrosivity). A CSTR desorber was proposed as a low CAPEX / low footprint alternative to the typical regenerator system. The system was previously demonstrated in the 2 kW_e demo [DE-FE0007502], and it was the initial design choice for the 0.5 MW_e pilot.

Location / Metal Type	Conditions	Unexposed samples (interface images)	Exposed samples (interface images)	Corrosion Rate (µm/yr)
Lean Storage / C1018	~380 hours at ~34 °C and ~6138 hours at ~25 °C	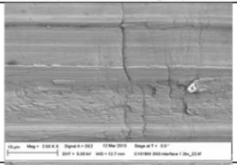	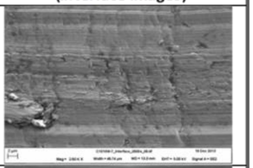	1.27
Absorber Sump / C1018	~389 hours at ~52 °C and ~6138 hours at ~25 °C	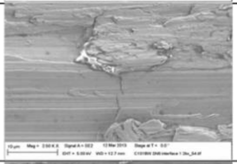	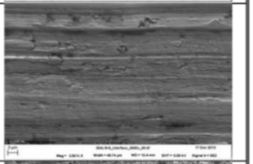	0.47
Desorber / C1018	~388hours at ~145 °C and ~6138 hours at ~25 °C	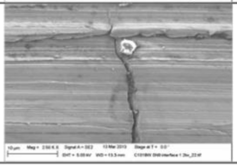	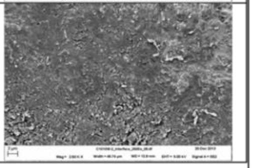	2188

Figure 9. **GAP-1_m/TEG Corrosivity**

Corrosion rates measured in the bench-scale demo (2 kW_e)

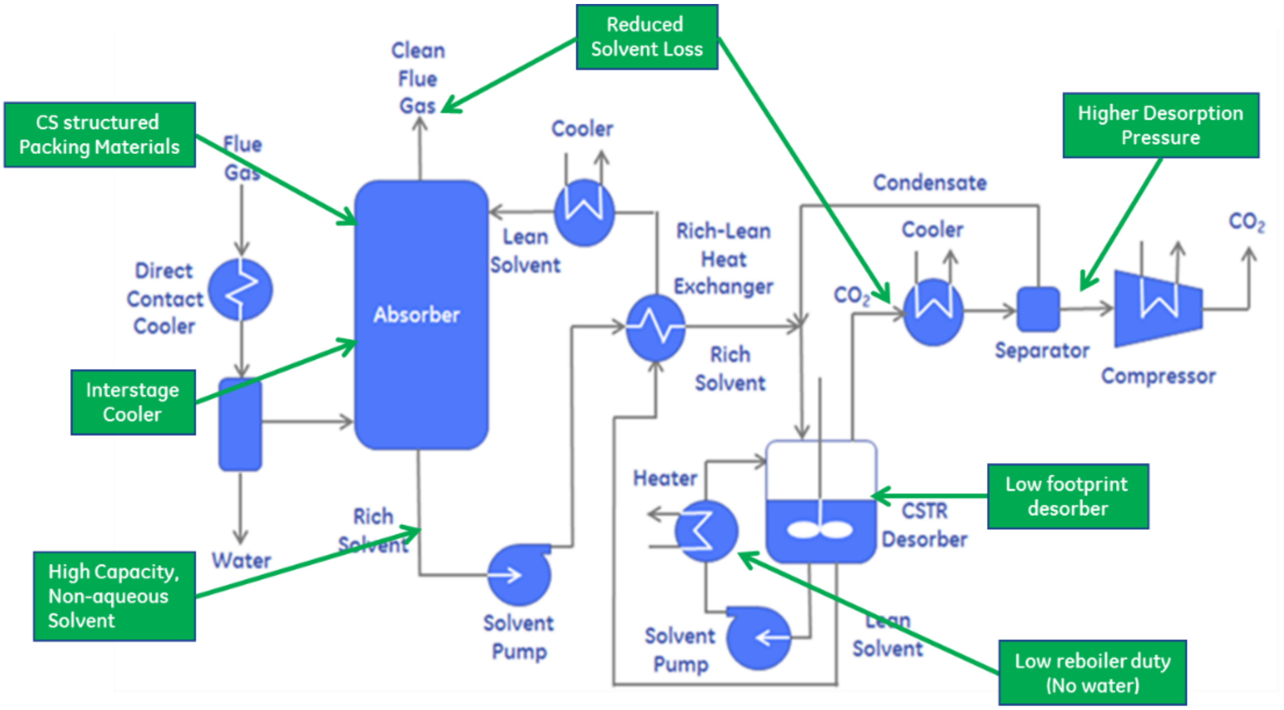

Figure 10. **CO_2 Capture Process for GAP-1_m/TEG**

CSTR – continuous stirred tank reactor

3. CSTR Campaign

A CSTR desorber system was designed, fabricated and integrated with the equipment available (absorber / water wash column, rich-lean exchanger, lean cooler) at the NCCC. The system was designed to operate continuously, using flue gas provided by the NCCC. The conceptual design of the hybrid system shown in **Figure 11**.

The skid design included a desorber that replaced the stripper column currently at the NCCC. The desorber consists of a continuous stirred-tank reactor into which the CO_2-rich solvent from the absorption column feeds. The reactor has an agitator to keep the content of the reactor well mixed. The reactor also has a recycle loop with a heat exchanger. This loop is used to heat the contents of the reactor and to increase mass transfer of the desorbed CO_2 from the solvent to the gas phase. The skid also includes a partial condenser that recovers solvent vapor from the CO_2 leaving the reactor vessel (not shown in the picture).

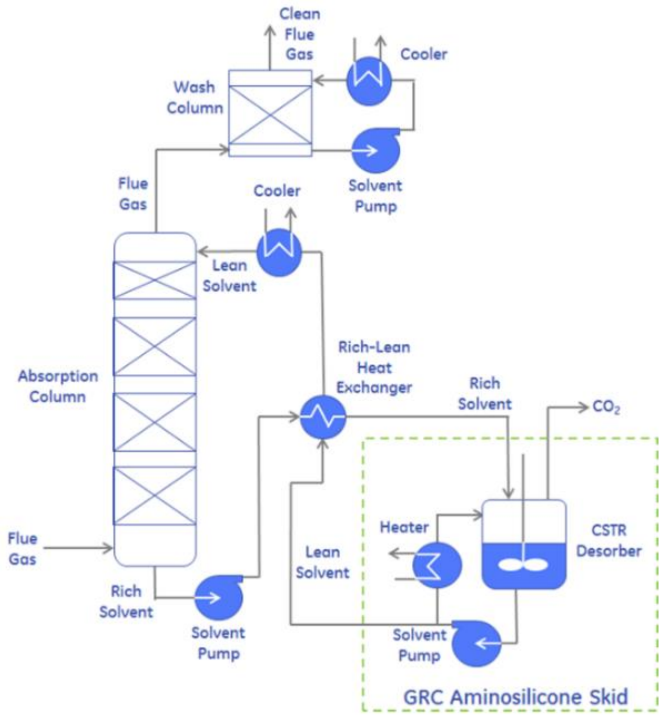

Figure 11. **CSTR – PSTU Integration:** Conceptual Design

3.1. CSTR System

The overall timeline of the CSTR campaign is shown in **Figure 12**.

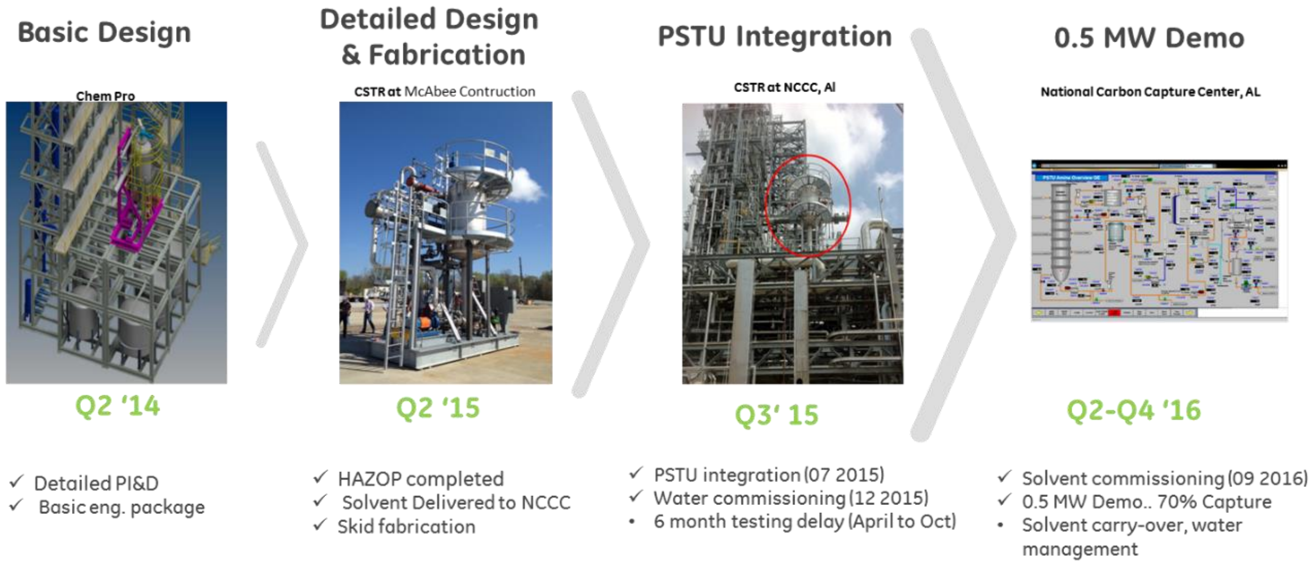

Figure 12. **CSTR Campaign:** Overall Timeline

3.1.1. CSTR System Design and Fabrication (Q1 2014 – Q2, 2015)

GE Global Research contracted ChemPro Group, an engineering firm, to complete the basic and detailed engineering package for the CSTR system. The initial design package included detailed P&IDs, equipment specifications for all major equipment (including pumps, heat exchangers, and the continuous stirred-tank reactor), and material and energy balances. **Figure 13** shows an aerial view of the mezzanine level of the PSTU, with the proposed location of the CSTR skid. **Figure 14** shows a 3D model of the CSTR skid, incorporated into the PSTU. **Figure 15** shows the 3D model of the CSTR skid structure. The basic engineering design was completed in Q2 2014, and the detailed engineering was completed in Q3 2014. McAbee Construction, contracted by ChemPro, completed the skid fabrication in Q1 2015 (**Figure 16**)

Figure 13. **CSTR Design:** PSTU showing the footprint of the GE skid

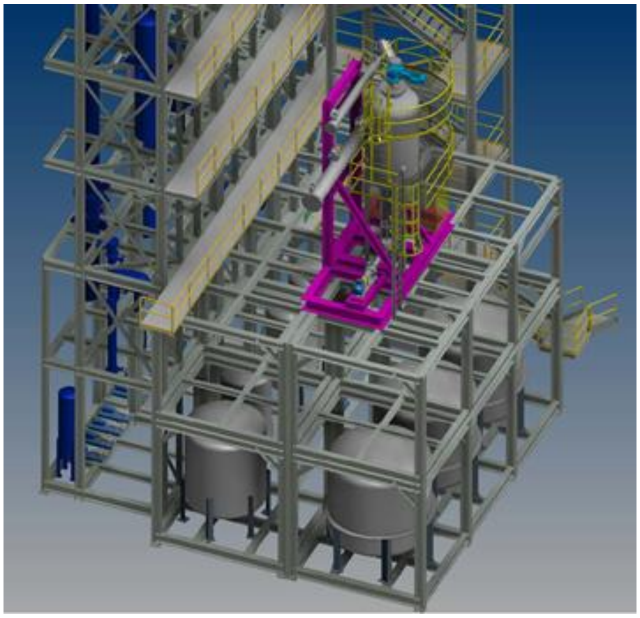

Figure 14. **CSTR Design:** GE CSTR – PSTU Integration (3D model, Chempro)

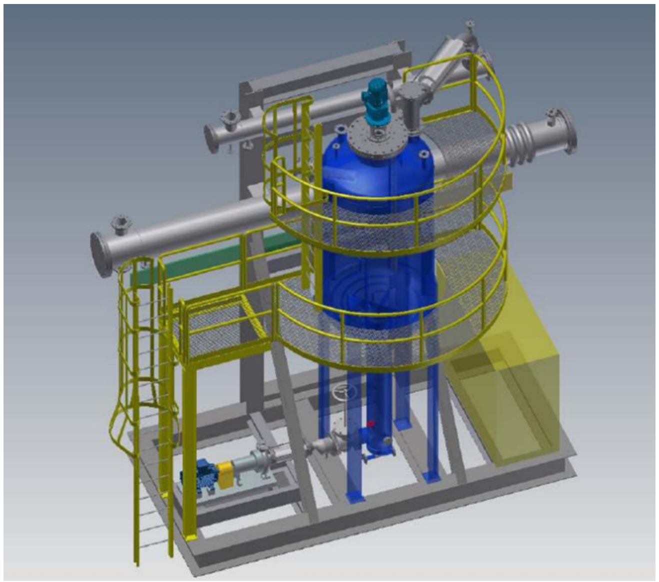

Figure 15. **CSTR Design:** Skid Structure (3D model, Chempro)

Figure 16. CSTR Fabrication: Skid during commissioning (Q1 2015, McAbee)

3.1.2. Material Selection

Compatibility of materials of construction is crucial for the integrity of the capture system. Some of the ubiquitous and critical components are seals and gaskets. From prior work, it was found that Viton® seals did not withstand prolonged exposure to aminosilicones. EPDM was considered as a replacement material for seals and gaskets on the PSTU, but it was unclear if this material would withstand a heated mixture of GAP-1_m/TEG.

To evaluate the EPDM elastomer, small samples of the white rubber were placed in flasks with various solvents, as shown in **Table 1**, and heated for 6-10 days at 140 °C under N_2. Both pure GAP-0 and GAP-1_m (Samples A and B) showed little effect on the EPDM sample with only a very small amount of white hazy material being formed/extracted after 10 days at 140 °C. While no apparent damage was done to the rubber sample C, the GAP-1_m/TEG mixture generated a scummy layer that contained black specks that floated on the solvent mixture.

Table 1. Test samples for EPDM stability

Sample	Solvent	Observation
A	GAP-0	Small amount of white hazy material extracted from rubber. No apparent dimensional or color change, and rubber sample was still elastomeric. Some absorption of solvent into rubber as seen by weeping after surface removal of solvent.
B	GAP-1m	Small amount of white hazy material extracted from rubber. No apparent dimensional or color change, and rubber sample was still elastomeric. Some absorption of solvent into rubber as seen by weeping after surface removal of solvent.
C	GAP-1m/TEG (60:40)	Scum/rag level floating on top of solvent with black material present. However, there was no apparent dimensional and only a very slight color change, and rubber sample was still elastomeric. Some absorption of solvent into rubber as seen by weeping after surface removal of solvent.
D	TEG	Small amount of white hazy material extracted from rubber. No apparent dimensional or color change, and rubber sample was still elastomeric. Some absorption of solvent into rubber as seen by weeping after surface removal of solvent.
E	GAP-1m/TEG (60:40)	Scum/rag level floating on top of solvent with black material present. However, there was no apparent dimensional and only a very slight color change, and rubber sample was still elastomeric. Some absorption of solvent into rubber as seen by weeping after surface removal of solvent.

Believing that the TEG was responsible for this effect, EPDM sample D was heated for 6 days with pure TEG with no rag/scum layer or black specks appearing. Repeating the C sample with E, black material appeared after 2-3 days and did not appear to increase for the six day duration of the heating. In all cases, regardless of the condition of the solvent, the EPDM samples remained viable and unchanged based on visual and tactile inspection.

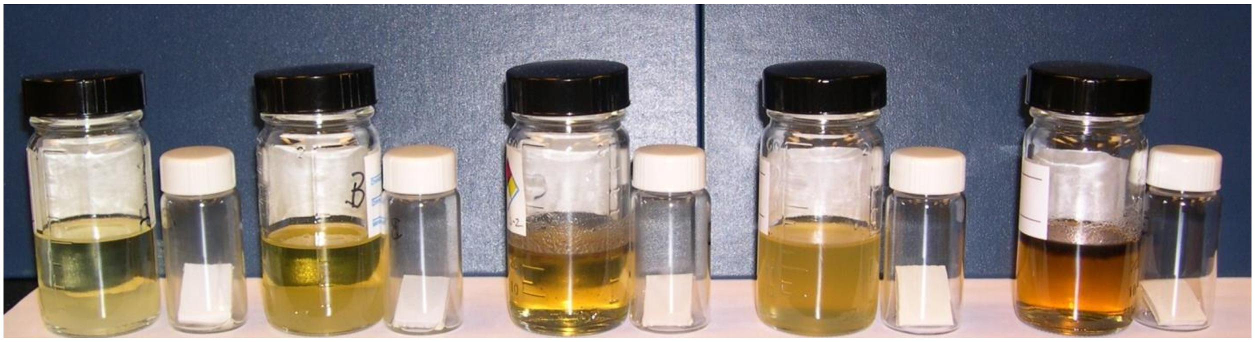

A **B** **C** **D** **E**

Figure 17. **Material Qualification:** Gasket & seal material selection
EPDM samples and solvents after thermal treatment in solvent.
See **Table 1** for sample description.

A more quantifiable measure of the rubber integrity was made via tensile testing. For these tests, dogbone-shaped samples were cut from a 3mm thick EPDM sheet. **Figure 18** and **Table 2** show the results obtained from virgin EPDM rubber samples. **Figure 19** and **Table 3** summarize the results for ethylene propylene diene monomer (EPDM) rubber aged at 140 ºC for seven days in a 60/40 mixture of GAP-1_m/TEG.

The virgin material showed a maximum load of 38 N and mean tensile stress of ~3.9 MPa and a tensile strain of ~1590% which is representative of a strong elastomer. After soaking in the solvent mixture, the maximum load jumped to ~62 N with a tensile stress increased to ~6.2 MPa and the stress increased to over 3000%. While the dimensions of the samples remained the same, it was apparent that some solvent had plasticized the rubber, thereby increasing its toughness.

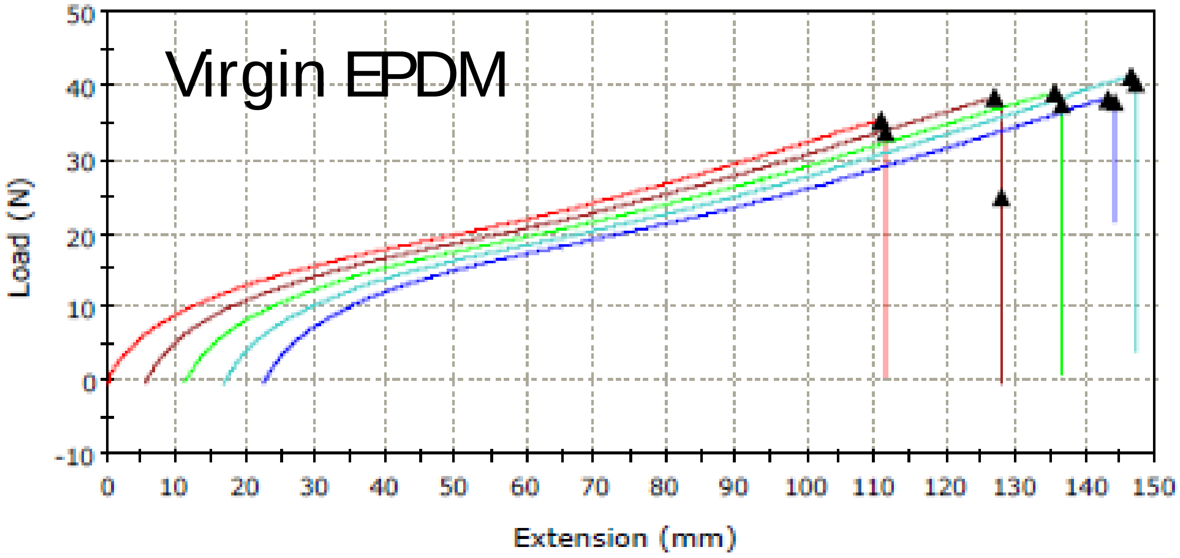

Figure 18. **Material Qualification:** Instron tensile plot (EPDM virgin samples)

Table 2. **Material Qualification:** Virgin EPDM Instron

	Maximum Load	Tensile stress at Maximum Load	Tensile strain at Maximum Load	Load at Break (Standard)	Tensile stress at Break (Standard)	Tensile strain at Break (Standard)
Sample	(N)	(MPa)	(%)	(N)	(MPa)	(%)
1	35.28	3.56	1449.73	33.64	3.4	1460.07
2	38.23	3.86	1589.43	24.79	2.5	1599.77
3	38.87	3.93	1624.85	37.33	3.77	1636.82
4	41.15	4.16	1699.95	40.13	4.05	1708.12
5	38.15	3.85	1583.57	37.61	3.8	1596.63
Coefficient of Variation	5.47157	5.47157	5.71596	17.30884	17.30884	5.64438
Maximum	41.15	4.16	1699.95	40.13	4.05	1708.12
Mean	38.33	3.87	1589.51	34.7	3.51	1600.28
Median	38.23	3.86	1589.43	37.33	3.77	1599.77
Minimum	35.28	3.56	1449.73	24.79	2.5	1460.07
Range	5.87	0.59	250.22	15.35	1.55	248.04
Standard Deviation	2.09745	0.21186	90.85557	6.00627	0.60669	90.32598

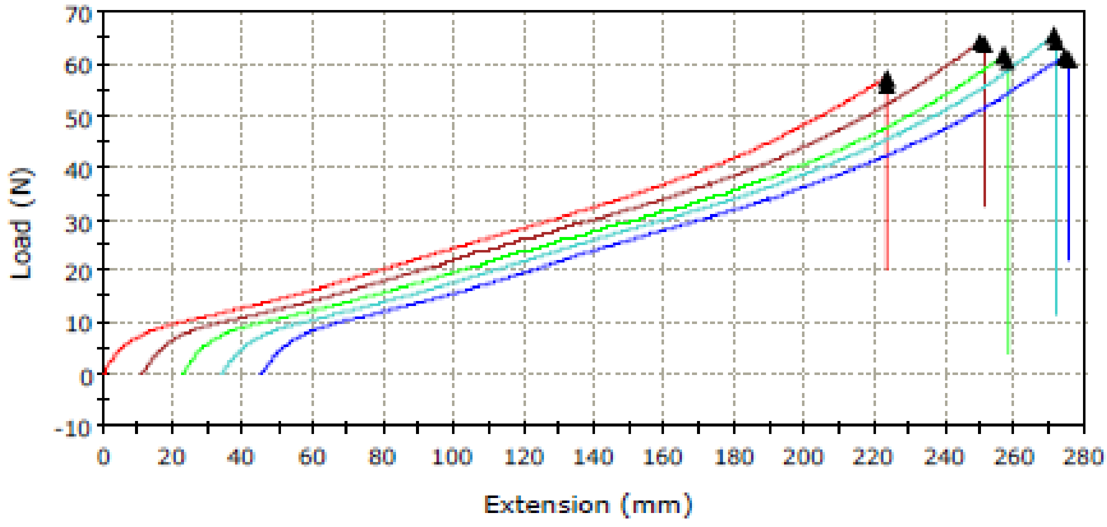

Figure 19. **Material Qualification:** Instron tensile plot (EPDM aged samples)
EPDM rubber aged at 140 ºC for 7 days in a 60/40 mixture of GAP-1/TEG.

Table 3. **Material Qualification:** Aged EPDM Instron
EPDM rubber aged at 140 ºC for 7 days in a 60/40 mixture of GAP-1/TEG.

	Maximum Load	**Tensile stress at Maximum Load**	**Tensile strain at Maximum Load**	**Load at Break (Standard)**	**Tensile stress at Break (Standard)**	**Tensile strain at Break (Standard)**
Sample	(N)	(MPa)	(%)	(N)	(MPa)	(%)
1	57.18	5.78	2920.15	55.65	5.62	2925.59
2	63.95	6.46	3120.51	63.63	6.43	3135.83
3	61.42	6.2	3065.5	60.55	6.12	3075.29
4	65.45	6.61	3111.72	64.21	6.49	3119.84
5	61.29	6.19	3006.72	60.71	6.13	3015.43
Coefficient of Variation	5.08924	5.08924	2.7293	5.56863	5.56863	2.80969
Maximum	65.45	6.61	3120.51	64.21	6.49	3135.83
Mean	61.86	6.25	3044.92	60.95	6.16	3054.4
Median	61.42	6.2	3065.5	60.71	6.13	3075.29
Minimum	57.18	5.78	2920.15	55.65	5.62	2925.59
Range	8.27	0.84	200.36	8.56	0.86	210.24
Standard Deviation	3.148	0.31798	83.1049	3.3941	0.34284	85.81913

3.1.3. Hazard and Operability Study (HAZOP)

A detailed hazard and operability study (HAZOP) of the skid design was conducted on 12/3 and 12/4 of 2014 at the NCCC. For the HAZOP, an independent facilitator and scribe were hired to guide the process. The facilitator sectioned the P&IDs for the skid into 11 nodes, each node corresponding to a portion of the skid dedicated to a unique function. The team, which included representatives from GE Global Research, the NCCC, and ChemPro group, evaluated possible failure modes for each node. For this evaluation, the frequency (F) of each failure mode occurring and the severity (S) in terms of health and safety, environment impact, and material loss were estimated on a scale of 1 to 4 (with 4 being the worst), and the resulting risk rank (R) was determined by calculating F×S. **Table 4** shows the matrix that was used for this evaluation, including guidelines for rating frequency and severity and the color coded region showing the resulting risk rank. Red risk ranks (D) are considered extreme risks, while green risk ranks (A) are considered minor. It should be noted that the risk for each failure mode was evaluated without taking into account existing safety measures or future abatement methods. After the risk was determined for each failure mode, recommendations were made by the team to abate the risk.

Table 4. **HAZOP study:** risk matrix

			Severity			
		H&S	No Injury	Minor Injury	Moderate Injury	Severe Injury
		Env. Impact	None	Contained	Impact on Site	Impact off Site
		Material Losses	<$10k	$10k to $100k	$100k to $1M	>$1M
			1	**2**	**3**	**4**
Frequency	1x in more than 15 yr	**1**	A	A	A	B
	1x in 6 - 15 yr	**2**	A	A	B	C
	1x in 1 - 5 yr	**3**	A	B	C	D
	more than 1x per yr	**4**	A	C	D	D

In the HAZOP, 39 failure modes were identified. However, of these failure modes, only one received a D risk rating and another received a C risk rating.

Figure 20 shows the results of the analysis for the failure mode that received a risk rating of D. This failure mode is caused by the high pressure in the solvent feed to the CSTR resulting in a gasket leak in the rich/lean heat exchanger. As shown in **Figure 20**, a number of causes for high pressure in the solvent feed were identified. Additionally, recommendations were given to abate the risk, such as having a high pressure shut off on the feed pump, and shielding the rich/lean heat exchanger to contain any solvent that might escape.

Figure 21 shows the results of the analysis for the failure mode that received a risk rating of C. This failure mode is caused by the over-pressure of the CSTR. As shown in **Figure 21**, the CSTR is already equipped with an indicating rupture disk in case of over pressure. One of the recommendations was to have a signal from the indicating rupture disk sent to the control room, so that the operator can see if the rupture disk has released. The design team implemented all recommendations from the HAZOP team during commission phase of the project.

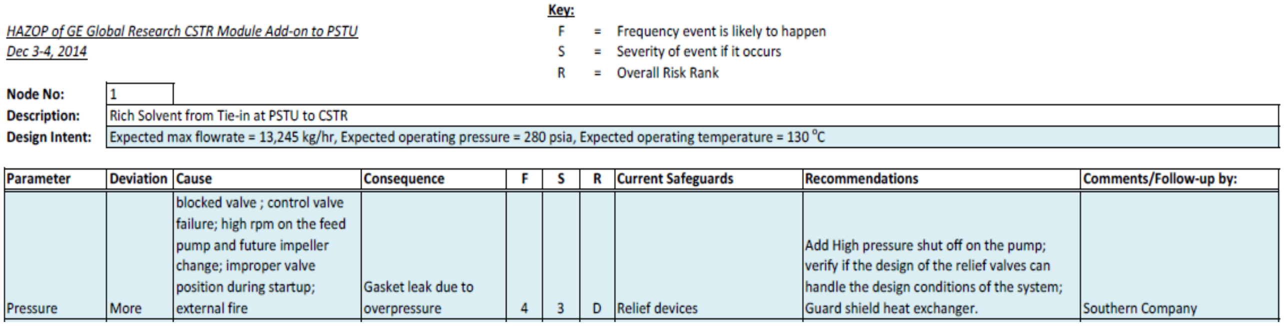

HAZOP of GE Global Research CSTR Module Add-on to PSTU
Dec 3-4, 2014

Key:
F = Frequency event is likely to happen
S = Severity of event if it occurs
R = Overall Risk Rank

Node No:	1
Description:	Rich Solvent from Tie-in at PSTU to CSTR
Design Intent:	Expected max flowrate = 13,245 kg/hr, Expected operating pressure = 280 psia, Expected operating temperature = 130 °C

Parameter	Deviation	Cause	Consequence	F	S	R	Current Safeguards	Recommendations	Comments/Follow-up by:
Pressure	More	blocked valve ; control valve failure; high rpm on the feed pump and future impeller change; improper valve position during startup; external fire	Gasket leak due to overpressure	4	3	D	Relief devices	Add High pressure shut off on the pump; verify if the design of the relief valves can handle the design conditions of the system; Guard shield heat exchanger.	Southern Company

Figure 20. **HAZOP study:** Failure mode analysis for high pressure in the solvent feed

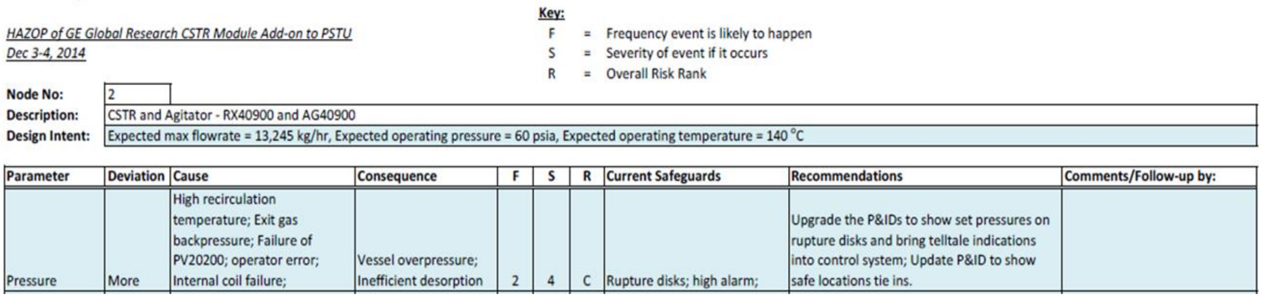

HAZOP of GE Global Research CSTR Module Add-on to PSTU
Dec 3-4, 2014

Key:
F = Frequency event is likely to happen
S = Severity of event if it occurs
R = Overall Risk Rank

Node No:	2
Description:	CSTR and Agitator - RX40900 and AG40900
Design Intent:	Expected max flowrate = 13,245 kg/hr, Expected operating pressure = 60 psia, Expected operating temperature = 140 °C

Parameter	Deviation	Cause	Consequence	F	S	R	Current Safeguards	Recommendations	Comments/Follow-up by:
Pressure	More	High recirculation temperature; Exit gas backpressure; Failure of PV20200; operator error; Internal coil failure;	Vessel overpressure; Inefficient desorption	2	4	C	Rupture disks; high alarm;	Upgrade the P&IDs to show set pressures on rupture disks and bring telltale indications into control system; Update P&ID to show safe locations tie ins.	

Figure 21. **HAZOP study:** Failure mode analysis for high pressure in the CSTR

3.1.4. Pilot Scale Solvent Supply

Two separate sources of GAP-1_m solvent were identified as potential suppliers for the solvent to be used in the pilot test operation. Solvent samples were received at GE GRC and the qualification process included full compositional analysis, performance evaluation for CO_2 capture uptake, and thermal stability tests. The supplier of choice was downselected based on consideration of shipping costs, scale-up capacity, on-time delivery, and reliability.

Part of the evaluation of the GAP-1_m from the domestic supplier entailed thermal stability testing with several levels of β-isomer contamination. Samples supplied contained <1%, 4%, 8% and 12% β-isomer. The most stable mixture of the four materials was the large-scale batch of GAP-1_m that had the highest beta content at ~12%. **Figure 22** summarizes the three- month test in which the sample containing 12 % β-isomer was heated at 150 °C for 90 days with periodic sampling for GC analysis. A modest decrease in GAP-0 content with a concomitant increase in GAP-1, GAP-2 and GAP-3 was observed. This was in stark contrast to the 1%, 4% and 8% samples in which a precipitous drop was seen in the first two weeks. 20-40% of the GAP-0 was lost with a doubling of the GAP-1 and GAP-2 content during this time period. 12% beta GAP-1m met also the qualifications for total CO_2 uptake and impurities profiles and it was selected to be produced for the pilot-scale program. 10 Mt of GAP-1_m solvent was delivered to NCCC site in Q2 2015 (**Figure 23**).

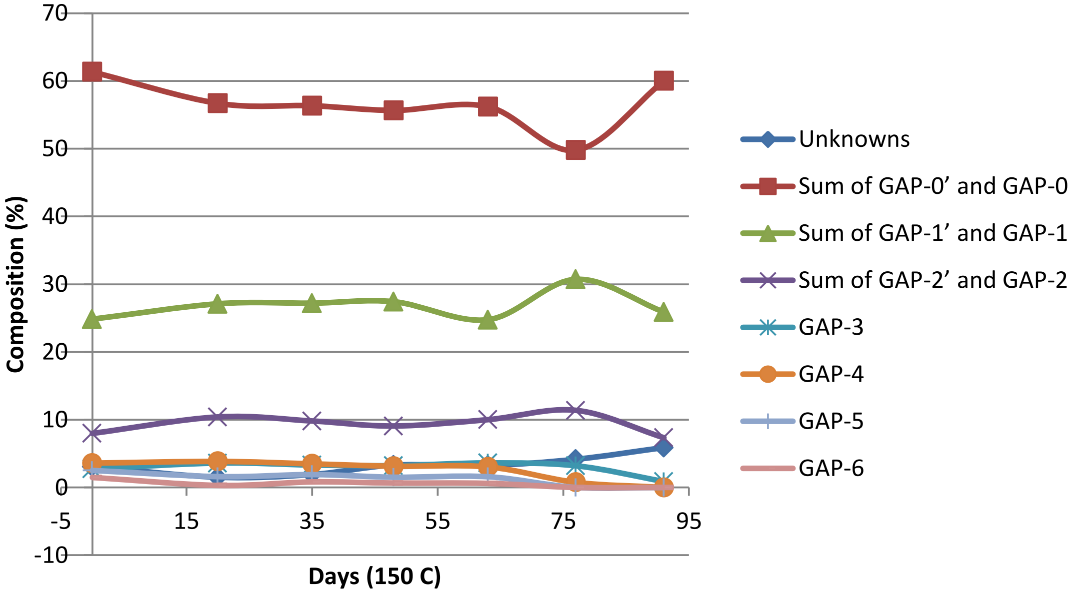

Figure 22. **Solvent Supply:** Qualification (Thermal stability)

Thermal stability of GAP-1_m with ~12% Beta Isomer

Figure 23. **Solvent Supply:** Solvent delivered at NCCC (10 Mt, Q2 2015)

3.1.5. Waste Water Process Development

During operation of the PSTU with the GAP-1_m/TEG solvent, there were two potential sources of waste water from the process, as shown in Figure 24. At the exit to the absorption tower, a water wash tower is used to capture any aminosilicone and TEG leaving the column as vapor or aerosol. As these components accumulate in the wash water, a fraction of the wash water is purged so that clean make-up water can be added. The second source of waste water is water that evaporates from the solvent during heating in the desorber. The CO_2 and water stream generated will pass through a partial condenser to recover the majority of the aminosilicone, but a small amount of aminosilicone will remain in the CO_2 stream and condense out with the water in the total condenser. During the design phase of the CSTR system, two methods were explored to minimize the solvent loss in the aqueous effluents: (i) purification through activated carbon bed, and (ii) water recycle in the lean storage tank. The two methods are discussed below.

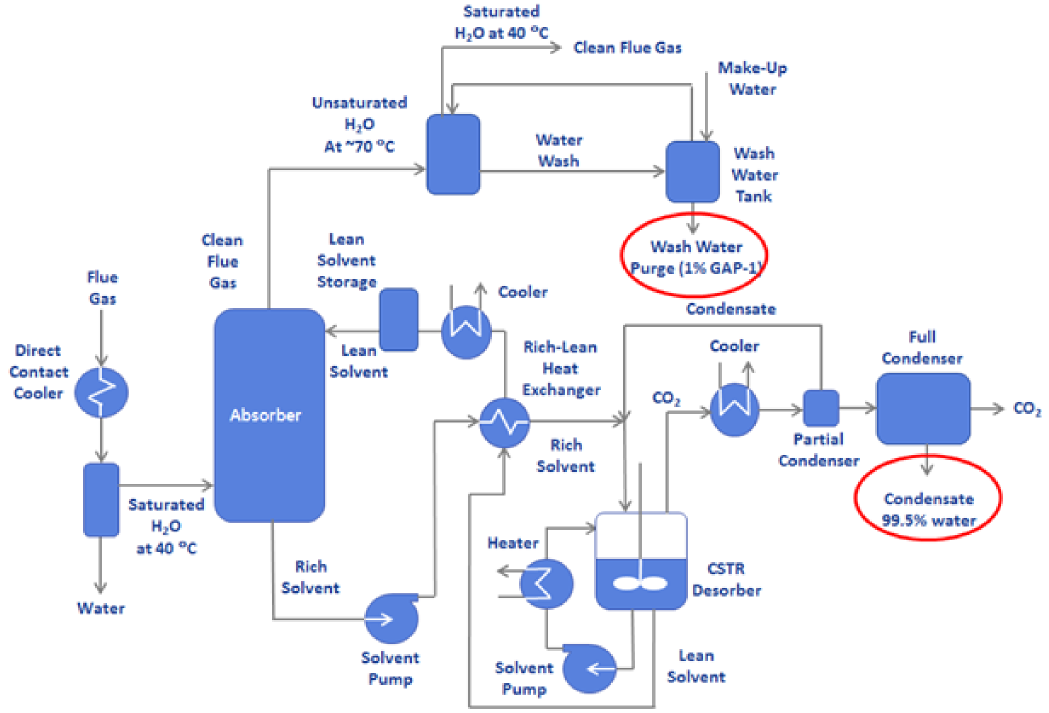

Figure 24. **GAP-1m/TEG Process Flow Diagram:** Waste water streams

3.1.5.1. Waste Water Purification: Activated Carbon Adsorption

Both lab- and bench-scale experiments were performed to evaluate the efficiency of using activated carbon for the removal of aminosilicones from waste water streams. Two methods were examined as potential analytical tools for the analysis of aminosilicones in water. The first was high-pressure liquid chromatography – electro spray/time-of-flight mass spectrometry (HPLC-ES/ToF MS) and the second was total organic carbon (TOC). Synthetic waste water sample was prepared by mixing 3.0 g of GAP-0 and 323 g DI water. This mixture was heated at 70 ^{o}C for 24 hours. The clear, water-white liquid was analyzed and then treated with carbon. 30 g of activated carbon (Norit SG II) was loaded into a chromatography column (20 x 150 mm bed of carbon), and 250 mL of synthetic waste water was passed through the column. **Table 5** shows that there was a large discrepancy between the two methods for the untreated sample. However, the treated material was in close agreement. This difference could be due to the fact that the concentration of the untreated sample exceeds the dynamic quantitative range for the mass spectrometer, even at 20-fold dilution. It is also possible that the response factors for the aminosilicones and aminosilanols are different than the cyclohexylamine standard used in the test.

Table 5. **Waste Water Treatment by Activated Carbon Adsorption:** Analytical Method Comparison

Method	Before Treatment (ppm)	After Treatment (ppm)
HPLC-ES/ToF MS	16,432	113
TOC	26,184	84

HPLC-ES/ToF MS - high pressure liquid chromatography – electro spray/ time-of-flight mass spectrometry; **TOC** - total organic carbon

While there is some difference in absolute measurements for aminosilicone content analysis between the TOC and HPLC methods, both appear to be acceptable methods for determining the presence of aminosilicones in aqueous solutions that range between ~100ppm and 3%. Although the TOC method cannot identify specific species in solution, it is a rapid and easily employed analytical procedure that can be deployed at the pilot plant site to provide a sense of the organic contamination in the waste water streams. In addition, it appears that under the conditions studied, activated carbon treatment of highly contaminated waste water (1.6-2.6% aminosilicone) is an effective means of greatly reducing the aminosilicone level.

In order to further test the efficacy of the carbon filter for removing aminosilicone and TEG from waste water, a series of experiments were commissioned to be performed at Engineering Performance Solutions, a company that specializes in testing materials for filtration.

For these experiments, a small bed of the activated carbon used in the full-scale carbon bed was produced by taking the full-scale carbon pellets and grinding them down to a finer particle size. The smaller particles were then placed in a mini-column. Solutions were made of 0.5 wt% aminosilicone in water, 0.5 wt% TEG in water, and 0.25 wt% aminosilicone and 0.25% TEG in water. Each of these solutions was run through a fresh bed at a flow rate that resulted in a contact time representative of the Empty Bed Contact Time (EBCT) of the full-scale process. The effluent from the carbon bed was measured using Total Organic Carbon (TOC) measurements, so that break-through curves could be generated for each solution. **Figure 25** shows the breakthrough curve for 0.5 wt% aminosilicone in water. It was observed that the TOC was less than 10% of its final value for roughly 2000 bed volumes. The TOC then jumped to approximately 50% of its final value for another 5000 bed volumes, before complete breakthrough.

Figure 26 shows the corresponding curves for 0.5 wt% TEG in water (Train 1) and 0.25 wt% aminosilicone and 0.25 wt% TEG in water (Train 2). The TEG appears to demonstrate 100% breakthrough almost immediately. Interestingly, for the mixture of aminosilicone and TEG in water, 100% breakthrough also appears almost immediately. This suggests that the TEG may interfere with the carbon beds' ability to remove aminosilicone. Therefore, it was concluded that absorbers containing the tested activated carbon are not highly efficient in removing traces of aminosilicone from aqueous streams containing TEG.

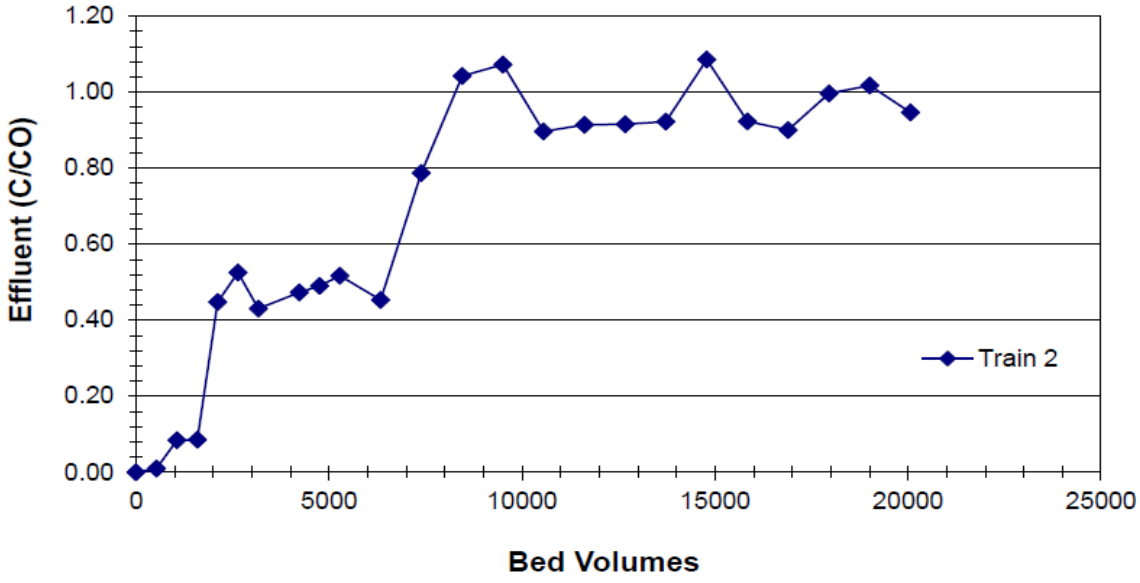

Figure 25. **Waste Water Purification:** Carbon bed test (GAP-1_m in water)
Breakthrough curve for 0.5 wt% aminosilicone in water through carbon bed
Analysis based on total organic carbon (TOC) method

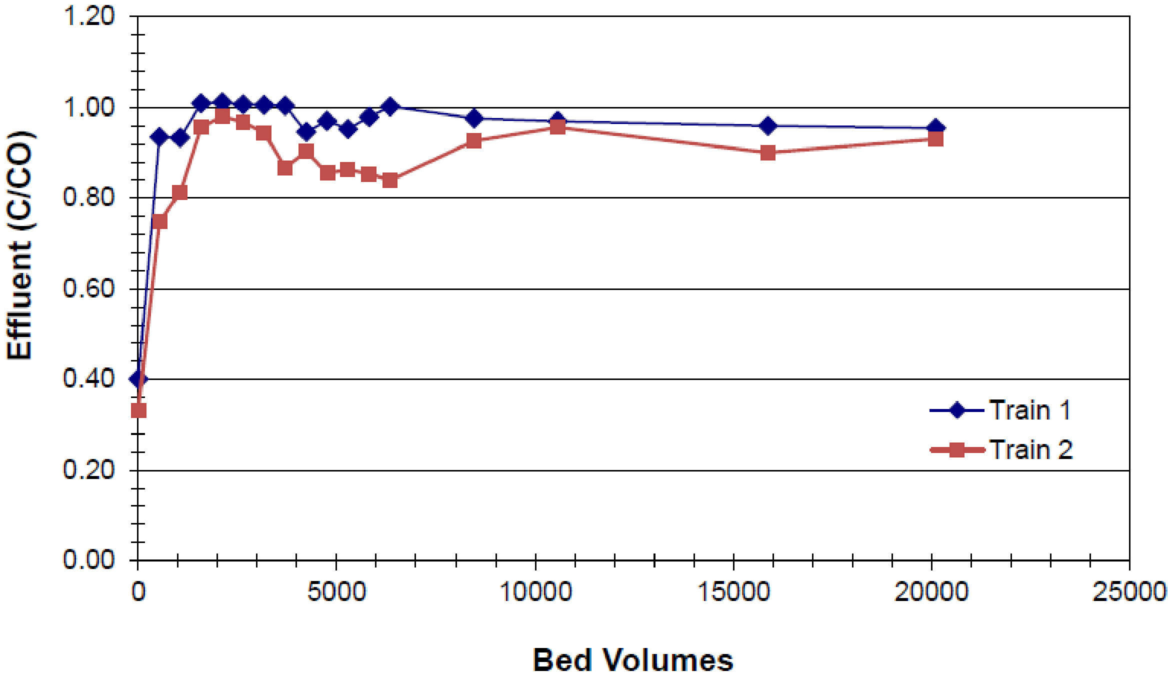

Figure 26. **Waste Water Purification:** Carbon bed test (TEG and GAP-1_m/TEG)
Breakthrough curves for: 0.5 wt% TEG in water (Train 1) and 0.25 wt% aminosilicone and 0.25 wt% TEG in water (Train 2). Analysis based on total organic carbon (TOC) method

3.1.5.2. Waste Water Recycling Process

In order to minimize the waste water produced, it was determined that the waste water streams can be recycled back to the lean solvent storage tank, as shown in **Figure 27**.

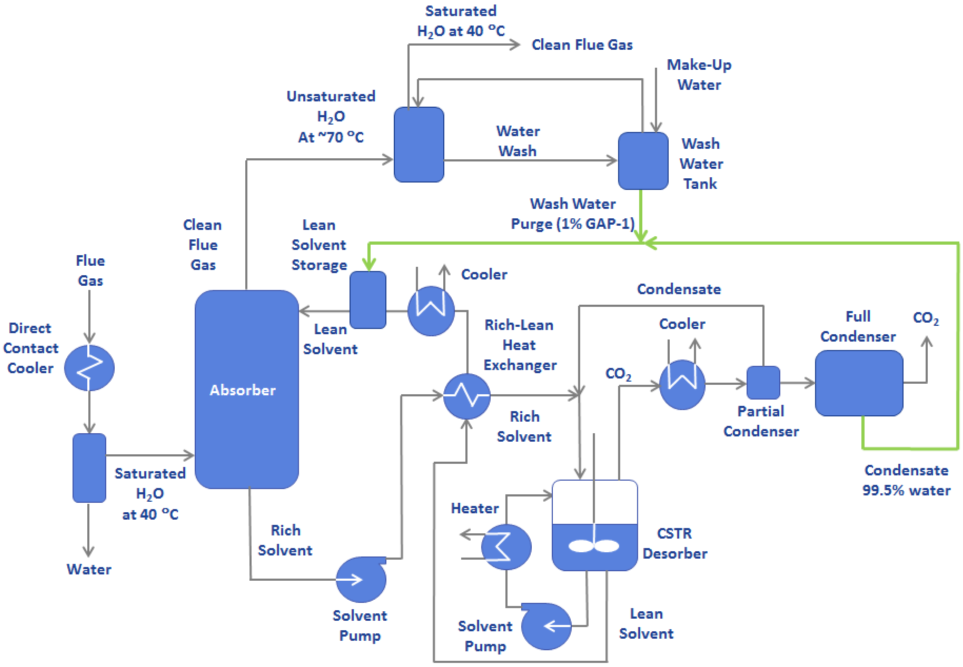

Figure 27. **Waste Water Recycle:** Process flow diagram
Waste water streams recycled to the lean solvent storage tank

Recycling the water to the lean solvent storage tank has several advantages. First, it has been shown that having controlled amount of water in the solvent decreases the rate of thermal degradation. Second, controlled amount of water lowers the partial pressure of CO_2 in the desorber headspace, and hence decreases the desorption temperature. Finally, recycling water reduces the solvent loss in the aqueous streams, and decreases the waste water produced during the operation. Based on all these advantages, this configuration was adopted during both CSTR and SSC campaigns.

3.2. Analytical Methods Development

GE Global Research and NCCC analytical team developed several analytical methods to assess the performance and degradation of the GAP-1_m/TEG solvent during the CSTR / SSC campaigns. **Table *6*** lists the method utilized during the campaign.

Table 6. Analytical Methods

Quantifier	Analytical Method
GAP-1_m/TEG in waste water	TN
% CO_2 in rich solvent	Carbamate Titration
Free Amine	Amine Titration
GAP-1_m : TEG urea	^1H NMR
% H_2O	Karl Fisher Titration

Total Nitrogen (TN):

As described earlier, this technique was used to determine the level of aminosilicone present in the wash water samples. The sample was acidified, and combusted. While this procedure cannot differentiate between species present in the sample, it is a very common method used in water evaluation. As there were no other sources of nitrogen present beside the GAP-1_m/TEG sample, we were able to correlate the TN to the amount of aminosilicone solvent present.

Carbamate Titration:

The extent of reaction of CO_2 with the amine solvent was determined by titrating the carbamate in the GAP-1_m/TEG solvent. A known amount of GAP-1_m/TEG solvent (1.5 – 3 g) was diluted with a pH adjusted methanol solution (50 mL, pH 11.3). Upon degassing CO_2, the pH of the methanol solution dropped depending on the CO_2 content. The mixture was then titrated back to a pH of

11.3 with potassium hydroxide. A fixed endpoint method was utilized. The sample weight, titrant normality, and volume of titrant consumed were all used to calculate the %CO_2 in the initial sample.

Amine Titration:

Free amine content was determined by titration with hydrochloric acid. Approximately 0.1 g of sample was added to a 10 mL 2-neck round bottom flask equipped with a magnetic stir bar and a pH electrode. The sample was diluted with approximately 8-10 mL of MeCN and stirred. pH measurements were recorded while adding hydrochloric acid solution (0.1 N). After the pH 7 end point was reached, titrant was added until a pH of 3 was achieved. The equivalence point was determined by plotting pH vs titrant volume.

^{1}H NMR

Samples were taken periodically for proton NMR analyses, to determine if the ratio of TEG : aminosilicone remained constant during the campaign, and to monitor for significant build-up of urea by-products. These tests were conducted at GE GRC on a 400-MHz instrument using $CDCl_3$ as the solvent. The ratio of O-CH_2CH_2-O protons in TEG to the CH_3-Si protons in GAP-X was determined, and the weight ratio of the two components defined. In addition, the integration of the resonance at ~3.2ppm showed the amount of urea that may have been formed due to thermal degradation.

3.3. CSTR – PSTU Integration and Water Commissioning (Q3-4 2015, Q2 2016)

CSTR system was delivered to NCCC site in June 2015, and its integration with the PSTU was completed in October 2016. System integration proceeded in the following sequential steps: (i) rigging the CSTR system to the 4th floor of PSTU (**Figure 28** / **Figure 29**); (ii) pipe connections between the CSTR system and the PSTU, (iii) pressure testing of the CSTR reactor and auxiliary equipment with air, (iv) heat tracing and (v) process control interface development for CSTR-

PSTU integrated system (**Figure 30**). A series of commissioning, start-up, and operating documents were created specific to the GE's CSTR system installed in the PSTU and transferred to NCCC. The list of procedures generated is listed in **Table 7**.

Table 7. **CSTR – PSTU Integration:** Operating Documents

Process Step	**Operating Documents**
Preparations for Start-up	• Verify Completion/Installation • Safety Check • Electrical and Instrument Continuity Check
Initial Start-up	• Preparation for Start-up with Water • Cooling Water and Tempered Water System Fill • Demineralized Water System Fill • Reactor/Recirculation System Fill • Steam System Fill • System Shutdown and Draining
Solvent Mixing and Loading	• Solvent Mixing Procedure • Inventory Lean Solvent Storage • PSTU Solvent Filling Procedure • Filling GE System with Process Fluid
Process Start-up	• Normal Start-up • Normal Operation • Normal Shutdown • Emergency Shutdown
Draining and Cleaning Procedures	• Draining and Cleaning Procedures • Draining Procedure • Cleaning Procedure

Figure 28. **CSTR – PSTU Integration:** CSTR Rigging (Q3 2015)

Figure 29. **CSTR – PSTU Integration:** CSTR Installed at NCCC (Q3 2015)

Figure 30. **CSTR – PSTU Integration:** Process control interface

Commissioning of the PSTU – CSTR system was conducted in the following sequential steps: (a) cold water circulation (Q4 2015), (b) steam commissioning (12/2015 and Q2 2016), and (c) hot and cold solvent circulation (Q3 2016). During the cold water circulation and steam commissioning, the team identified and fixed two minor leaks in the rich-lean heat exchanger, and CSTR lid (around sight glasses). Finally, it was determined that the CSTR had been hooked up to intermediate pressure steam (<250 psig), instead of the medium pressure steam (<450 psig) specified in the design. Because of the lower pressure steam supply, a pressure control valve on the CSTR system that was designed for the higher expected pressure drop had to be removed, and the interlock system was modified to accommodate this change.

3.4. Solvent Commissioning (Q3 2016)

Commissioning of the CSTR - PSTU system with GAP-1_m/TEG solvent was conducted by flowing both cold and hot solvent through the absorber-desorber system to check the operability of both the CSTR system and the rest of PSTU (absorber, pump, rich-lean exchanger, lean cooler) with the non-aqueous GAP-1_m/TEG solvent. The team implemented strict waste water and solvent management procedures to address handling the non-aqueous GAP-1_m/TEG solvent in the PSTU. First, all the pressure relief points of the system were piped to containment drums to eliminate the risk of solvent leaks. Any waste water resulted from the process was transferred to collection tanks and disposed off-site. PSTU sump collecting rain water drainage was monitored through automatic TN measurements. Flue gas was automatically turned off in case of over pressure or over temperature events. Finally, HAZOP and SOPs were updated after solvent commissioning and before starting the CSTR campaign.

During the first attempts at operation with flue gas, the liquid level in CSTR was difficult to control leading to solvent carry-over in the downstream mist separator and total condenser. The root cause of solvent carryover was determined to be the high solvent water content (11 wt.%). The rapid changes in liquid level were attributed to the development of CO_2 and water vapor bubbles in the solvent, which resulted in a reduction in the effective density of the solvent in the CSTR (**Figure *31***). Foam development was confirmed by visual inspection through the CSTR sight glass. To address this behavior, the water content of the solvent was reduced to approximately 5 wt. % prior to further testing. In addition, a manual valve mounted downstream of the recirculation pump was adjusted to increase the local pressure on the suction side of the recirculation pump and the high pressure leg of the pressure differential liquid level measurement. The result of this adjustment was stable CSTR operation at 5 wt.% water. Once the water loading was kept below 5 wt.%, CSTR continuous operation was commenced in Q4, 2016. **Figure 32** shows stable CSTR operation at 0.2 MW_e and 2.5 % wt.% H_2O.

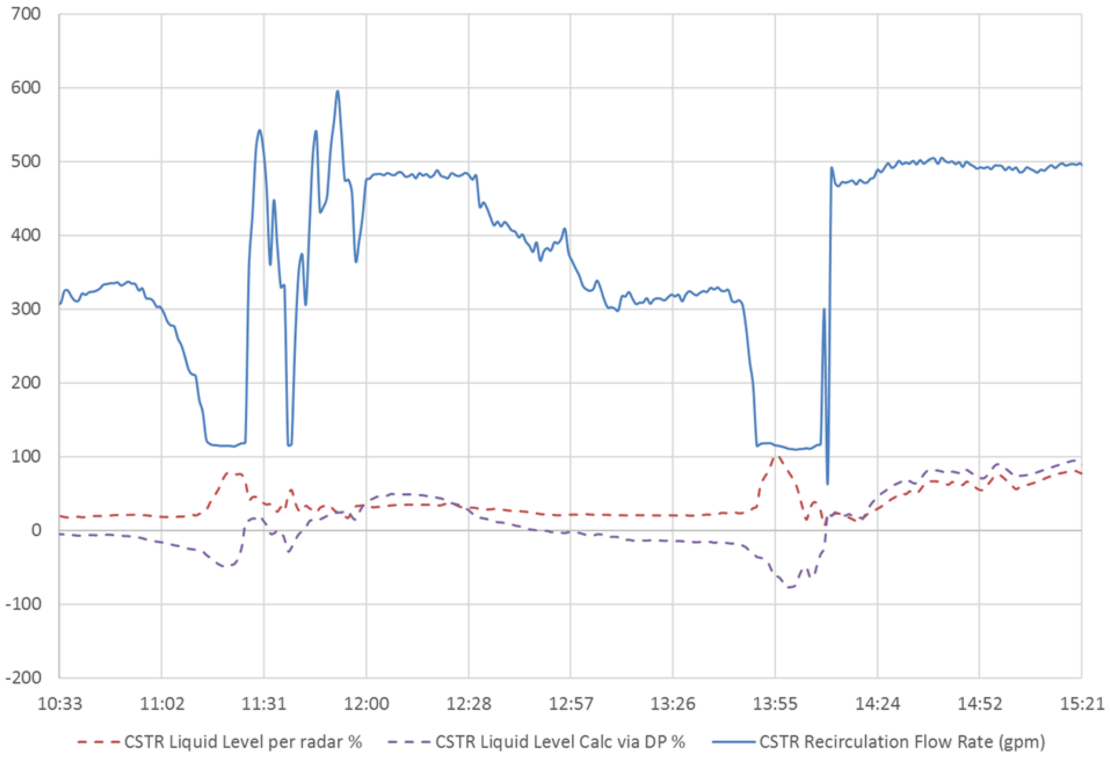

Figure 31. **CSTR Commissioning:** Solvent foaming at 11 wt.% H_2O

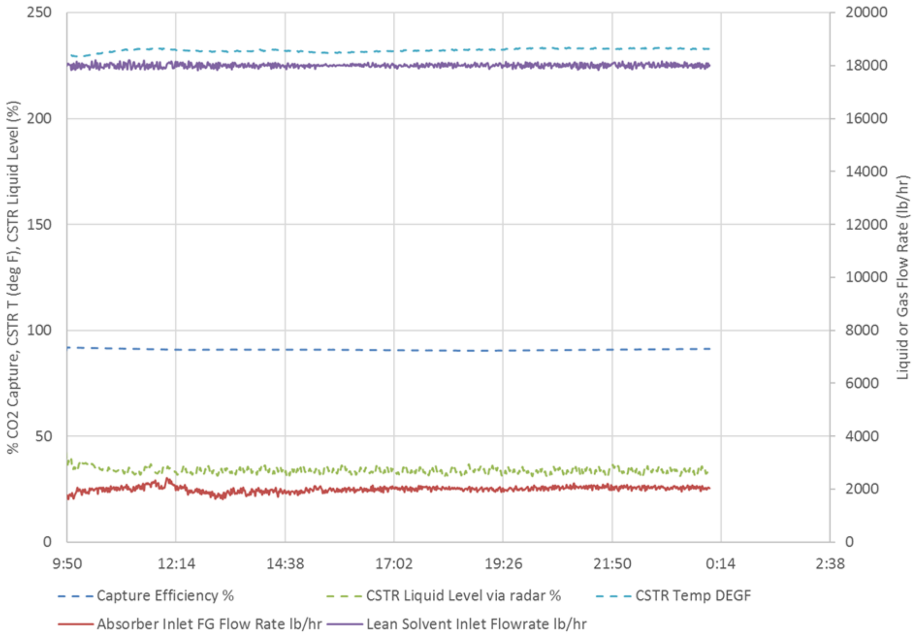

Figure 32. **CSTR Commissioning:** Stable operation at 2.4 wt.% H_2O and 0.2 MW_e

3.5. CSTR Campaign (Q4 2016)

Five-hundred hours of flue gas testing was performed in the NCCC PSTU with the CSTR while varying the stoichiometry (GAP : CO_2 = 2-4), and desorber temperature (230 F – 265 F). Operating conditions and desing Liquid level in CSTR was kept constant at 33%. Water level was maintained below 5 wt.% by manually transferring it from the mist separator tank (602) to the lean storage tank (401). Desorber pressure was varied between 7 to 10 Psig. Attempts to reduce desorber pressure below 7 Psig led to solvent carryover in the CSTR overhead. CO_2 capture efficiency has calculated based on gas phase CO_2 content of the clean flue gas stream. Solvent degradation was evaluated based on the % amine measured in the lean solvent (**Figure 33**).

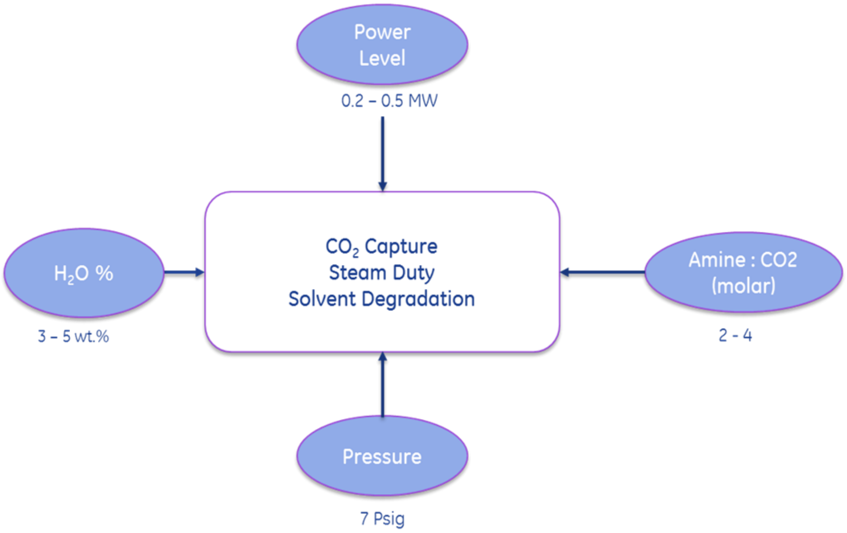

Figure 33. **CSTR Campaign:** Design of Experiments

Table 8: **CSTR Campaign:** Process Conditions

Condition	**1**	**2**	**3**	**4**	**5**	**6**	**7**
Power Level (MW_e)	0.2			0.35	0.5	0.5	0.5
Flue Gas (FG) (lb/hr)	2000	2000	2000	3750	5000	5000	5000
Liquid (lb/hr)	12000	12000	12000	18000	1800	18000	18000
$T_{desorber}$ (F)	233	233	233	248	248	255	265
$P_{desorber}$ (Psi)	7	7	7	7	7	7	7

<u>Water Management</u>: manual water addition from mist separator tank (602) to lean storage tank (401).

Table 9: **CSTR Campaign:** Flue gas conditions

	NO	**O_2**	**CO_2**	**NO_2**	**T**
	ppm	% vol.	% vol	ppm	F
Avg	34.2	6.6	12.6	0.55	134
Stdev.	8.1	0.8	0.5	0.21	2.9

Table 10: **CSTR Campaign:** Solvent Composition

Sample	Total Amine wt.%		CO_2 wt.%	TEG	Water
	wet	dry	wt.%	wt. %	wt.%
Initial	52.84	53.7	3.34	40.7	3.2
Condition 1	52.4	53.5	3.34	40.7	2.1
Condition 2	49.4	51.6	3.22	40.8	4.3
Condition 3	49.3	51.2	2.8	39.5	3.8
Condition 4	48.9	50.8	1.8	41.2	3.8
Condition 5	47.4	49.5	1.6	41.6	4.2
Condition 6	42.6	44.1	1.4	42.6	3.5
Condition 7	38.9	41.8	1.3	39.2	7.0

During the first week of the continuous CSTR campaign (Conditions 1-3, **Table 8** and **Table 9**), the system was operated at 0.2 MW_e, and a liquid flow rate that corresponded to a molar feed ratio of approximately 3.85 mol GAP-1_m/mol CO_2. CSTR temperature was held constant at 233 °F, and the lean solvent water content varied between 2 – 6 wt.%. During this period, CO_2 capture rates of 91-96% were observed. Higher CO_2 capture rates and lower absorber temperature correlated with increased solvent water content. Water concentration was maintaining by manually transferring the condensate accumulated in the total condenser (S-602) to the lean storage tank (401).

In the second week of the CSTR campaign, the gas flow rate was gradually increased to 5000 pph (0.5 MW_e), as shown in **Table 8** (Conditions 4-7). Attempts were made to increase the liquid flow rate to maintain constant molar GAP-1 : CO_2 ratio, but the PSTU rich solvent pump could not keep up with the higher liquid flow rate. Thus, the liquid flow rate was set to the maximum operable rate as limited by the rich solvent pump, which corresponded to a molar feed ratio of ~ 1.55 mol GAP-1_m/mol CO_2. CSTR temperature was increased from 233 ^oF to 265 ^oF.

During the third week of the continuous CSTR campaign, several attempts were made to operate the CSTR at lower pressure, to determine if higher desorption rates could be achieved at lower temperatures. However, operability of these test conditions proved to be problematic. Reducing CSTR pressure caused foaming of the liquid inventory in the CSTR. As this two-phase mixture entered the CSTR recirculation loop, pump PU40910 performance suffered, giving a lower output flow rate than expected. The flow meter read lower than anticipated, which tripped the interlocks that shut down the CSTR steam supply. As a result, steady-state operation could not be achieved at low CSTR pressure. These conditions were explored more during the SSC campaign.

3.5.1. CSTR Campaign: 0.5 MW$_e$ Demo

Performance of the CSTR with GAP-1$_m$/TEG solvent was demonstrated at 0.5 MW$_e$ for 48 hours (**Figure 34**). Process conditions are listed in **Table 8** (Condition 5). GAP-1$_m$: CO$_2$ molar ratio was maintained at 1.5. Desorption conditions were kept constant at 248 ^{o}F and 7 Psig, respectively. Solvent composition is listed in **Table 10** (Condition 5). CSTR liquid level was kept constant at 33 % with no indication of solvent carry-over in the CSTR headspace. Specific steam utilization was 1.1 (lb. CO$_2$: lb. steam). CO$_2$ capture efficiency reached only 65%.

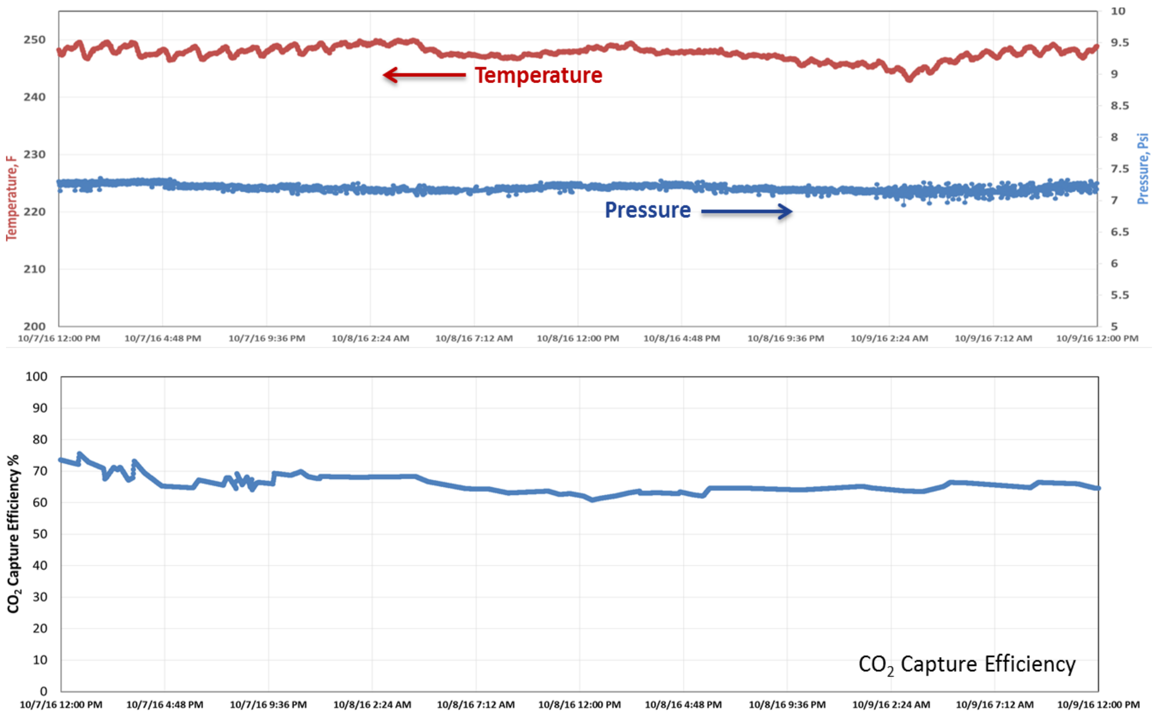

Figure 34. **CSTR Campaign:** 0.5 MW$_e$ Demo

Process conditions listed in **Table 8** (Condition 5)

3.5.2 CSTR Campaign: Effect of stoichiometry and desorption temperature

CO_2 capture efficiency was greatly affected by amine to CO_2 stoichiometry and desorption temperature as shown in **Figure 35**.

CO_2 capture efficiency exceeded 90% under a large excess of amine (GAP : CO_2 = 3.85, 0.2 MW_e), even though the desorption temperature was only 233 ^oF. It dropped to 87% at lower amine excess (GAP : CO_2 = 1.9) even after the desorption temperature increased to 248 ^oF. Increasing flue gas flow rate to 5000 pph while maintaining liquid flowrate at 18,000 pph decreased the amine to CO_2 stoichiometry to 1.55. This led to a CO_2 capture efficiency of 65%. Increase in desorption temperature to 265 ^oF at constant stoichiometry (GAP : CO_2 = 1.55) led to a marginal improvement in CO_2 capture efficiency of 71%.

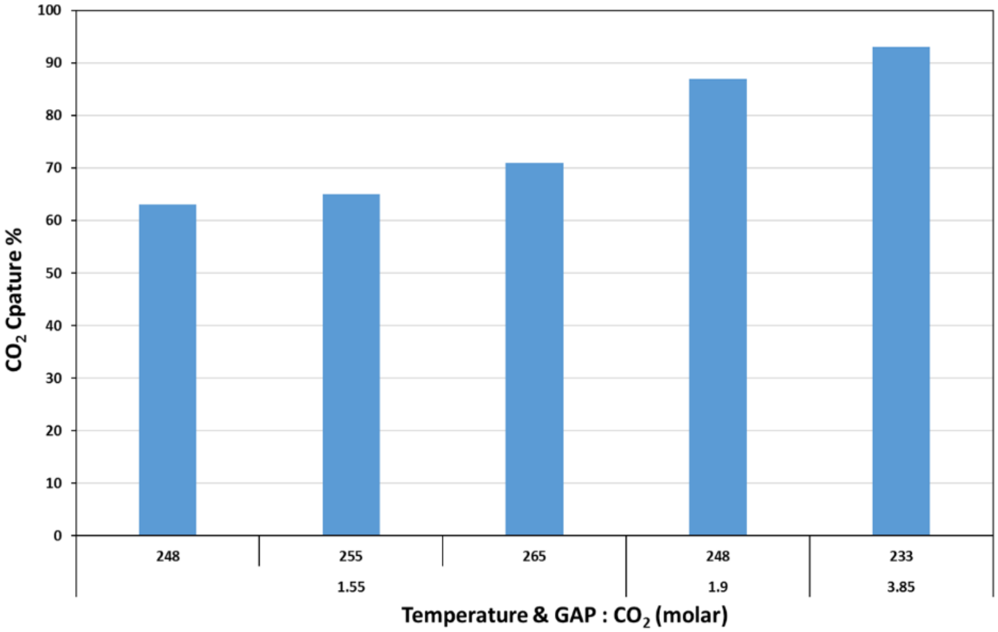

Figure 35. **CSTR Campaign:** CO_2 Capture Efficiency = f (T, GAP : CO_2 (molar))
Process conditions listed in **Table 8.**

Temperature increase and the maximum temperature in the absorber beds as a function of desorption temperature and amine to CO_2 stoichiometry are shown in **Figure 36**. For Conditions 1-3 (**Table 8**), lower desorption temperature (233 °F) and high excess of amine (GAP-1 : CO_2 = 3.85) led to overall lower absorber temperatures, and uniform absorption among the three absorber beds. Increasing desorber temperature from 233 °F to 248 °F and to 265 °F led to overall higher absorber temperatures (from 140 °F to 165 °F) and higher exotherms in the top bed, as the solvent entering the absorber top became leaner.

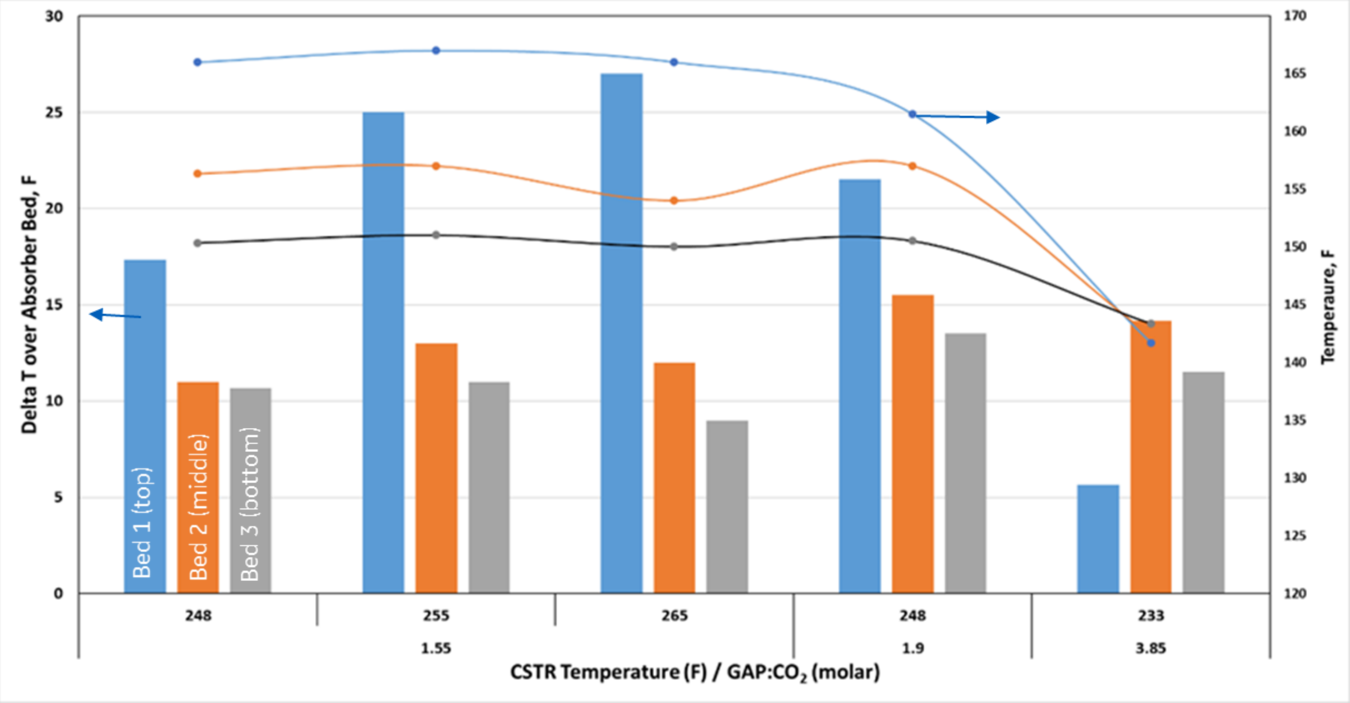

Figure 36. **CSTR Campaign:** Absorber operation = f (T, GAP : CO_2 (molar))

Process conditions listed in **Table 8.**

CO_2 loading in the lean and rich GAP-1_m/TEG working solution varied significantly as a function of desorption temperature and amine to CO_2 stoichiometry as shown in **Figure 37**. At low desorber temperature (233 °F) and high excess amine (Condition 1-3, **Table 8**), the active working capacity is very low due to an inefficient desorption process. Upon increasing the desorption temperature to 265 °F, the CO_2 content of the lean solvent dropped to 0.54 wt.% and active working capacity increased to 2.67%. However, this is only 30% of the theoretical working capacity of the solvent. As mentioned previously, we attributed this behavior due to insufficient cooling capacity of the lean cooler HX at 0.5 MW_e, and inability of the CSTR to be operated at higher water content and lower desorption pressure. These conditions were explored more during the SSC campaign.

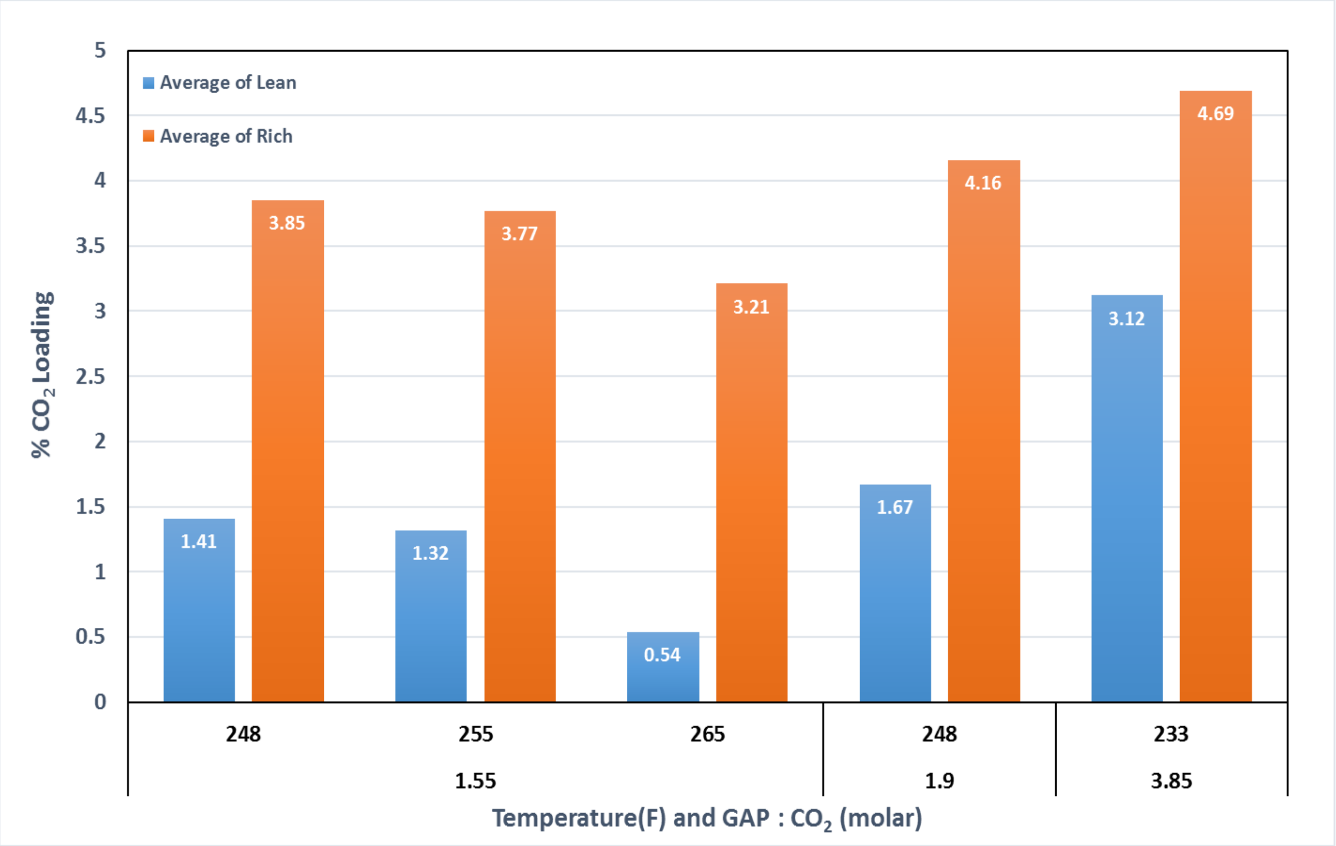

Figure 37. **CSTR Campaign:** Working Capacity = f (T, GAP : CO_2 (molar))
Process conditions listed in **Table 8.**

3.5.3. CSTR Campaign: Solvent Degradation

During the CSTR campaign, the solvent experienced desorption temperatures in the range of 233-262 °F, which caused thermal degradation to occur. The accumulation of degradation products in the solvent was monitored via the total amine content that was quantified in solvent samples taken throughout the test period and shown in **Figure 38**. The solvent lost approximately 15 wt. % amine capacity in the first two weeks of the CSTR campaign. The increased rate of degradation in the second week of the campaign is attributed to an increase in the CSTR operating temperature and reduced amount of water in the working solution. Before the third week of testing, some fresh GAP-1_m was loaded into the system to compensate for thermal degradation (not shown in **Figure *38***). Following this make-up, the solvent lost approximately 5.4 wt% amine capacity in the following week.

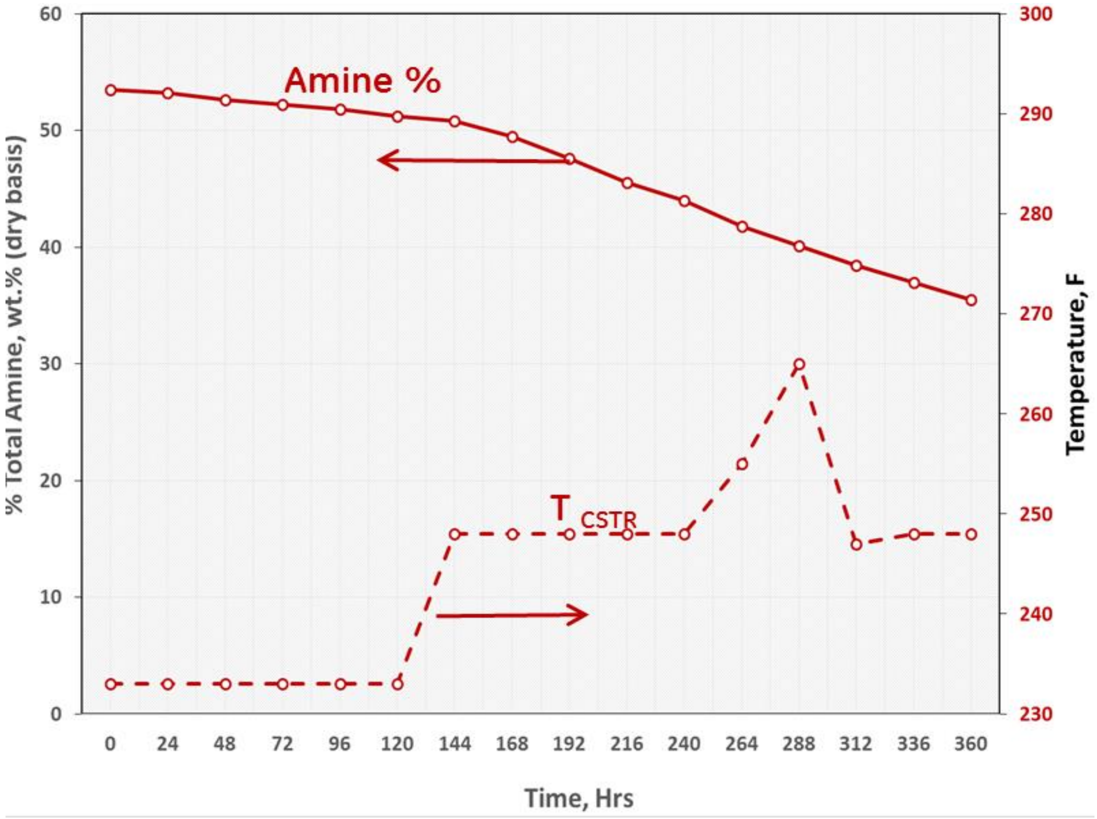

Figure 38. **CSTR Campaign:** Amine Degradation in Lean Solvent
Process conditions listed in **Table 8.**

At the end of the CSTR campaign, all samples collected at NCCC were shipped to GE for post-run analyses. These samples consisted of aminosilicone samples from the absorber as well as water samples from the 501 tank.

One of the analyses deemed critical to understanding the loss of amine, and therefore the carbon capture capacity of the solvent, was proton nuclear magnetic resonance (^{1}H NMR) spectroscopy. It was previously shown that exposure of the aminosilicone carbamate to an elevated thermal environment resulted in the formation of urea-containing by-products. These by-products could be readily seen by ^{1}H NMR. In addition, this technique was also useful in determining the relative GAP-1_m/TEG ratios, the β-isomer content and the GAP number.

Figure 39 shows the visual transition the solvent underwent with increased time spent in the system. It is obvious that the solvent mixture became quite dark over time which is expected, as amines readily discolor upon oxidation to highly colored species. However, these color bodies may only be present in very small quantities, so deep discoloration may not be indicative of poor performance.

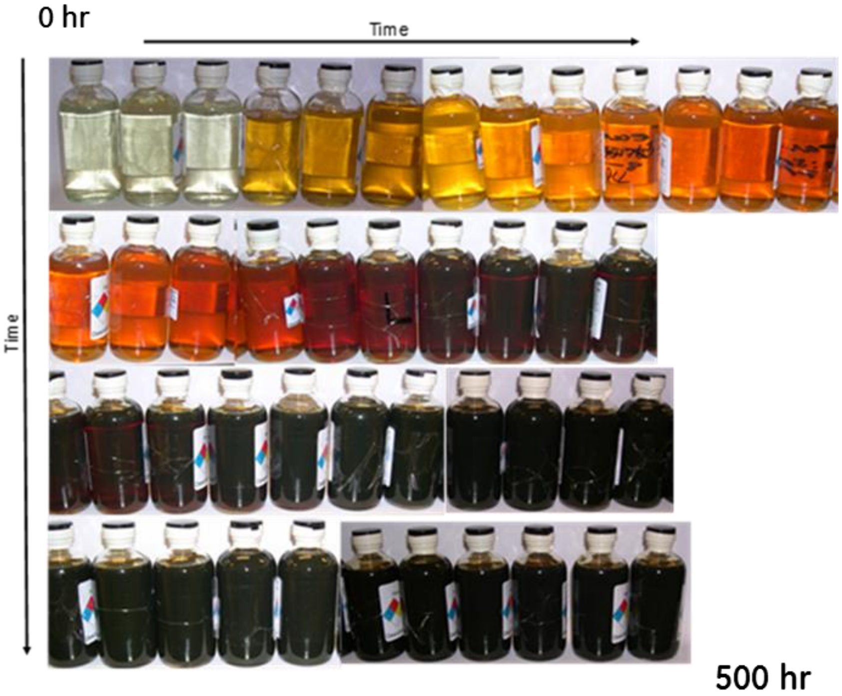

Figure 39. CSTR Campaign: Lean samples = f (time)

A variety of analyses were conducted to determine how the GAP-1_m/TEG solvent mixture performed and changed during the campaign. These tests included ^{1}H NMR and GC analyses, titrations, and CO_2 uptake experiments which provided information on the GAP # of the aminosilicone, the amine content of the system, mass balance of the components, and urea formation.

^1H NMR examination of the samples provided a wealth of information. First, the GAP-# was calculated based on the ratio of the methylene groups adjacent to the Si atom relative to the total number of methyl groups on silicon. The original aminosilicone solvent started with a GAP-# of 0.96 indicating that it was very close to the desired starting number of 1. **Figure 40** shows that this value steadily decreased with time. This was expected as a re-equilibration reaction can occur under basic conditions and with heat and water present. This re-equilibration reaction not only generates an aminosilicone with a smaller average GAP# but also results in the formation of cyclic silicones such as D_4 and D_5. Scheme 1 shows the process by which these materials are formed. There is a significant increase in the GAP-# at 366 hours, but this corresponded to fresh solvent (with a GAP-# of 0.96) being added to the system. The variation in values at 505 h is the result of samples taken when relatively fresh material from the SSC was added to the system.

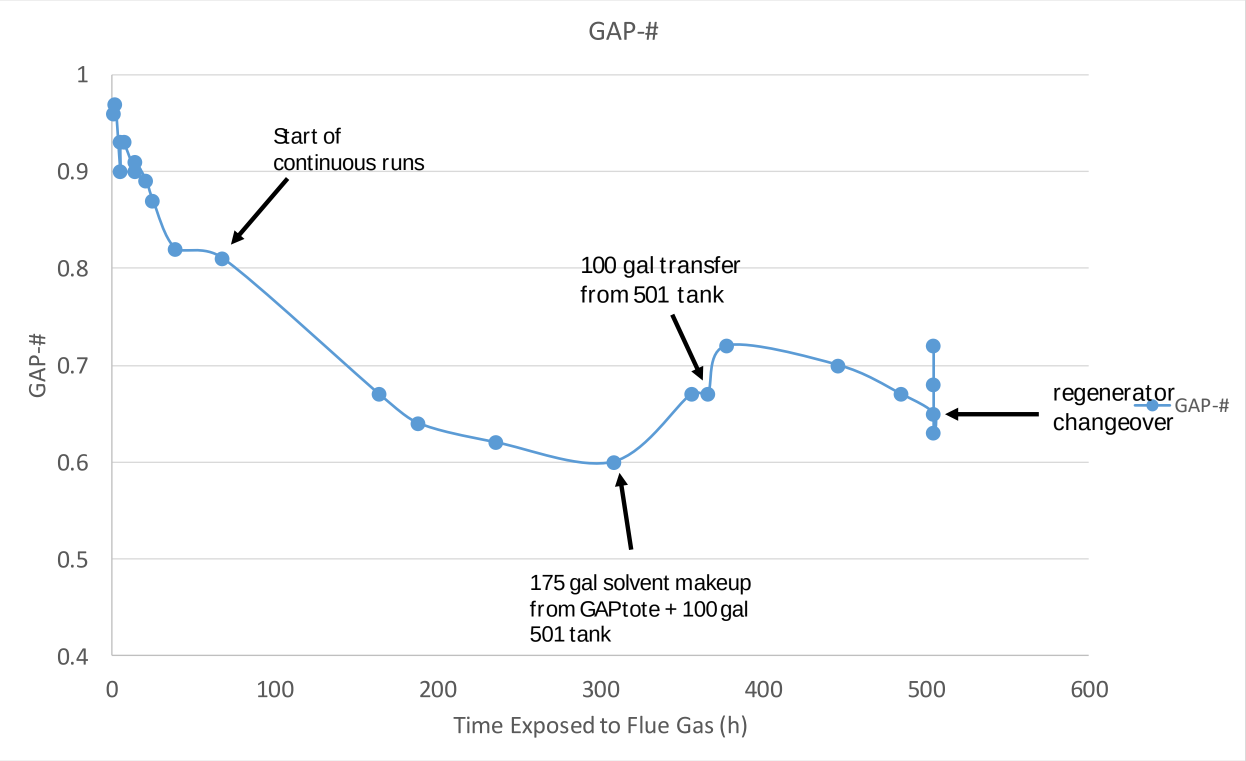

Figure 40. **CSTR Campaign:** GAP # = f (time)

Scheme 1. Re-equilibration of GAP-1

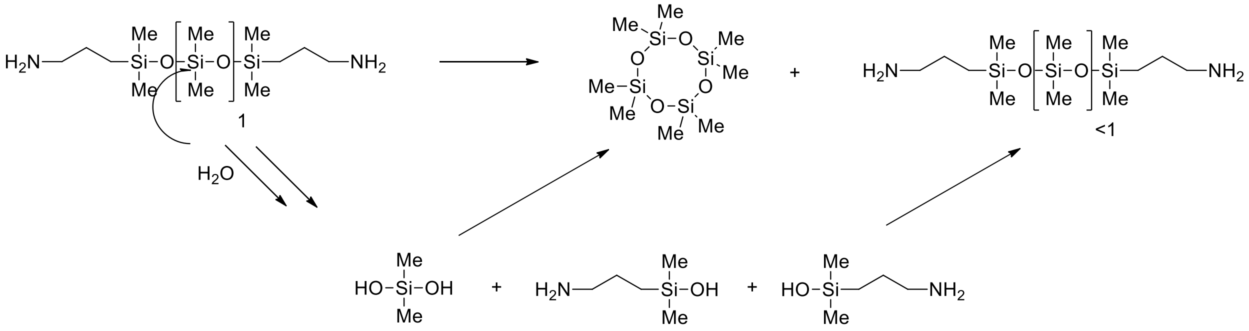

Amine and urea content could also be determined from NMR spectra. A series of aged samples are shown in **Figure 41**. The 1694 sample, with only 5 h exposure to flue gas showed very little urea present and the integration of the amine peak at 2.6 ppm indicated that 96% of the original amine was still present. As time progressed, more urea was formed. The peaks circled in red are confirmed urea peaks while those in green are likely other urea containing by-products. This conclusion is based on the peak shapes and chemical shift. More aged samples begin to show small amounts of other unidentified products, circled in blue.

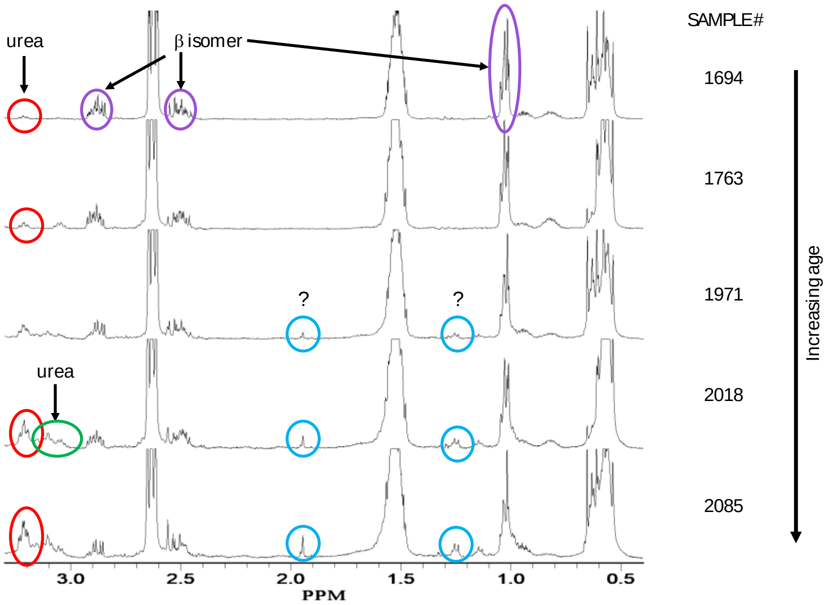

Figure 41. **CSTR Campaign:** ^{1}H NMR spectra of aged absorber samples

Figure 42 shows the increase in urea content of the solvent over time. The urea decomposition products may be formed via a variety of pathways as shown in Scheme 2. Whichever path is responsible; all indicate that high temperatures and low water levels intensify the problem.

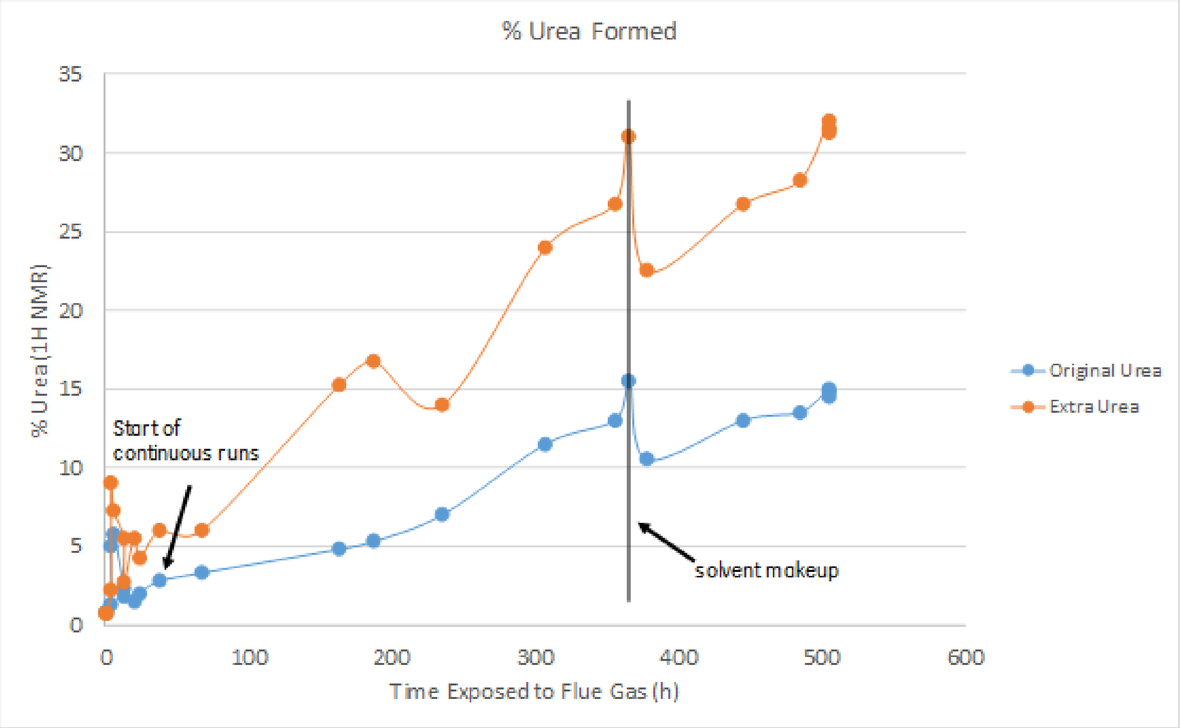

Figure 42. **CSTR Campaign:** Urea formation in absorber samples = f (time)

The blue line assumes only the urea that was circled in red in **Figure 41**. The orange line is likely the more accurate urea level that includes both the red and green circled peaks in **Figure 41**. The decrease in urea content at 366 h is again due to fresh solvent introduction into the system. The seemingly anomalous values in the orange curve at 164 and 188 h are unexplained at this point.

Scheme 2. Urea formation

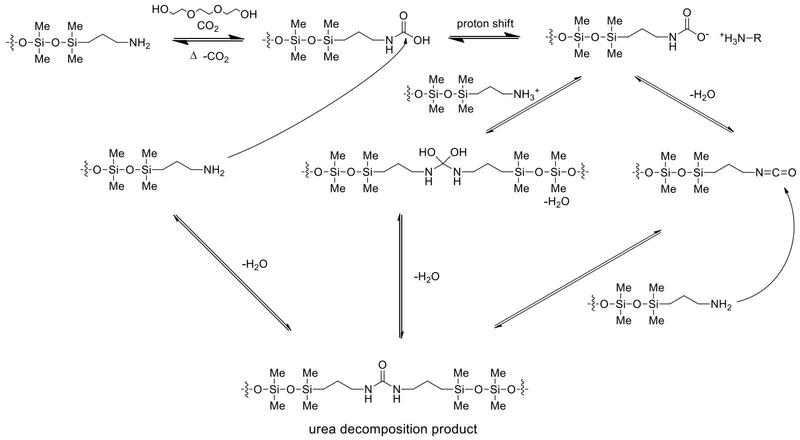

The active amine content of the solvent mixture is the most critical parameter to assay. This value dictates the efficiency of the solvent mixture. **Figure 43** shows several plots relating to both the amine content of the solvent mixture, as well as the component analysis or mass balance of the system. The orange curve represents the amine titration data obtained from NCCC. This is in weight percent of the total solvent mixture. In a perfect system of only GAP-1/TEG and no water, that value would start and remain at 60%. However, the initial loading of GAP-1/TEG started around 53.4%, which is reflected in the curve. As the campaign progressed, the amine content decreased, which was commensurate with the increase in urea content. The blue curve shows the amount of amine remaining that was calculated from the NMR spectra. These numbers are higher because they represent the total amount of amine in the solvent mixture as determined by relative ratios of alpha and gamma protons on the aminopropyl functional group in GAP-X. This value should start at 100% and comes close at >97% with the early samples. Integration uncertainties account for ~3%. This curve follows the same trajectory as the % Amine NCCC curve except for a "bump" at 236 hours. It is unclear why there is this discrepancy. In both curves, the sharp increase in amine content at 378 hours is due to replenishment of the solvent.

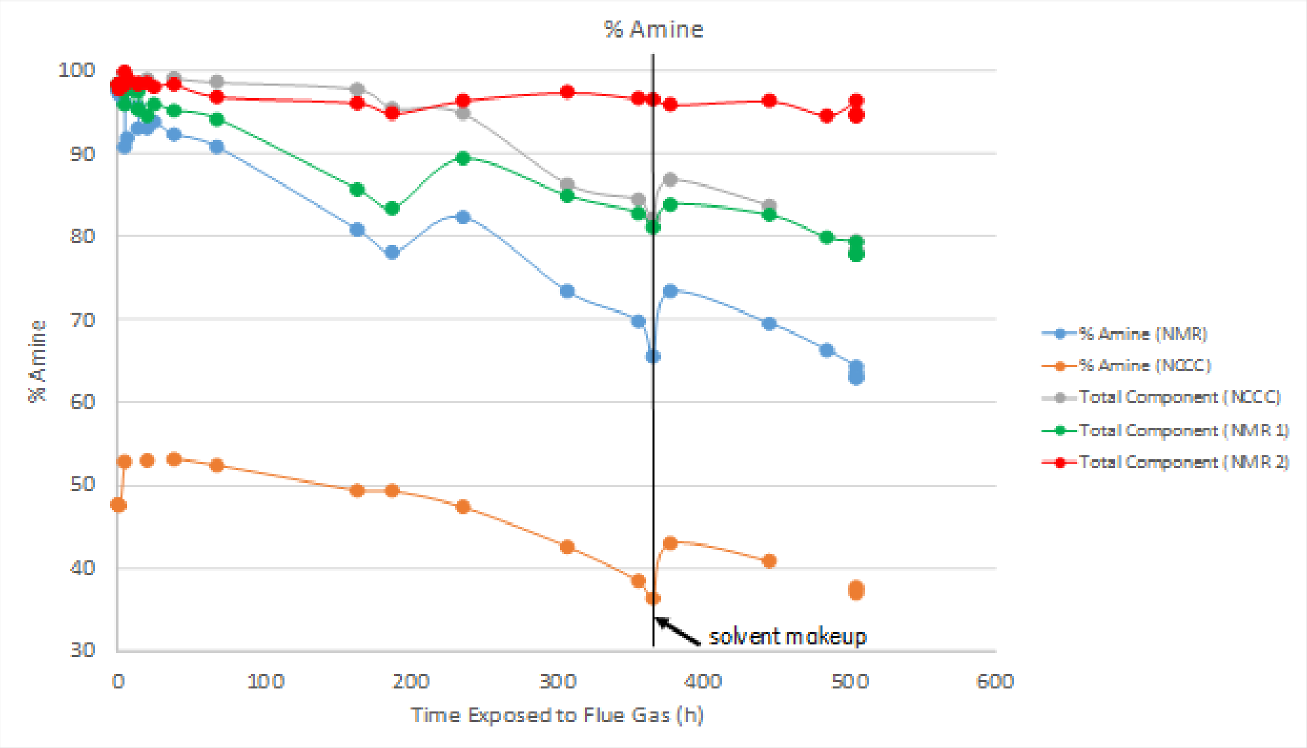

Figure 43. **CSTR Campaign:** Amine Content and Mass Balance = f (time)

The total component analysis provided by NCCC (gray curve), mirrored the % amine content closely. These data only accounted for the presence, or absence, of amine and did not consider any degradation products, such as urea. If only confirmed urea materials (red circled compounds in **Figure 41**) were added to the amine total, then the green curve in **Figure 43** was obtained. This shows comparable values to the gray curve at extended times, with only about 80% of the mass accounted for at the end of the campaign. However, if all the suspected urea derivatives were included in the mass balance calculation, then the red curve is obtained. This shows that about 95% of all the material is accounted for. This result also indicates that thermal degradation to urea-containing materials constitutes the major decomposition pathway. This does not rule out oxidative degradation, which is surely occurring, but it does imply that this is a less important reaction.

To identify and more fully characterize the decomposition products generated during operation, GC (gas chromatography) and LC/MS (liquid chromatography/mass spectrometry) were employed on the absorber samples. **Figure 44** shows the change in a series of GC chromatograms taken of aged absorber samples. Early samples showed the expected homologous series of GAP-X aminosilicones along with the β-isomer. As the campaign progressed, by-product peaks began appearing and the higher homologues of the GAP-X series began diminishing. The latter observation is consistent with re-equilibration occurring to give lower GAP-# materials and cyclic silicones. The by-product peaks may be indicative of the urea-containing decomposition products, but GC/MS was unable to unambiguously identify them.

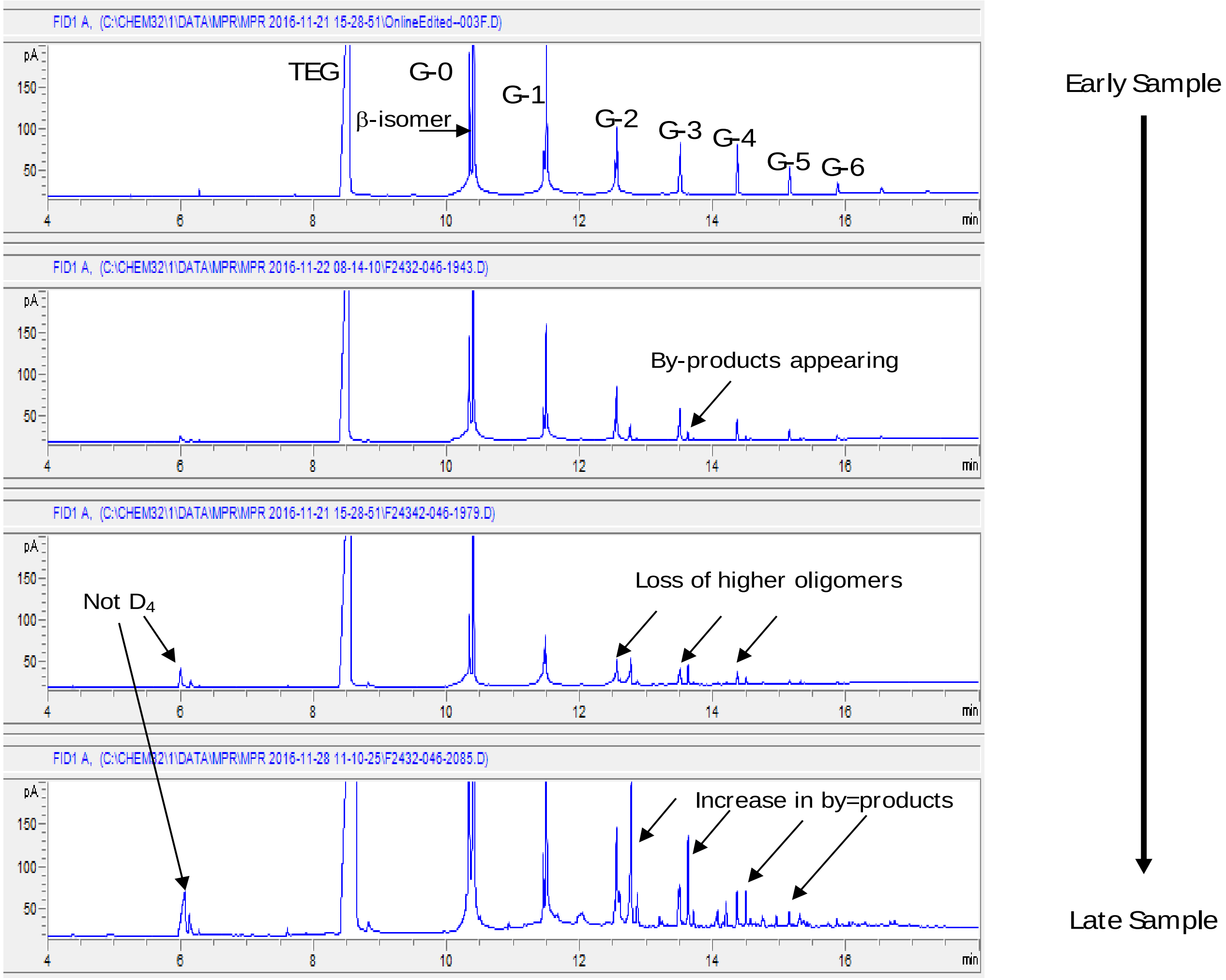

Figure 44. **CSTR Campaign:** GC chromatograms of aged absorber samples

As mentioned before, re-equilibration of the aminosilicones would generate cyclic silicones. It was clear from the decrease in the GAP-# that such cyclics had to be forming but their fate and location within the process were unknown. Several possible locations for these small molecules were possible. The first was to have them remain in the solvent mixture. This was ruled out because no evidence was seen in the GC traces above and, if these materials were resident in the absorber samples, the observed GAP-# would have remained constant as there is no way to distinguish Si-methyl protons apart in the ^{1}H NMR.

An alternate location for the cyclics was in the condenser water samples. Since the cyclics are more volatile than the linear aminosilicones (174 and 210 °C respectively for D_4 and D_5 versus

~285 °C for GAP-1), they might be expected to be carried out with the exhaust gas and trapped in the water wash and/or condensers. Samples from both the 501 and 602 tanks were examined by GC as shown in **Figure 45**.

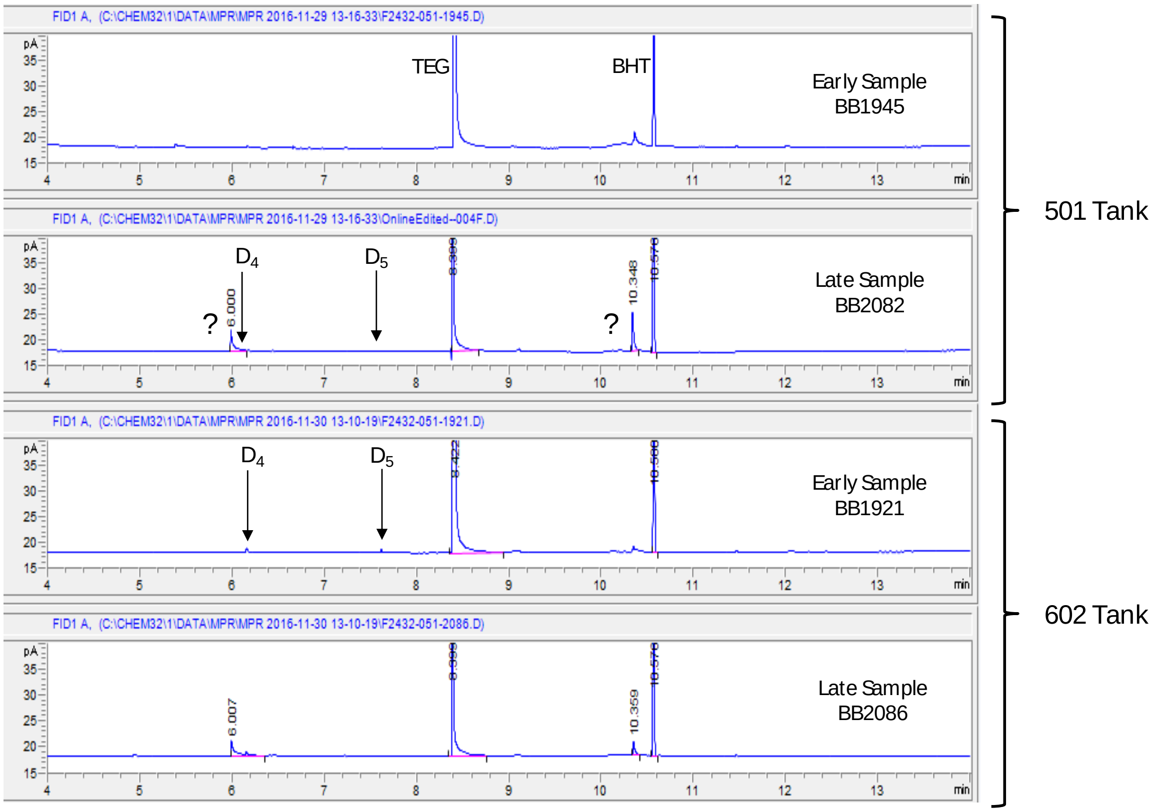

Figure 45. **CSTR Campaign:** GC chromatograms of water samples

It is evident that the major compound present in these samples is TEG. The BHT identified is from the antioxidant added to the THF solvent used to solubilize the water samples prior to injection. There are two unidentified peaks at 6.0 and 10.3 minutes, but they do not correspond to the D_4 and D_5 cyclics. The early sample from the 602 tank does show very small traces of these cyclic silicones, but not in sufficient quantity to account for the GAP-# dropping from 0.96 to 0.6.

The water samples taken by NCCC and tested for amine are shown in **Table 11**. NCCC reports amine content as weight % as GAP-1. GE values match closely with those from NCCC. However, from the GC data in **Figure 44**, no GAP materials were present. This implies that some basic component is present in the water samples. Earlier work has shown that ammonia is produced during thermal cycling of the solvent, which could be the basic constituent of the aged solvent. If dissolved ammonia is present, then the wt% as ammonia is approximately a factor of 10 lower than that for GAP-1.

Table 11. **CSTR Campaign:** Amine content in water samples

Sample	**Flue Gas Time (h)**	**Location**	**Wt% Amine** (as GAP-1, NCCC)	**Wt% Amine** (as GAP-1, GE)	**Wt% Amine** (as NH_3, (GE)
BB1945	164	501 Tank	1.97	-	-
BB2082	505	501 Tank	4.83	4.61	0.49
BB1921	60	602 Tank	7.16	6.75	0.71
BB2086	505	602 Tank	3.04	2.81	0.30

While not as large a contributor to the loss of activity as urea formation, oxidation of GAP-1 was occurring. The myriad of decomposition products formed at low levels precluded any identification by NMR and the silicon-containing materials did not provide useful data via GC/MS analysis.

3.5.4. Gas Analysis

Gas adsorption samples were collected during the CSTR campaign as following: (i) from the water wash gas exhaust, (ii) ELPI aerosol measurements, and (iii) CO_2 quality sample as summarized in **Table 12**.

Table 12. **CSTR Campaign:** Gas quality samples collected from outlet of water wash

Date	L (lb/hr)	G (lb/hr)	CSTR T (deg F)	Solvent H2O (%)	Gas Adsorption	ELPI / Aerosol	CO2 Quality
10/4/2016	18000	2000	230	4.2-8.9%	X		
10/10/2016	18500	5000	255	3.4-3.7%	X		
10/11/2016	18500	5000	262	3.5-7%			X
10/21/2016	18500	3750	248	target 5%	X	X	

Gas adsorption samples were collected according to the following procedure. The water wash vapor effluent was passed through a condensing system. The condensate was collected and the vapor slip from the condenser was captured on gas adsorption tubes. Details of the gas adsorption tubes are shown in **Table 13**. At each sampling interval, two tubes of each type were sampled, and all tubes were shipped to GE for analysis.

The results of gas adsorption analysis are shown in **Table 14**. Nitrosamines that are not listed were not detected above the limit of quantification of 0.011ug/tube in any samples. The analysis for ethylene glycol, D4, D5, and D6 are not quantitative. These species were detected in all samples.

Four replicates of aerosol particulate concentration and size measurements were sampled. The results are summarized in **Figure 46**. Most of the particles detected were smaller than 0.006 microns, and all particles were smaller than 0.087 microns in diameter. Direct composition measurement of the aerosol particles is not available from this method.

Table 13. **CSTR Campaign:** Adsorbent tubes for water wash vapor sampling

Adsorbent type	Tube size (mm)	Vendor	Analysis Company	Analytes of interest
226-10-06	6x70	SKC, Inc.	Analytics Corp.	Ammonia
226-30-18	6x70	SKC, Inc.	Analytics Corp.	Methyl amine, Ethyl amine
226-119	6x100	SKC, Inc.	Analytics Corp.	Formaldehyde, Acetaldehyde
226-01	6x70	SKC, Inc.	Analytics Corp.	Ketones (Acetone)

32010001	N/A	Ellutia, Inc.	RJ Lee	Nitrosodimethylamine, Nitrosodiethylamine, Nitromethylethylamine, Nitrosodi-n-propylamine
Carbotrap 300 (GE-supplied)	6x178	Gerstel	GE	Aminosilicone, Carbamate, TEG, D4, D5, D6, Ethylene oxide, Ethylene glycol, Dimethyl aminopropyl silanol

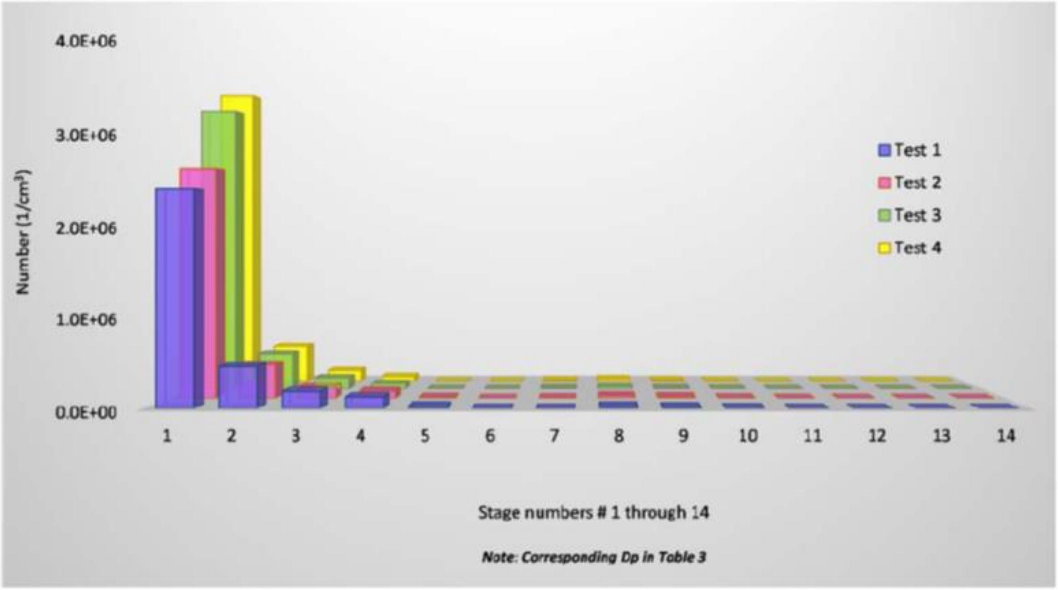

Figure 46. **CSTR Campaign:** ELPI aerosol particle count and size measurement

Table 14. **CSTR Campaign:** Gas adsorption analysis

Date	units	10/4/2016	10/10/2016	10/11/2016	10/21/2016
Formaldehyde	ppm	<0.0034	0.00543	N/A	0.00383
		<0.0034	0.00604	N/A	
Ammonia	ppm	437	38.1	N/A	42.1
		254	34	N/A	
Acetone	ppm	7.82	7.75	N/A	8.51
		9.42	8.33	N/A	
Ethylamine	ppm	<0.181	<0.181	N/A	<0.181
		<0.181	<0.181	N/A	<0.181
Methylamine	ppm	<0.262	<0.262	N/A	<0.262
		<0.262	<0.262	N/A	<0.262
N-nitrosodi-n-propylamine	ug/tube	0.059	<0.011	N/A	<0.011
		0.055	<0.011	N/A	
N-nitrosodimethylamine	ug/tube	<0.012	<0.012	N/A	0.018
		<0.012	<0.012	N/A	
Ethylene Glycol	Presence*	Present	Present	N/A	Present
		Present	Present	N/A	
D4	Presence*	Present	Present	N/A	Present
		Present	Present	N/A	
D5	Presence*	Present	Present	N/A	Present
		Present	Present	N/A	
D6	Presence*	Present	Present	N/A	Present
		Present	Present	N/A	

Finally, the CO_2 product stream was analyzed for one set of conditions during the CSTR campaign. A nonhazardous gas sampling kit supplied by Airborne Laboratories was used, and the samples were shipped to Airborne Labs for analysis. The results are listed in **Table 15** indicating that 99+% CO_2 product was achieved.

Table 15. CSTR Campaign: CO_2 quality samples

Desorber			**CSTR**
Test Date			**10/11/2016**
		LOQ	
CO2 purity	vol%	5	99.4+
H2	ppmv	10	ND
O2 + Ar	ppmv	10	98
N2	ppmv	10	3200
CO	ppmv	2	2.4
Ammonia	ppmv	0.5	1
NOx	ppmv	0.5	1.5
NO	ppmv	0.5	na
NO2	ppmv	0.5	na
Total HCs	ppmv as CH4	0.1	1700
Total non-methane HCs	ppmv as CH4	0.1	1700
Methane	ppmv	0.1	0.9
Acetaldehyde	ppmv	0.05	27
Aromatic HCs	ppb as C6H6	2	ND
Total Sulfur content	ppmv	0.05	trace
SO2	ppmv	0.05	ND
HCN	ppmv	0.2	ND
Ethane	ppmv	0.1	0.1
Propylene	ppmv	0.1	78
Hexanes +	ppmv	0.1	240
H2S	ppmv	0.01	trace
Propionaldehyde	ppmv	0.1	54
Acetone	ppmv	0.1	27
Methanol	ppmv	0.1	17
t-butanol	ppmv	0.1	ND
Ethanol	ppmv	0.1	0.1
Methyl Ethyl Ketone	ppmv	0.1	0.7
2-Butanol	ppmv	0.1	150
Isoamyl Acetate	ppmv	0.1	trace
Unknown VOX	ppmv	0.1	210

3.6. CSTR Campaign: Summary

(i) The CSTR desorber system was designed, fabricated and integrated with the pilot solvent test unit (PSTU), replacing the PSTU Steam Stripper Column at NCCC.

(ii) Solvent management and waste water special procedures were implemented to accommodate operation of the non-aqueous solvent in the PSTU.

(iii) Performance of the GAP-1_m/TEG solvent with the CSTR was demonstrated for over 500 hours while varying temperature of the desorption (230 – 265 ^oF), solvent circulation rate (GAP-1_m : CO_2 (molar) = 1.5 – 4), and flue gas flow rates (0.2 – 0.5 MW_e). Solvent carry-over in the CO_2 product was minimized by maintaining water content below 5 wt.%, and desorption pressure at 7 psig.

(iv) CO_2 capture efficiency was 95% at 0.25 MW_e (GAP-1_m : CO_2 = 4 (molar), 233 ^oF desorption), and 65% at 0.5 MW_e (GAP_m : CO_2 (molar) = 1.55, 248 ^oF).

(v) Solvent loss was dominated by thermal degradation of the rich solvent.

4. Steam Stripping Column (SSC) Campaign

4.1. Motivation

Initial design for the GAP-1_m/TEG process utilized a CSTR for CO_2 desorption based on the excellent thermal stability of the lean GAP-1_m/TEG solvent. However, later studies indicated that higher rate of thermal degradation of the CO_2 containing GAP-1_m/TEG occurred. In light of these discoveries, alternate designs for the regenerator in the aminosilicone based solvent process have been considered to reduce solvent loss due to thermal degradation.

The CSTR design has a number of advantages with respect to the aminosilicone-based solvent. Because the solvent is relatively non-volatile, the CSTR allows the CO_2 and any water to desorb in a single stage, with very little loss of solvent. The simplicity of this design decreases the required capital cost as the technology moves to commercial scales. It is also a design that allows for simple, robust process control. One area where the CSTR design is lacking, in comparison to more traditional distillation tower designs seen in aqueous solvent processes, is that there is no sweep gas. In the aqueous CO_2 capture process, water is vaporized in the reboiler of the distillation column, and this water vapor acts as a sweep gas, lowering the partial pressure of CO_2 in the gas phase, and therefore increasing the driving force for CO_2 desorption. By using a similar design with the aminosilicone-based solvent, a water vapor sweep gas could be used to increase the driving force for CO_2, resulting in a lean solvent with much lower concentrations of CO_2 than are possible with a CSTR. This, coupled with the data showing that water decreases the rate of thermal degradation, makes a distillation column-type regenerator using steam stripping a promising technology for the aminosilicone-based solvent process.

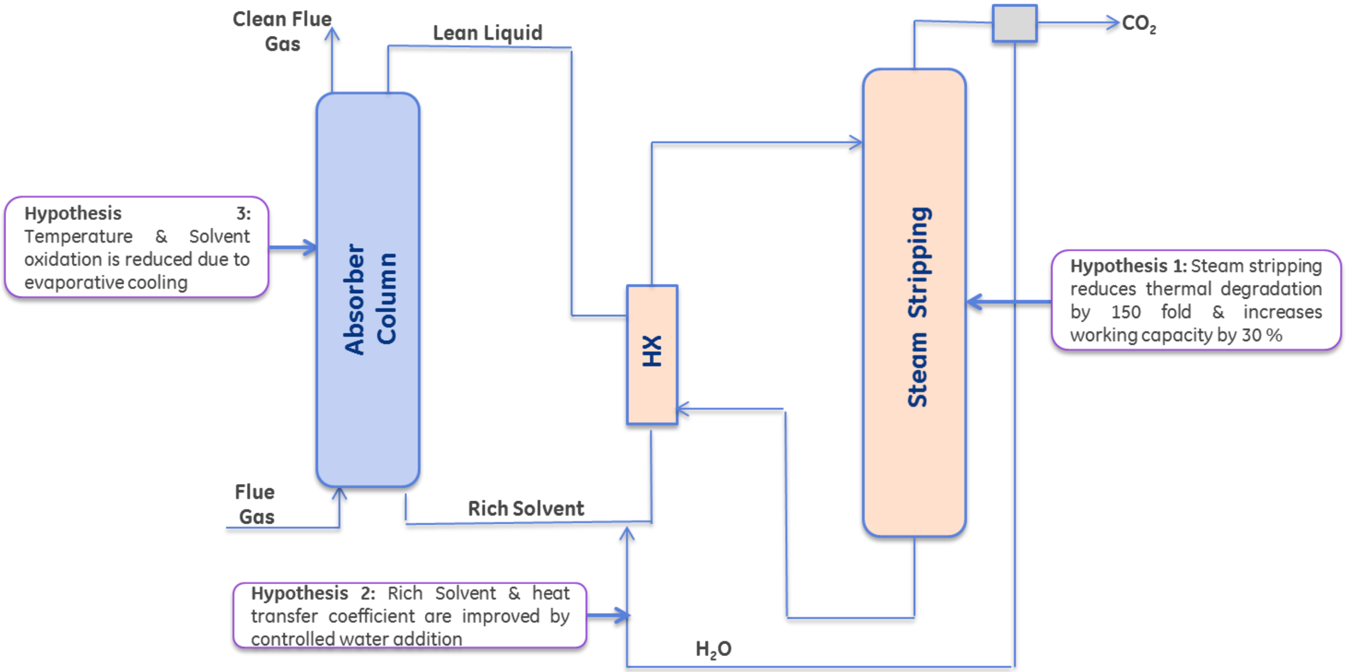

Figure 47. **Steam Stripping Process:** Solvent Management De-risk

Figure 47 describes the proposed steam stripping process. Controlled amounts of water (up to 20 wt.%) are added in the GAP-1_m/TEG working solution to induce steam stripping desorption, lower desorber temperature and hence reduce thermal degradation. Furthermore, controlled water addition is expected to improve heat and mass transfer process through reduction in solvent viscosity. Finally, temperature in the absorber will be lowered due to evaporative cooling, leading to decreased solvent oxidation rates.

Development of the steam stripping process was conducted in parallel to the CSTR campaign. The concept was first validated in a glass stripping column, followed by the demonstration in the bench-scale system (2 kW_e) at GE GRC with simulated exhaust. Finally, the process was scaled-up at 0.5 MW_e at NCCC, after the CSTR campaign was completed (**Figure 48**).

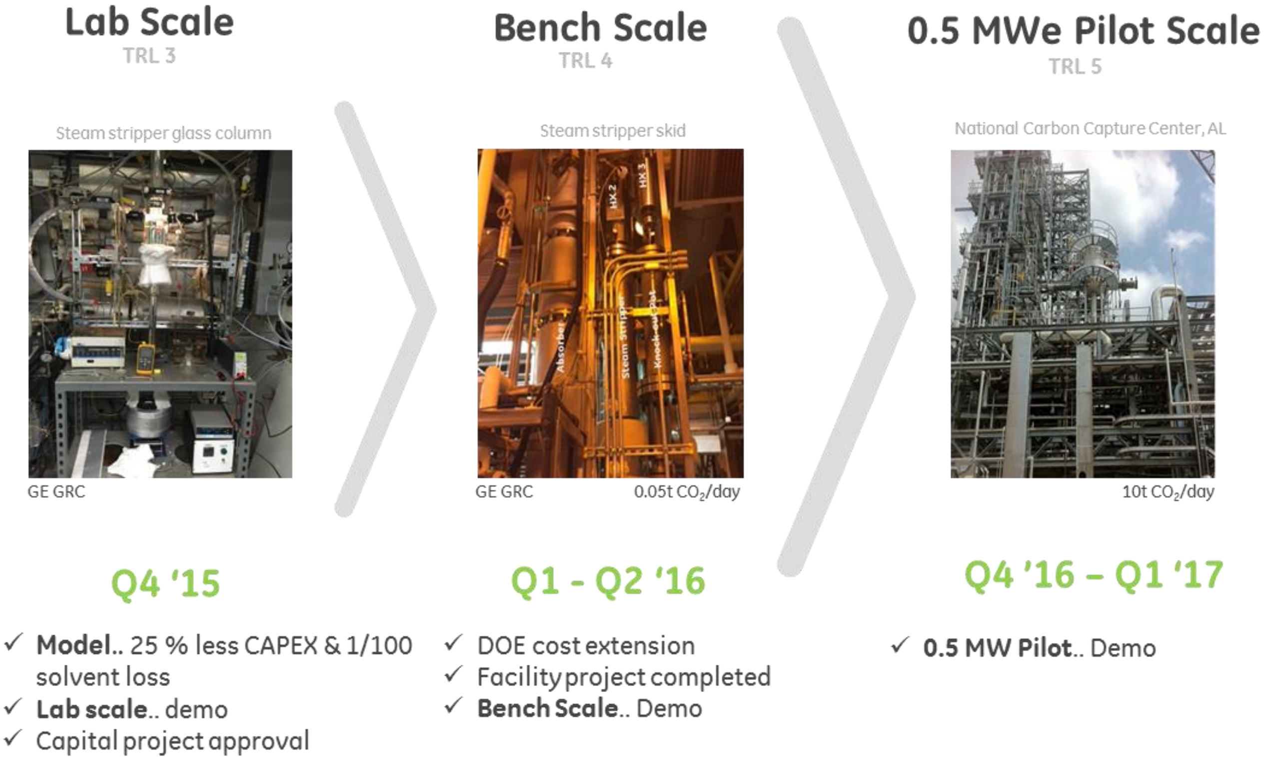

Lab Scale
TRL 3

Steam stripper glass column

GE GRC

Q4 '15

- ✓ **Model**.. 25 % less CAPEX & 1/100 solvent loss
- ✓ **Lab scale**.. demo
- ✓ Capital project approval

Bench Scale
TRL 4

Steam stripper skid

GE GRC 0.05t CO_2/day

Q1 - Q2 '16

- ✓ DOE cost extension
- ✓ Facility project completed
- ✓ **Bench Scale**.. Demo

0.5 MWe Pilot Scale
TRL 5

National Carbon Capture Center, AL

10t CO_2/day

Q4 '16 – Q1 '17

- ✓ **0.5 MW Pilot**.. Demo

Figure 48. **Steam Striper Process Development:** Timeline

4.2. SSC Campaign: Lab-scale demonstration (Q4 2015)

Experiments have been performed with a lab-scale stripping column to demonstrate the concept of steam stripping with the aminosilicone-based solvent. **Figure 49** shows a picture of the experimental set-up. In these experiments, CO_2-rich solvent containing 10 wt.% H_2O is fed into the top of the column. As the solvent flows down the column, it is heated by steam generated in the reboiler. The CO_2 that is liberated from the solvent flows up the column with the steam. The solvent, which becomes progressively leaner and hotter as it flows down the column, ultimately flows into the reboiler, where it is heated to vaporize the water in the solvent. Lean solvent is removed from the column directly above the reboiler for composition testing. A condenser is at the top of the column to remove water from the CO_2 product gas. The condensate generated is collected for analysis.

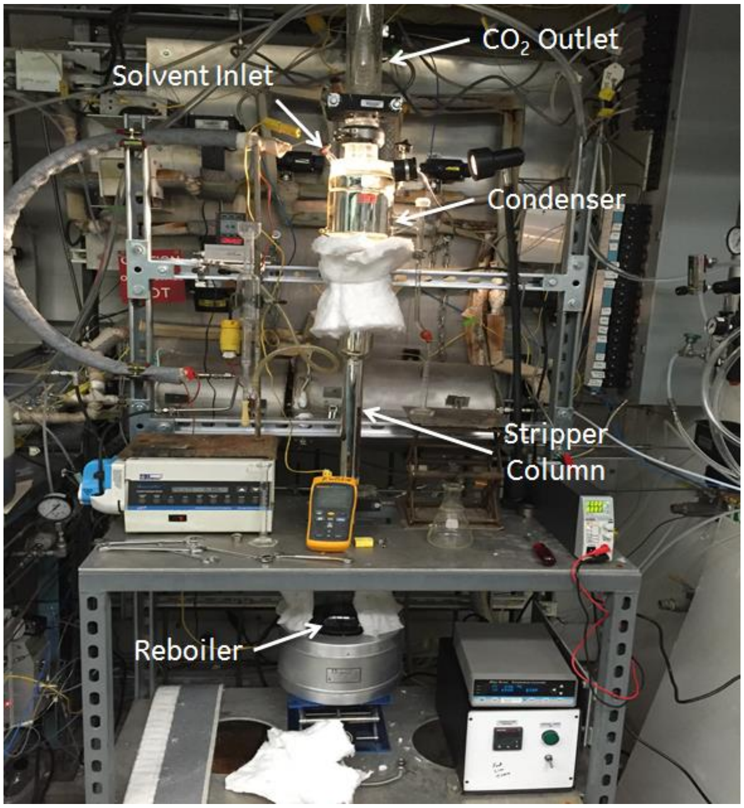

Figure 49. **Steam Stripping:** Lab-scale stripping column

Because the solvent becomes progressively leaner as it flows down to the hotter regions of the column, the stripper column design ensures that only the leanest solvent contacts the highest temperatures. This decreases the rate of thermal degradation. Additionally, because the driving force for CO_2 desorption is increased by the presence of the steam, a lower maximum temperature is possible while achieving efficient removal of CO_2. **Figure 50** shows results for reboiler temperatures of 110 and 120 °C. Even at a reboiler temperature of 110 °C, 89% of the CO_2 fed into the column with the rich solvent is desorbed. This is significantly higher than can be achieved at the same temperature with a CSTR.

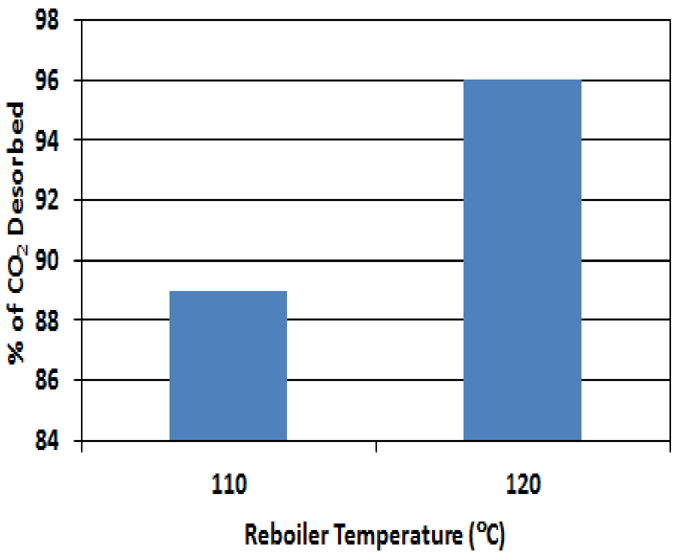

Figure 50. **Steam Stripping:** Lab scale demonstration

4.3. SSC Campaign: Bench scale demonstration (Q1-Q2 2016)

4.3.1. SSC Bench Scale: System Modification

CSTR bench-scale system (2 kW_e) at GE GRC was retrofitted with a steam stripping column (SSC). The conceptual design of the retrofitted system is shown in **Figure 51**. For the normal operation of the SSC, three-way valve **T_1** is switched such that the rich solvent stream exiting the absorber column is redirected through the rich heat exchanger (**HX 1**), and SSC. Rich solvent flowing downwards through the steam stripping column is contacted with the steam generated in the reboiler / CSTR. CO_2 generated from the desorption of the rich solvent is passed through the partial condenser (**HX 2)**, and total condenser (**HX 3)**. Lean solvent stream collected in the CSTR / reboiler is cooled in the lean heat exchanger (**HX 4**) before being sent to the top of the absorber column. The added functionality allows sequential testing of CSTR and SSC to evaluate both desorption processes under similar process conditions.

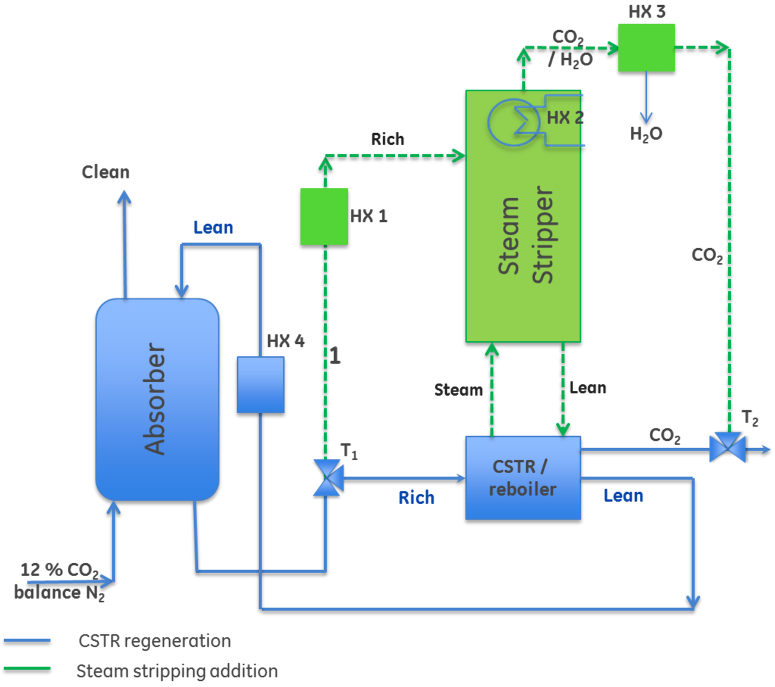

Figure 51. **Steam Stripping:** Bench Scale Conceptual Design

P&ID of the steam stripping column (SSC) is shown in **Figure 52**. Steam stripping column (6" (d) x 3' (H))) was manufactured by Atlantis Equipment Corporation, and was fitted with four thermocouples, and four sampling ports for monitoring temperature and concentration profiles within the column. Rich heat exchanger (**HX 1**), and the partial and total condensers (HX 2 and HX 3) were manufactured by YULA Corporation. All vessels were constructed of stainless steel, and rated for 300 Psi. Rich heat exchanger (**HX 1**) is heated with oil, while the **HX2** and **HX3** condensers are cooled with glycol solution. All process parameters (flow rates and temperatures, liquid level in the column / knock-out pot) are monitored and/or controlled by Cimplicity software. **Figure 53** shows the physical installation of the steam stripper, heat exchangers (HXs 2-3), reboiler vessel, and the 2" pipe connecting the bottom of the steam stripper column to the reboiler.

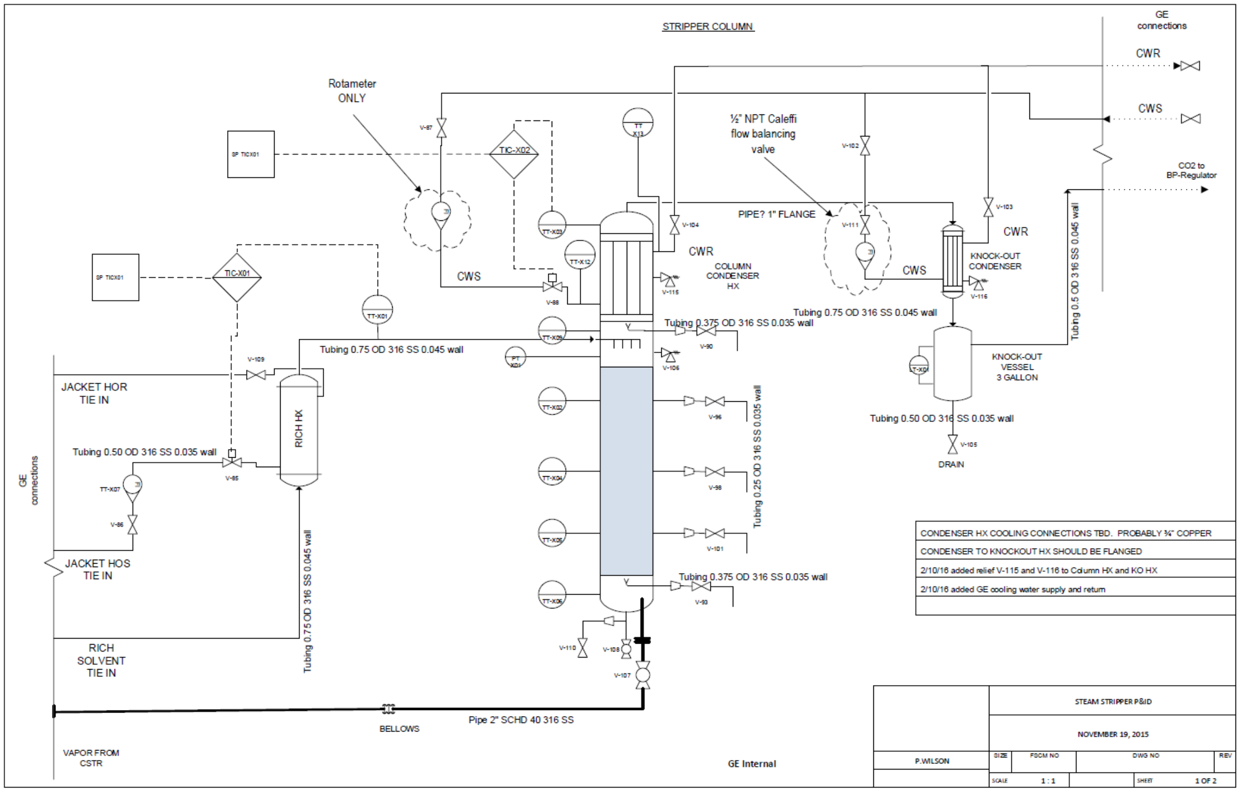

Figure 52. **Steam Stripping:** P&ID

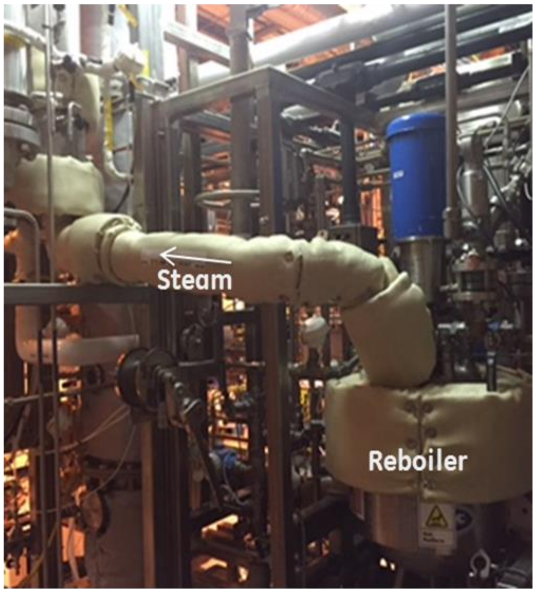

Figure 53. Steam Stripping: Bench-scale system (2kW$_e$) installed at GE GRC

4.3.2 SSC Bench Scale: Experimental Design

An experimental design was performed to evaluate the performance of the two desorption systems (i.e. CSTR and SSC) at 2KW$_e$ as a function of: (i) water content in the working solution, and (ii) GAP-1$_m$: CO_2 molar ratio. Maximum desorption temperature was kept at 108 °C (226 °F), and desorption pressure was kept at less than 1 PSIG. Performance of the GAP-1$_m$/TEG solvent was evaluated based on four criteria: % CO_2 capture, % SSC efficiency, hydrothermal stability and thermo-oxidative stability.

CO_2 capture was calculated based on the % carbamate measured by FTIR in the liquid samples collected at the bottom of the absorber and lean storage, respectively. Steam stripper efficiency was calculated based on the change in % carbamate in the liquid samples collected at the top and bottom of the column. Hydrothermal stability of the solvent was evaluated by quantifying degradation products via ^{1}H NMR and ^{29}Si NMR. Thermo-oxidation was evaluated by measuring % NH_3 in the clean stream simulated flue gas at the top of the absorber via gas FTIR. **Figure 54** highlights the main elements of the experimental design.

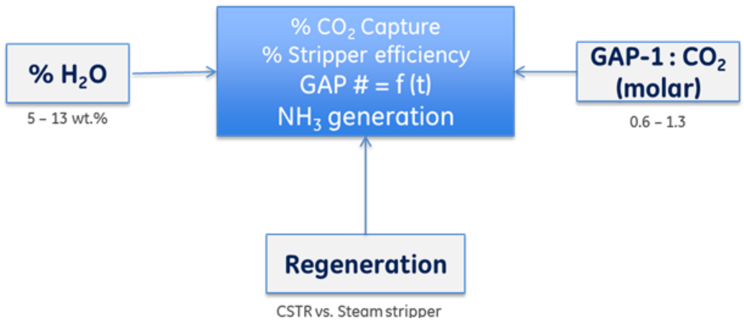

Figure 54. **Steam Stripping:** Experimental design
Effect of water, stoichiometry, and type of regeneration
Max T $_{desorption}$ = 108 ^{o}C (226 ^{o}F), P $_{desorption}$ < 1 Psig

% CO_2 Capture = f (H_2O%, and CSTR/SSC)

Performance of the 60 wt.% - 40 wt.% GAP-1$_m$ - TEG was first evaluated as function of the desorber system (CSTR vs. steam stripper) while varying water content between 6 and 13 wt. %. A detailed description of the experiments is provided below. Performance of the system is compared in **Table 16**, **Figure 56** and **Figure 57**.

Desorption with CSTR: Experimental Procedure

Simulated exhaust gas (200 SLPM; 12 % CO_2, 5 % O_2, 1 ppm SO_2, balance N_2; 40 ^{o}C) was fed at the bottom of the absorber column. GAP-1$_m$ /TEG (0.8 L / min, 40 ^{o}C) was fed at the top of the absorber column. This corresponds to a molar ratio GAP-1 : CO_2 = 1.3 : 1. Rich solvent, collected at the bottom of the absorber, was sent to the CSTR desorber. The temperature of the desorber was set at 108 ^{o}C, and the desorber pressure was 1 PSIG.

Desorption with SSC: Experimental Procedure

Simulated exhaust gas (200 SLPM; 12 % CO_2, 5 % O_2, 1 ppm SO_2, balance N_2; 40 ^{o}C) was fed at the bottom of the absorber column. GAP-1$_m$ /TEG (0.8 L / min, 40 ^{o}C) was fed at the top of the absorber column. This corresponded to a molar ratio GAP-1 : CO_2 = 1.3 : 1. Rich solvent, collected at the bottom of the absorber, was sent to the steam stripper regenerator. The setpoint temperature of the solvent leaving the rich heat exchanger was set at 95 °C; and the temperature of the reboiler was set at 108 ^{o}C. The reboiler pressure was 1 PSIG.

Performance of SSC and CSTR with controlled water addition was compared vs. the baseline case (CSTR with 2 % wt. water) in **Table 16**. The increase in water content from 3 wt. % to 10 wt. % (**Table 16**, Experiment 1 to Experiment 2) lowers the desorption/regenerator temperature from 125 °C to 108 °C. The lower desorption temperature renders lower heat-induced degradation of the GAP-1$_m$ solvent. Moreover, the amount of absorption solvent required for a given amount of CO_2 capture can desirably be reduced by up to 30 %, as compared to baseline case, reducing the size of the CO_2 capture plant.

Table 16. SSC Bench-Scale Demo: SSC vs. CSTR Performance

Experiments	**1***	**2**	**3**	**4**	**5**
% H_2O	3	10		13	
Regenerator	CSTR	CSTR	SSC	CSTR	SSC
GAP-1_m : CO_2 (molar)	1.8	1.3	1.3	1.3	1.3
Desorption Temperature, ^{o}C					
Steam stripper range	NA	NA	100 – 104	NA	100 - 104
Regenerator	125	108	108	108	108
% GAP-1 reacted					
Absorber, bottom	64	95	85	86	81
Steam Stripper, bottom	NA	NA	52	NA	27
Lean Storage	16	33	21	22	13
CO_2 Capture %	74	74	79	75	83

Lean solvent composition (dry-basis): 60 wt. % GAP-1 (Sivance) / 40 wt. % TEG. *Gas absorber inlet conditions:* 12 % CO_2, 5 % O_2, 1 ppm SO_2, (balance N_2); 40 ^{o}C. *Desorber pressure:* 1 Psig.

Performance of the CSTR vs. SSC is compared in **Figure 55** at varying water content. Performance of the two desorber systems was similar for 6 wt. % water. Higher water content (10 - 13 wt. %), and desorption in the steam stripper rendered increased % CO_2 capture (from 74 % to 83%), lower temperature of desorption (from 125 ^{o}C to 100-108 ^{o}C), and an increased solvent working capacity (30 % increase).

To better understand this behavior, temperature profiles in the SSC, and % SSC efficiency = f (water content) are shown in **Figure 56** and **Figure 57**, respectively. For working solutions with lower water content, there is limited steam circulation in the SSC as indicated by temperatures lower than 100 ^oC for the entire height of the column (6 wt. % water). In this case, most of the desorption is happening in the CSTR/reboiler (SSC efficiency ~ 10%). As water content in the working solution is increased to 10 and 13 wt. %, respectively, more steam is generated, and the efficiency of the stripping column increases to 58 % (10 wt. % H_2O) and 78% (13 wt. % H_2O), respectively. As expected, temperatures in the stripping column exceed 100 ^oC for most of the column height at water content above 10 wt. %. Performance of the CSTR vs. SSC is compared in **Figure 58** at varying GAP-1_m : CO_2 (molar) and 13 % wt. H_2O. % CO_2 capture efficiency is increased with solvent flowrates.

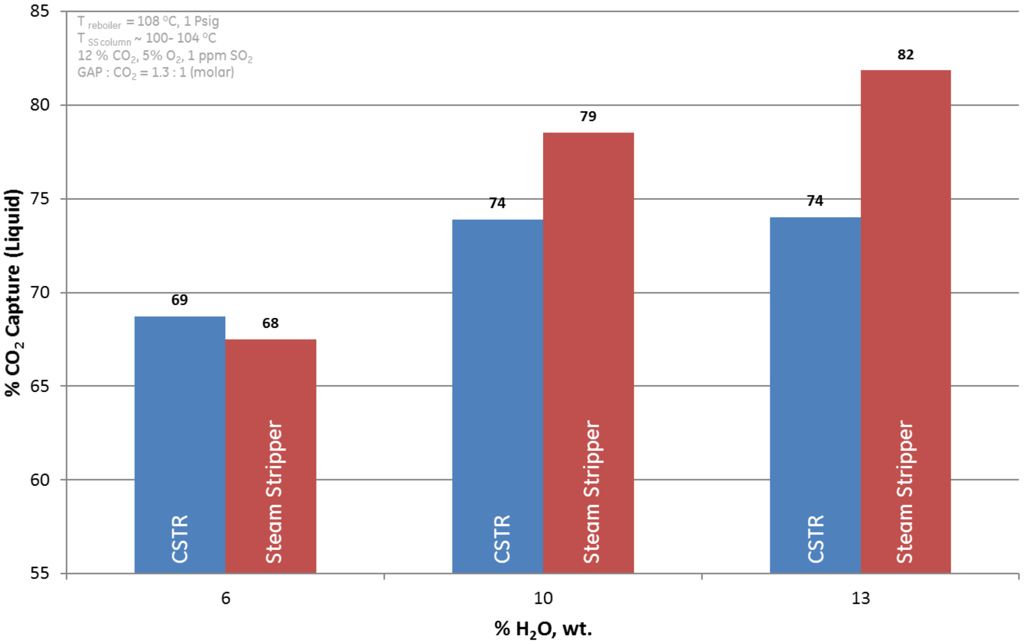

Figure 55. **SSC Bench Scale Demo:** % CO_2 Capture = f (H_2O%, desorption system)
Lean solvent composition (dry-basis): 60 wt. % GAP-1_m/ 40 wt. % TEG.
Gas absorber inlet conditions: 12 % CO_2, 5 % O_2, 1 ppm SO_2, (balance N_2); 40 ^oC. *Desorber pressure:* 1 Psig. T_{CSTR} = 108 ^oC, T_{SSC} = 100 – 104 ^oC. GAP -1_m : CO_2 (molar) = 1.3

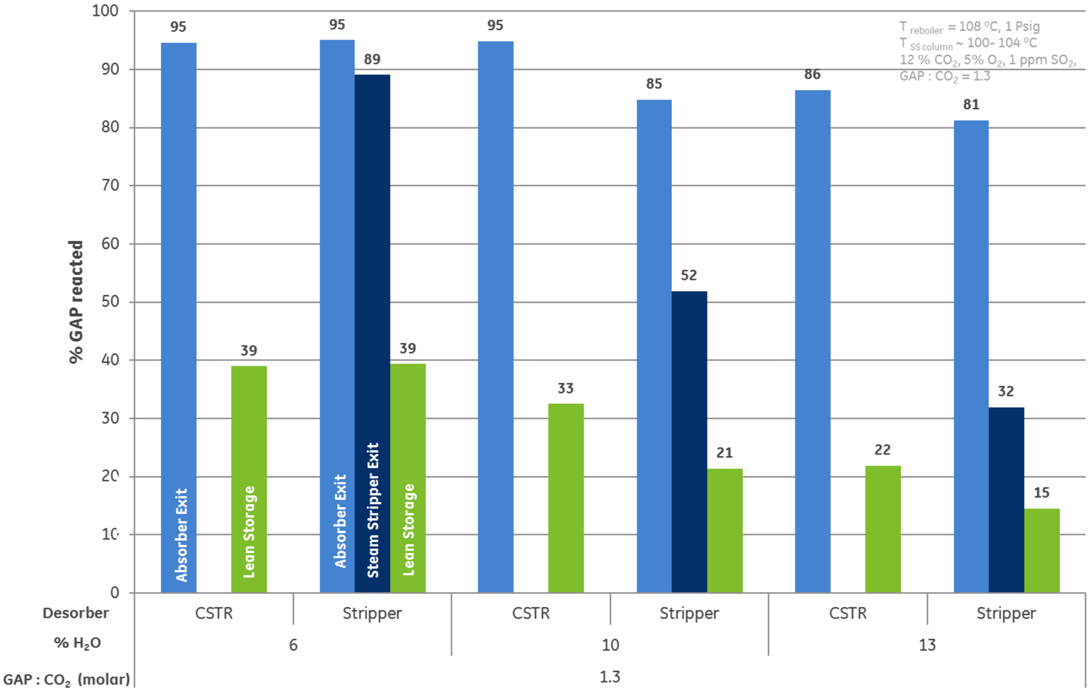

Figure 56. **SSC Bench Scale Demo:** % GAP carbamate (CSTR / SSC)
Conditions as in **Figure 55**

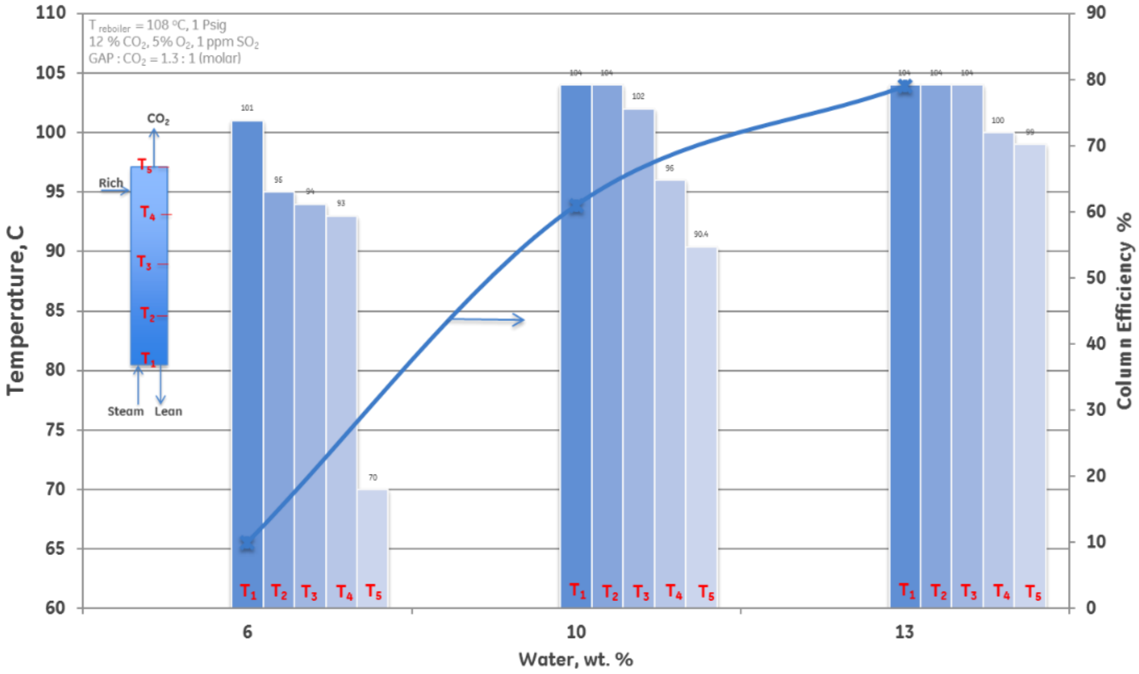

Figure 57. **SSC Bench Scale Demo:** SSC temperature profile

Conditions as in **Figure 55**

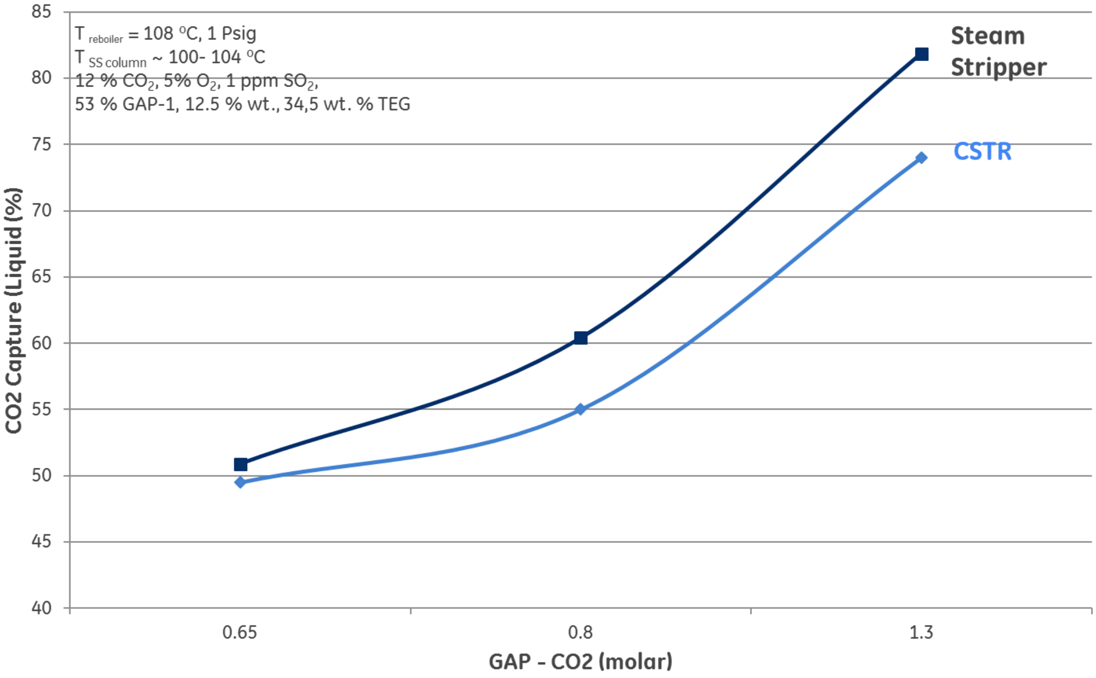

Figure 58. **SSC Bench Scale Demo:** CO_2 Capture Rate = f (GAP-1_m : CO_2 (molar))
Conditions as in **Figure 55**, 13 wt.% H_2O

4.3.3. SSC Bench-Scale: Hydrothermal stability

Hydrothermal stability of the aminosilicone solvent was evaluated by following the evolution of GAP-X numbers, during the bench-scale experiments. The overall hydrolytic reaction of GAP-X material is shown below:

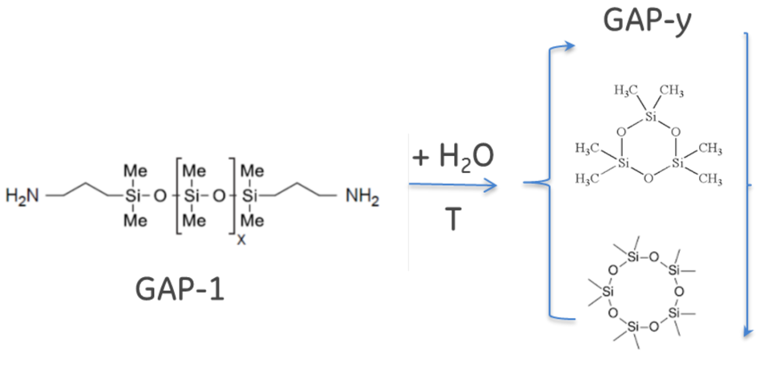

Liquid samples collected periodically from the lean storage tank during the entire period of the campaign were analyzed by ^{1}H NMR. **Figure 59** shows the evolution of GAP-X number as a function of heating time. GAP-x number decreased from 0.75 (fresh solvent) to 0.6 after 20 hours of heating at temperatures between 105-115 ^{o}C.

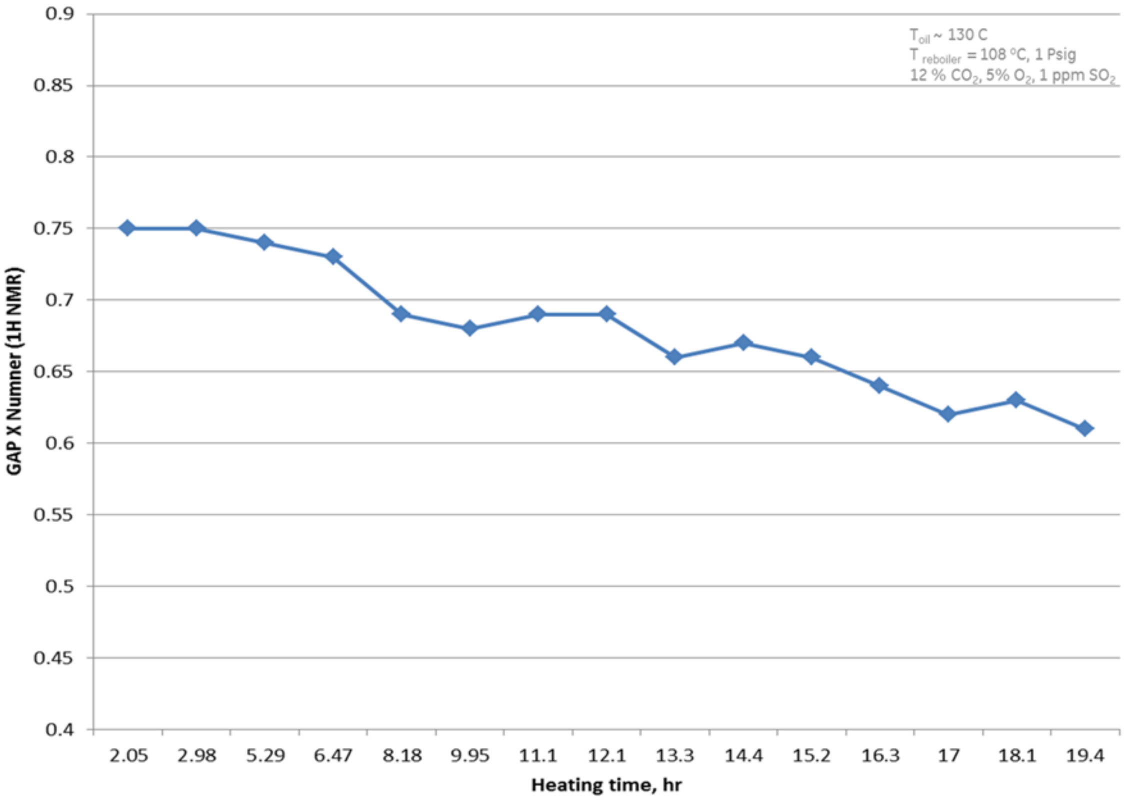

Figure 59. **SSC Bench-Scale Demo:** *GAP Number = f (heating time)*
Conditions as in **Figure 55**, 13 wt.% H_2O

Product distribution of the hydrothermal degradation of the GAP-1_m solvent was evaluated by collecting and analyzing liquid samples from different locations of the process, as shown in **Figure 60**. **Table 17** shows phase composition determined by ^{1}H NMR.

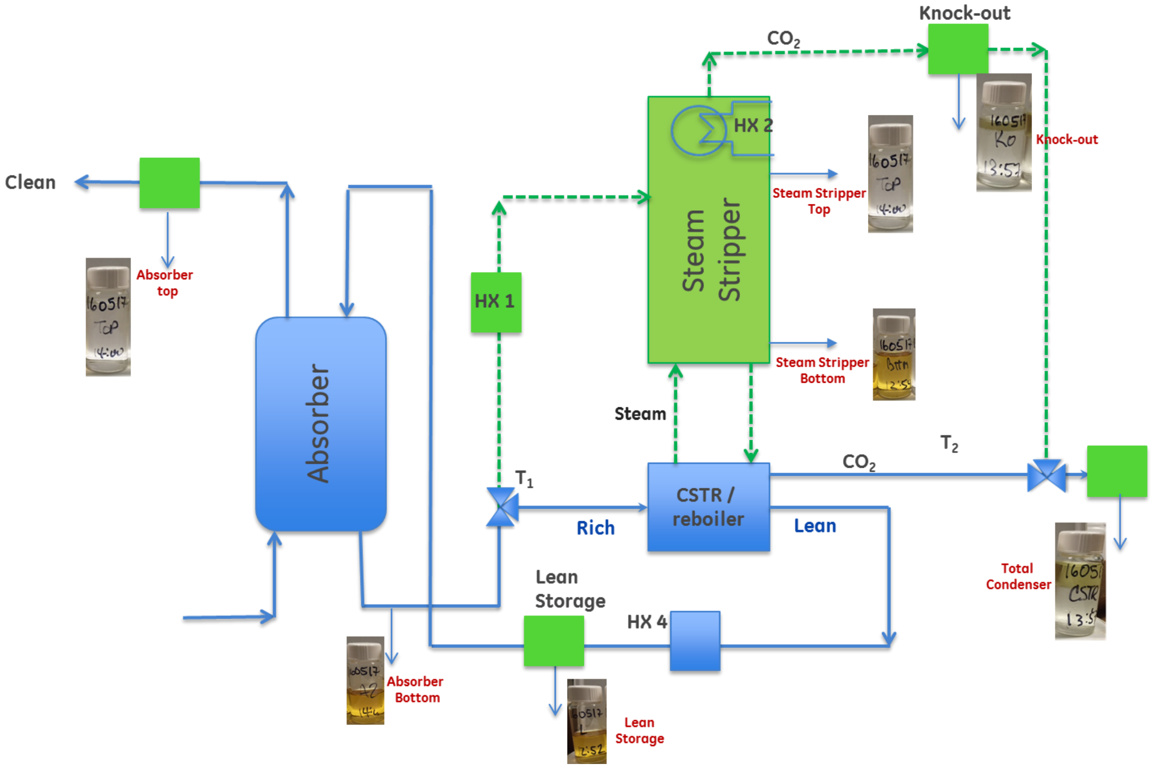

Figure 60. Hydrothermal stability: Sample collection

Table 17. **Hydrothermal Stability:** Product Composition (wt. %)

	Steam Stripper Top	Total Condenser (top layer)	Total Condenser (bottom layer)	Knock-out (bottom layer)	Knock-out (top layer)
Water	99.8	3.7	86	99.4	4
TEG	0.1	0.8	5.9	0.2	32.4
GAP-X	0.1	95.5	8.2	0.4	45.2

One phase, aqueous samples, were collected from the clean product stream (Absorber top sample), and the top of the steam stripper column (SSC top sample). These samples contain predominantly water (99+ wt.%) with traces of TEG and GAP-1_m degradation products (D_n, < 1 wt. %).

One phase, organic samples, were collected from the bottom of the steam stripper (SSC bottom sample), the bottom of the absorber (*Absorber bottom sample*), and the lean storage tank (Lean storage sample). These organic samples have the composition of the working solution (60 wt. % GAP-1_m, 40 wt. % TEG – dry basis). Two-phase, organic (top layer) – water (bottom layer), samples were collected from the knock-out condenser (*Knock-out sample*), and total condenser (Total Condenser sample).

4.3.4. SSC Bench-Scale: Summary

- An experimental design was performed in the bench-scale system ($2kW_e$) to evaluate the steam stripping desorption process vs CSTR while varying water content in the working solution, and amine to CO_2 stoichiometry. Temperature of the reboiler was kept constant at 108 ^oC and desorption pressure at 1 PSIG.

- Controlled water addition and SSC lowered desorption temperature by 20 ^oC and increased working capacity by 30 %.

- SSC efficiency was strongly correlated on the water content in the working solution. Most of the desorption occurred (> 75 %) in the SSC for water content > 10 wt. %. Performance of the SSC and CSTR were similar at low water content, as most of the desorption occurred in the reboiler.

- Hydrothermal stability: GAP number decreased from 0.75 to 0.6 in less than 20 hours of heating.

4.4. SSC 0.5 MW_e Pilot-Scale (Q4 2016 – Q1 2017)

Testing the aminosilicone solvent utilizing the steam stripper column (SSC) at NCCC was conducted with the overall objective of reducing the thermal degradation of the solvent through decreased desorber temperature, and controlled water addition. The campaign was conducted in three phases: commissioning (Phase 1 – Nov. 2016), parametric study and optimization (Phase 2 – Dec. 2016), and solvent degradation and water loading optimization (Phase 3 – Feb. 2017).

Commissioning of the steam stripper column was conducted by gradually increasing the amount of water in the solvent (from 5 wt.% to 15 wt.%) while decreasing desorber temperature (from 255 ^{o}F to 235 ^{o}F) and pressure (from 7 Psig to 2 Psig). **Figure 61** describes the overall experimental design implemented in phase 1.

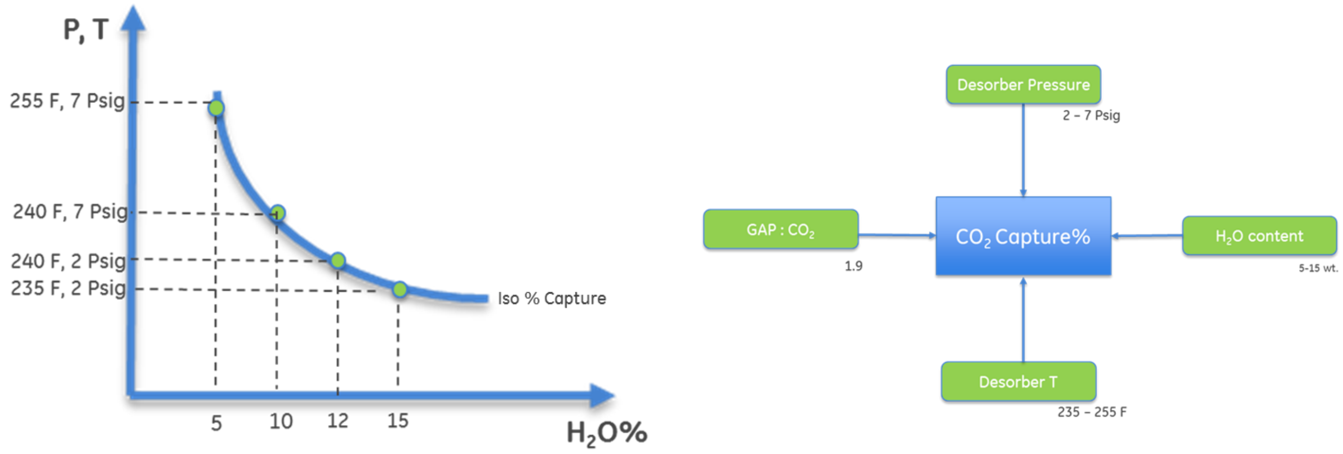

Figure 61. Steam Stripper Commissioning: Experimental Design

4.4.1. 0.5 MW_e SSC Phase 1: Commissioning (Nov. 2016)

Initial experiments were performed to evaluate performance of the regenerator column at increasing water content, while lowering desorber temperature and desorber pressure. The following sections describe the sequence of process conditions tested to evaluate the performance of the SSC with the non-aqueous aminosilicone solvent. **Table 18** summarizes the conditions utilized during the commissioning phase.

4.4.1.1 Experimental Conditions

Flue gas flowrate was maintained at 2,500 pph. Flue gas composition is listed in **Table 19**. The commissioning was conducted with the spent GAP-1_m/TEG solvent utilized in the CSTR campaign. Lean solvent working solution composition is listed in **Table 20**. Working solution flow rate was kept at 12,000 pph +/- 5%. GAP-1_m : CO_2 (molar) ratio was 1.8 +/- 10%. Amine content was 38 wt.% (dry basis).

Table 18. SSC commissioning: Process Conditions

Parameter	**1**	**2**	**3**	**4**
Flue Gas (FG) (lb/hr)	2500	2500	2500	2500
Liquid (lb/hr)	12000	12000	12000	12000
$T_{desorber}$ (°F)	255	240	240	235
$P_{desorber}$ (Psi)	7	7	2	2
H_2O (wt.%)	5	10	12.5	15
Water Management	Auto: 602 tank (1) to 401 tank (2)	*Manual*: 501 tank (3) to 401 tank Auto: 602 tank to 401 tank	*Manual*: 501 tank to 401 tank Auto: 602 tank to 401 tank	*Auto*: 501 tank to 401 tank Auto: 602 tank to 401 tank

(1)602 tank: mist separator tank; (2)401 tank: lean storage tank; (3)501 tank: water wash tank

Table 19. SSC commissioning: Flue Gas Composition

O2 (% vol, dry)		**CO2 (% vol, dry)**		**NO2 (ppm)**		**NO (ppm)**		**SO2 (ppm)**	
Average	Std. Dev	Average	Std. Dev	Average	Std. Dev	Average	Std. Dev	Average	Std. Dev
6.99	0.39	12.06	0.34	0.75	0.54	34.9	14.5	0.6	0.74

Table 20. **SSC commissioning:** Solvent composition

SAMPLE #	Description	Collection date	TOTAL AMINE wt. % (TITRATION)		TEG wt. % (GC)	WATER wt.%. (KARL FISHER)
			Wet basis	Dry basis		
BB02122	Absorber IN	11/2/16 17:00	35.4	39.3	33.3	10.1
BB02124	Absorber IN	11/3/16 8:30	34.3	38.3	33.5	10.5
BB02132	Absorber IN	11/4/16 8:45	33.6	38.4	33.3	12.5
BB02135	Absorber IN	11/4/16 14:50	32.3	38.3	32.8	15.6

Condition 1*: 5 % H_2O, 7 Psig and 255 ^oF Desorption*

The starting conditions were similar to the ones used in the CSTR campaign: 5 % H_2O, 255 ^oF desorber temperature, and 7 Psig desorber pressure. CO_2 capture efficiency, measured based on the gas phase analysis, was 80%. Temperature profile in the regenerator column is shown in **Figure 62**, indicating that only the bottom 10% of the regenerator column was under the steam conditions. Regenerator liquid level was constant at 60% indicating normal operation of the column with the non-aqueous aminosilicone solvent. Limited or no carry-over was recorded in the total condenser or 602 mist separator. Absorber temperature did not exceed 160 ^oF. Temperature increase in the three absorber beds was as following: 30 ^oF (top bed), 10 ^oF (second bed) and 7 ^oF (third bed) indicating that most of the absorption occurred in the first bed of the column.

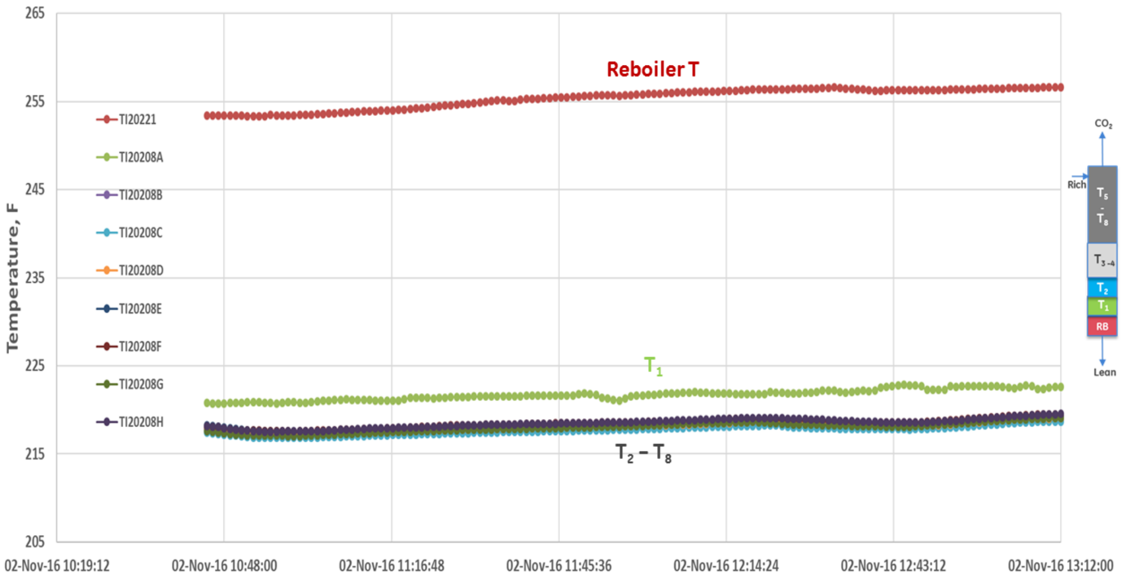

Figure 62. **SSC Commissioning:** Desorber T Profile for Condition 1
5 % H_2O, 7 Psig, 255 ^oF desorber temperature, FG = 2,500 lb/hr; Liquid = 12,000 lb/hr;

***Condition 2**: 10 wt. % H_2O, 7 Psig and 240 ^oF Desorption*

Water level in the working solution was increased from 5 wt. % (condition 1) to 10 wt.% by adding 90 gallons of water from 602 tank (mist separator) to lean storage tank (401). During the run, water was continuously transferred from 602 tank to 401 tank to keep the liquid level in lean storage tank, 401 at 30% fill. Desorber temperature was dropped to 240 ^oF. All the other process conditions were kept as for condition 1.

CO_2 capture efficiency, measured based on the gas phase analysis, was 77%. Only the bottom 15% of the regenerator column was under the steam conditions. Regenerator liquid level was constant at 60% indicating normal operation of the column with the aminosilicone solvent. Limited or no carry-over was recorded in the total condenser or 602 separator. Absorber temperature did not exceed 160 ^oF. Temperature increase in the three absorber beds was as following: 37 ^oF (top bed), 12 ^oF (second bed) and 9 ^oF (third bed). % CO_2 in the rich and lean working solutions were 3.2 wt. % and 0.98 wt.%, respectively.

***Condition 3**: 12.5 wt. % H_2O, 2 Psig and 240 ^oF Desorption*

Water level in the working solution was increased from 10 wt. % (condition 2) to 12.5 wt.% by adding 30 gallons of water from 501 tank (water wash tank) to the lean storage tank (401). During the run, water was continuously transferred from 602 tank to 401 tank to keep its liquid level at 30% fill. Desorber temperature was maintained at 240 ^oF. Desorber pressure was lowered to 2 Psig. All the other process conditions were kept the same as for condition 1.

CO_2 capture efficiency, measured based on the gas phase analysis, was 90%. Only the bottom 15% of the regenerator column was under the steam conditions. Increased water content and reduced desorber pressure rendered higher temperature in the bottom of the regenerator column due to higher steam circulation (**Figure 63**). Regenerator liquid level was constant at 60% indicating normal operation of the column. Limited or no carry-over was recorded in the total condenser or 602 separator. Max absorber temperature was 162 ^oF (top bed). Temperature increase in the three absorber beds was as following: 42 °F (top bed), 19 °F (2nd bed) and 9 °F (3rd bed). % CO_2 in the rich and lean working solutions were 3.2 wt. % and 0.45 wt.%, respectively.

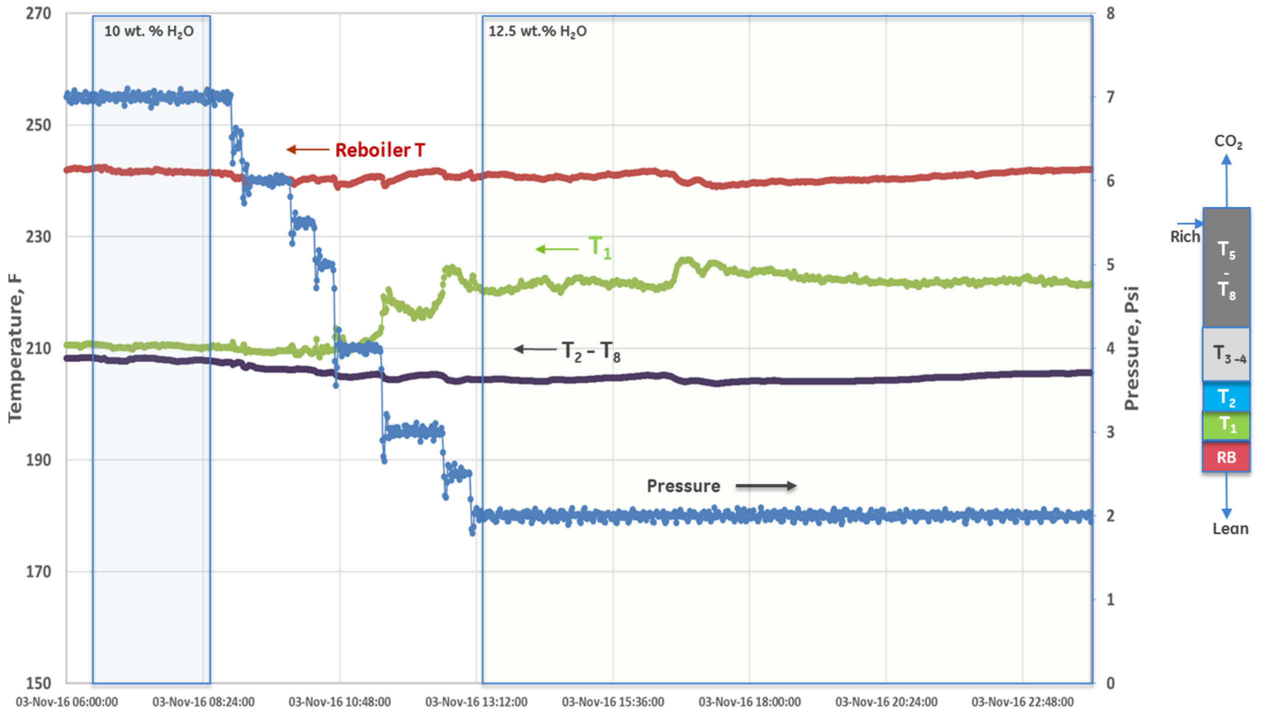

Figure 63. **SSC Commissioning:** Desorber T Profile for Condition 3
Process conditions listed in **Table 18**

***Condition 4**: 15 wt. % H_2O, 2 Psig and 235 °F Desorption*

Water level in the working solution was increased from 12.5 wt. % (condition 3) to 15 wt.% by adding additional 50 gallons of water from 501 tank (water wash tank) to the lean storage tank (401). During the run, automatic water control was implemented by controlling liquid level in the 401 lean storage through water addition from the water wash tank (501). Desorber temperature was lowered to 235 °F. Desorber pressure was maintained at 2 Psig. All the other process conditions were kept the same as for condition 1.

CO_2 capture efficiency, measured based on the gas phase analysis, was 90%. Increased water content rendered higher temperature in the bottom of the regenerator column due to higher steam circulation (**Figure 64**). Limited or no carry-over was recorded in the total condenser or 602 mist separator. Maximum absorber temperature was 162 °F (top bed). Temperature increase in the three absorber beds was as following: 50 °F (top bed), 19 °F (second bed) and 8 °F (third bed). % CO_2 in rich and lean working solutions was 3.2 wt. % and 0.15 wt.%, respectively.

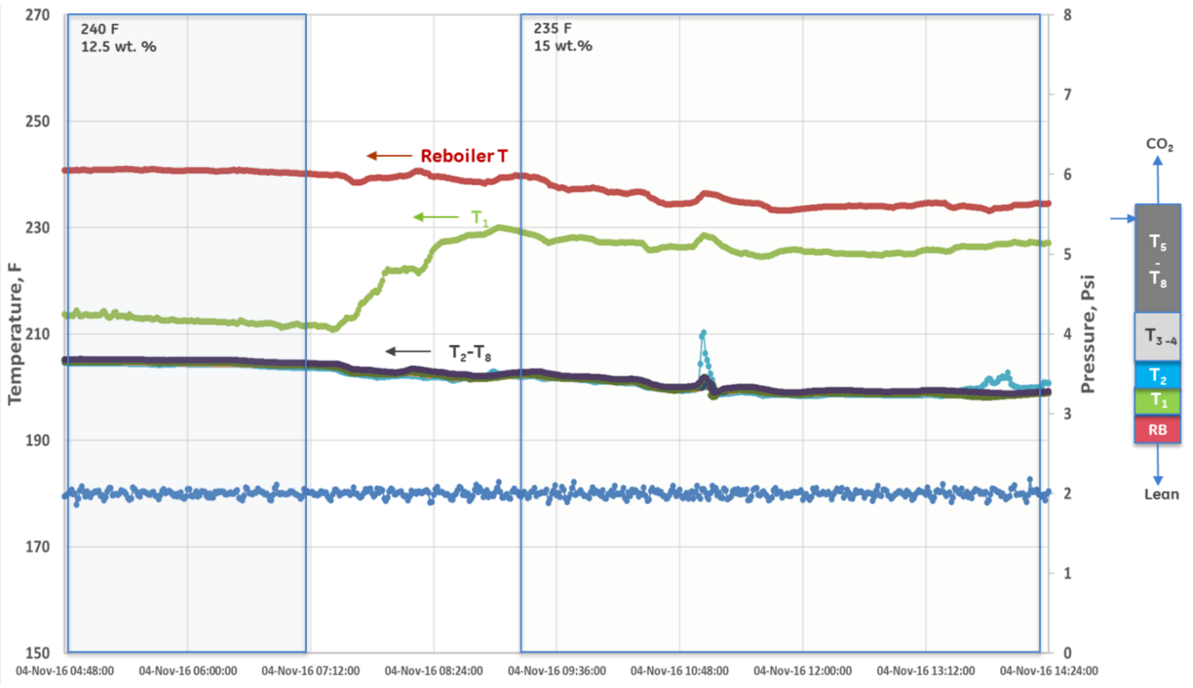

Figure 64. **SSC Commissioning:** Desorber T Profile for Condition 3
Process conditions listed in **Table 18**

4.4.1.2 SSC Performance = f (% water, desorption pressure and temperature)

Performances of the SSC and CSTR are similar at 5 wt. % H_2O (73% (CSTR) vs. 79% (SSC), **Figure 65**). The steam circulation in the regenerator is limited to the bottom of the column, and most of the desorption happens in one stage (i.e. in the reboiler) as in case of the CSTR. CO_2 capture reached 90% efficiency while increasing water content from 5 wt.% to 15 wt.% and decreasing desorber pressure from 7 Psig to 2 Psig, even though the desorber temperature was lowered from 255 °F to 235 °F. This trend can be attributed to the increased steam circulation in the regenerator column that lowers the partial pressure of CO_2, and drives the desorption equilibrium towards leaner working solution.

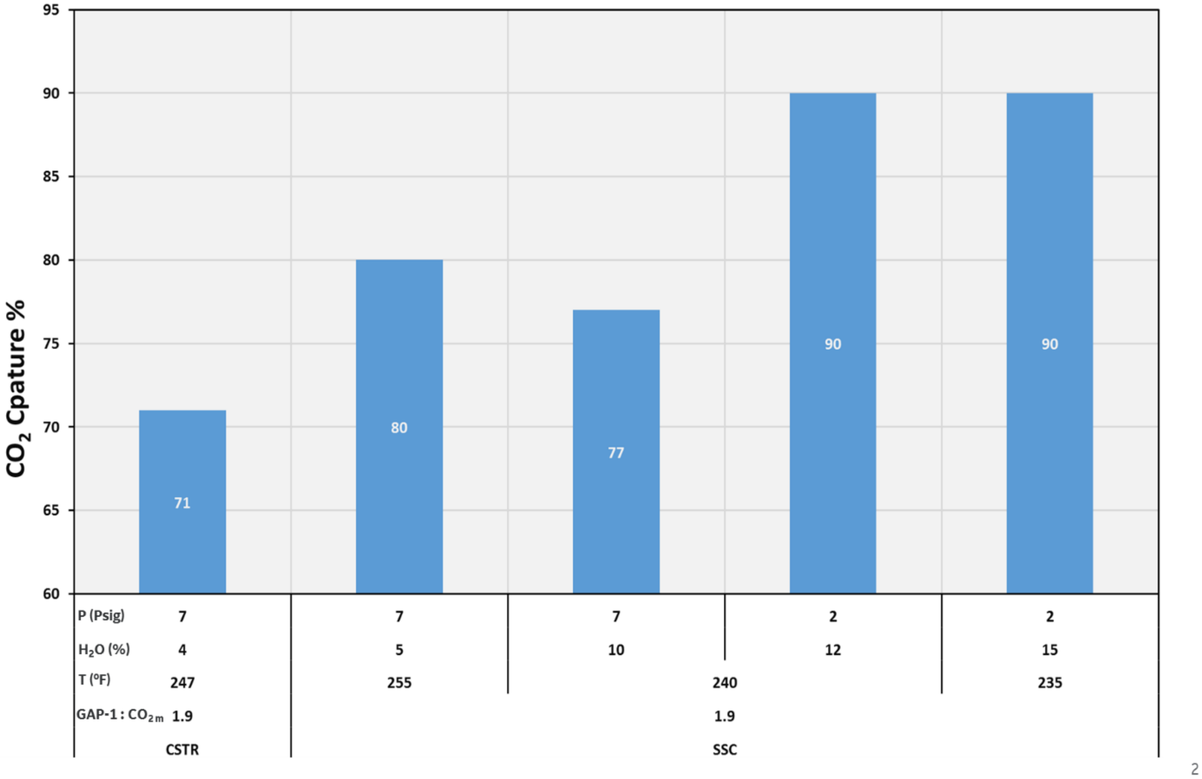

Figure 65. **SSC Commissioning:** CO_2 Capture Efficiency =f (CSTR vs. SSC)
Process conditions listed in **Table 18**

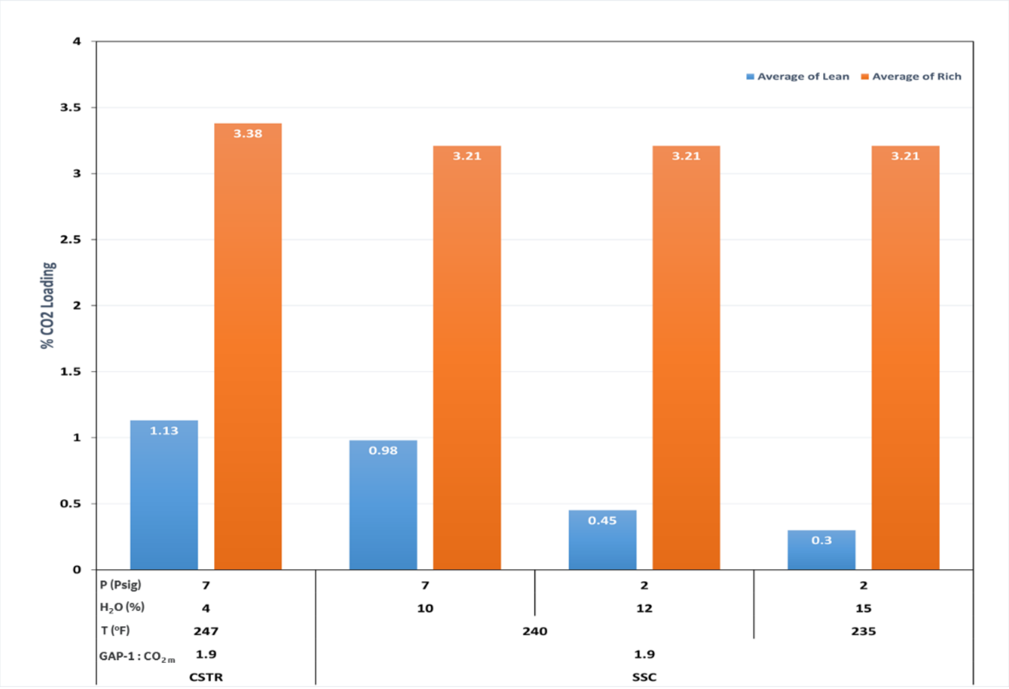

Figure 66. **SSC Commissioning:** CO_2 Capture Efficiency =f (CSTR vs. SSC)
Process conditions listed in **Table 18**

Figure 66 compares % CO_2 in the lean and rich solutions while increasing water content and reducing desorber pressure and temperature. Higher water content and lower desorber pressure decreased the %CO_2 in the lean solvent to 0.3 wt.% (15 wt.% H_2O, 2 Psig and 235 °F, SSC) due to a more efficient desorption process.

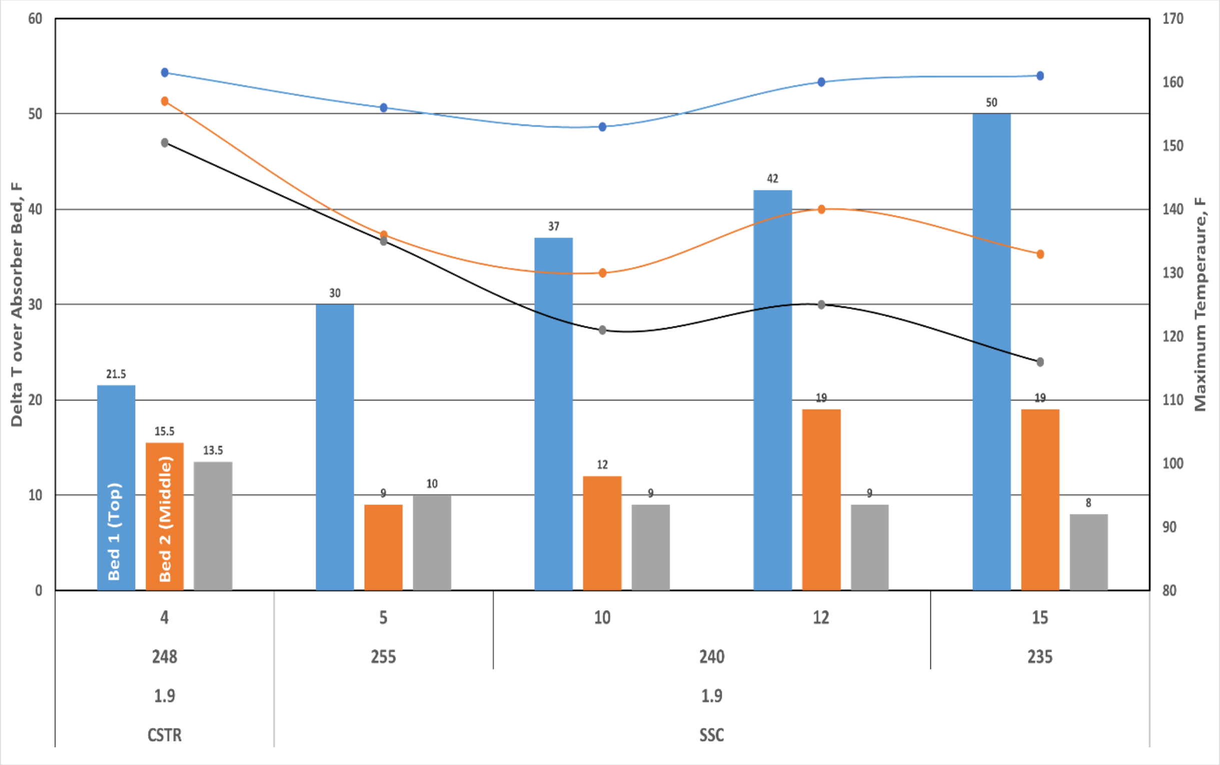

Figure 67. **SSC Commissioning:** Absorber temperature =f (CSTR vs. SSC)
Process conditions listed in **Table 18**

Distribution of the CO_2 absorption in the absorber beds, and maximum temperature in each of the beds were greatly influenced by the water loading in the working solution, and desorber conditions, as shown in **Figure 67**. High water content and low pressure desorption led to higher exotherms in the top bed: 30 ^oF (255 ^oF desorption, 5 wt.%, 7 Psig) < 37 ^oF (240 ^oF desorption, 10 wt. %, 7 Psig) < 42 ^oF (240 ^oF desorption, 12 wt. %, 2 Psig) < 50 ^oF (235 ^oF desorption, 15 wt.%, 2 Psig). Under these conditions, the desorption process in SSC is more efficient, yielding a much leaner solvent. This leads to a more efficient absorption process and more heat generation in the top bed. Lower temperature increase in the bottom beds is indicating that the absorber is oversized for the conditions tested.

Maximum temperature in the bottom absorber bed is lowered by the increased water content in the working solution: 135 ^oF (5 wt. % H_2O) > 121 ^oF (10 wt.% H_2O) > 116 ^oF (15 wt.% H_2O). This effect could be attributed to the endothermic process of water evaporation from the working solution into flue gas. The phenomenon is beneficial as it can reduce the cooling duty of the absorber.

4.4.1.3. SSC performance: 2 kW$_e$ (bench scale, GRC) vs. 0.25 MW$_e$ (pilot, NCCC)

Performance of the GAP-1$_m$/TEG with SSC was compared at two different scales: 0.25 MW$_e$ (NCCC pilot) and 2 kW$_e$ (GE GRC). Under similar conditions (240 ^oF and 2 Psig desorption, 13 wt.% H_2O), CO_2 capture performance at both scales was between 85 – 90% (**Table 21**). Comparing the temperature profile in the SSC between the two scales (**Figure 68**) indicates that only 10% of the column is under the steam conditions at 0.25 MW$_e$. Absorber temperature profiles are shown in **Figure 69**. Maximum absorber temperature at 2 kW$_e$ scale was 70 ^oC with no intercooling.

Table 21. Performance of the SSC: 2 kW$_e$ vs. 0.25 MW$_e$

Conditions	Bench Scale (2 kW$_e$)	NCCC (0.25 MW$_e$)
Run	07072016	11042016
H$_2$O wt. %	13.5	12.5
T (F)	239	240
GAP : CO$_2$ (molar)	1.37	1.92 (total) 1.34 (active)
P$_{desorber,}$ (Psig)	3 - 4	2
CO$_2$%		
Rich	6.5	3.2
SSC	2.9	
Lean Storage	1.4	0.45
CO$_2$ Capture %	84-86	89-91

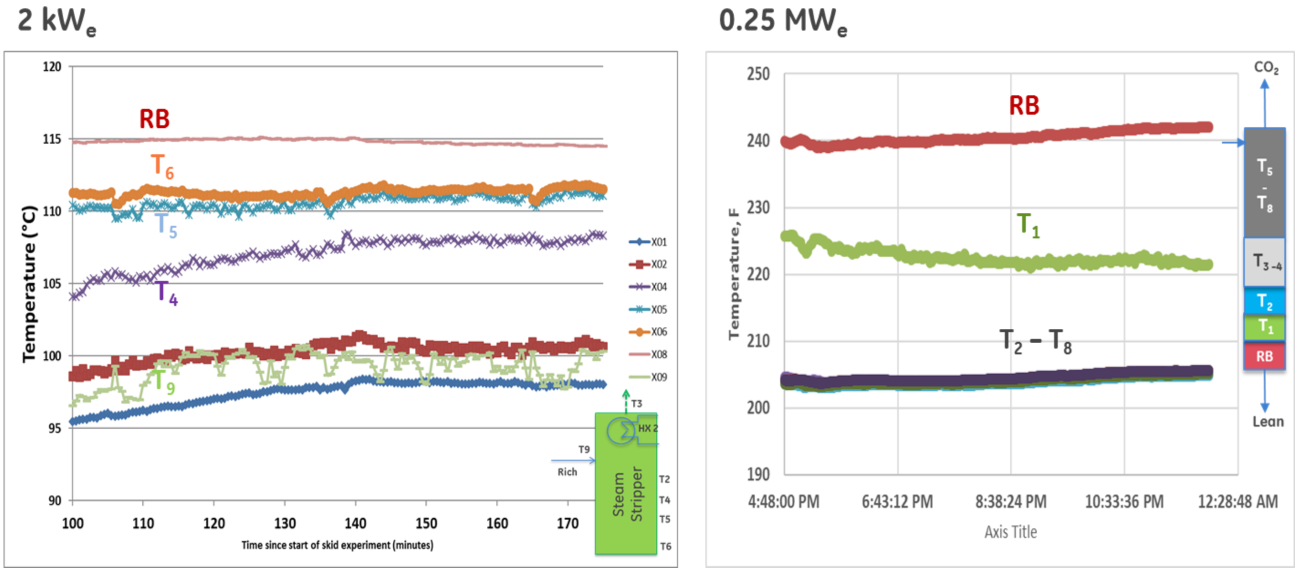

Figure 68. **SSC temperature profile:** Bench-Scale (2 kW$_e$) vs. Pilot-Scale (0.25 MW$_e$)

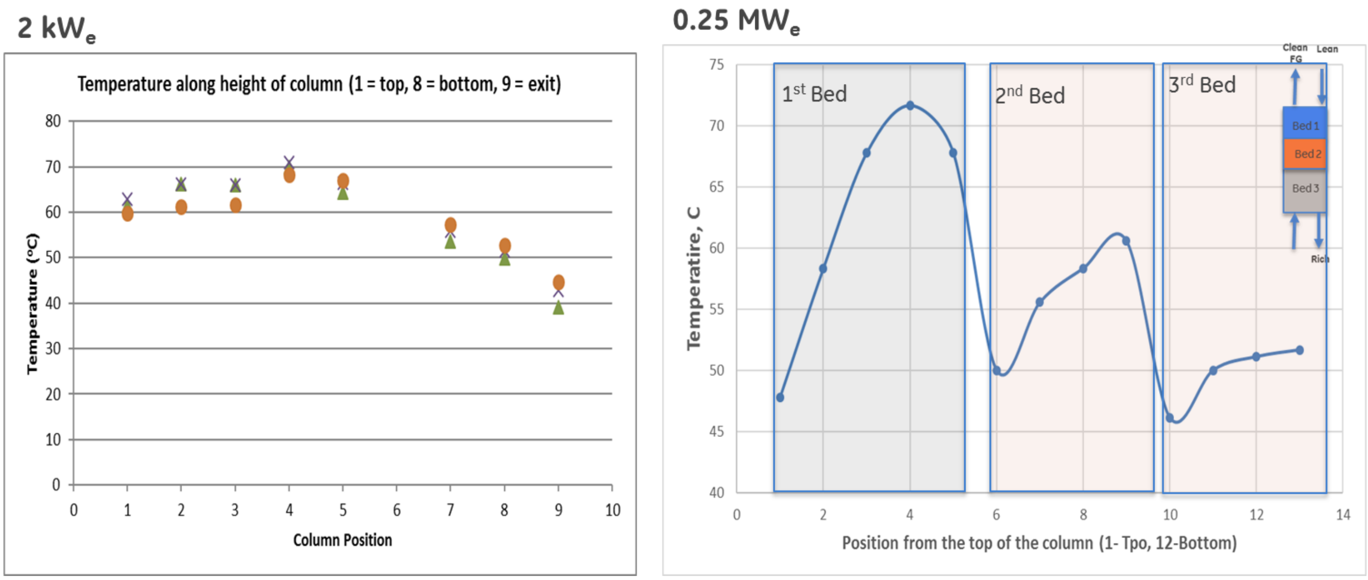

Figure 69. **Absorber temperature profiles:** Bench scale (2 kW, no inter-stage cooling) vs. Pilot Scale (0.25 MW$_e$, 2 inter-stage cooling)

4.4.1.4. 0.5 MW_e SSC Commissioning: Summary

1. Steam stripping column at NCCC was successfully commissioned with GAP-1_m/TEG-1 solvent. No solvent carry-over was observed at water content < 15 wt.%, and low desorption pressure operation. Automatic water management was demonstrated by maintaining liquid level in the lean storage tank (401) through automatic transfer from the water wash tank (501). Stable low pressure desorption was demonstrated.

2. The following performance was demonstrated (0.25 MW_e) with the steam stripper column:
    a. 90 % capture efficiency was demonstrated at 240 ^oF (12 % H_2O) and 235 ^oF (15+% H_2O)
    b. Absorber temperature was decreased by up to 20 ^oF upon increasing water content to 15 wt.%
    c. Steam circulation in the regenerator column was improved by decreasing desorber pressure, and increasing water content (12-15 wt.% H_2O)

4.4.2. 0.5 MW_e SSC Campaign Phase 2: Optimization

Phase 2 of the SSC campaign at NCCC was conducted to optimize performance of the GAP-1_m/TEG at 0.5 MW_e scale (**Figure 70**). First, the molar ratio GAP-1_m : CO_2 was lowered by increasing the flue gas flow rate from 2500 lb/hr (0.25 MW_e) to 5000 lb/hr (0.5 MW_e), while keeping liquid flow rate constant at 13,000 lb/hr. Next, steam duty was optimized at 0.5 MW_e by lowering the water content in the working solution while maintaining CO_2 capture efficiency between 87 - 93 %. Desorber temperature and pressure were maintained below 235 °F and 2 Psig, respectively, to minimize solvent thermal degradation. **Table 22** and **Table 23** list the process conditions and flue gas composition utilized during the campaign.

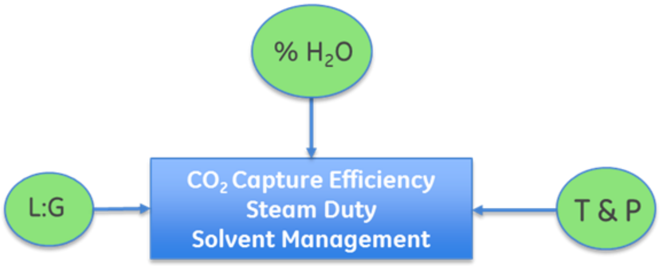

Strategy:

- **Optimize steam duty..** Decrease water % & reduce steam circulation in the regenerator
- **Lower GAP : CO_2..** Increase FG at constant liquid flowrate
- **Desorber T & P..** Maintain 230 F < T < 235 F; 2 Psig

Figure 70. **SSC campaign (Phase 2):** Solvent Circulation and Steam Duty Optimization

Table 22. **SSC campaign (Phase 2):** Process conditions

Condition	**5**	**6**	**7**	**8**	**9**	**10**
Objective	Solvent circulation flow rate			0.5 MWe Demo	Steam Optimization	Pressure Effect
Flue Gas (FG) (lb/hr)	2500	3750	5000	5000	5000	5000
Liquid (lb/hr)	12000	12000	12000	13000	15000	15000
$T_{desorber}$ (F)	230	235	235	235	235	235
$P_{desorber}$ (Psi)	2	2	2	2	2	5

Water Management: automatic water addition from water wash tank (501) to lean storage tank (401).

Table 23. **SSC campaign (Phase 2):** Flue gas conditions

	NO	**O_2**	**CO_2**	**NO_2**	**T**
	ppm	% vol.	% vol	ppm	F
Avg	34.1	6.6	12.5	0.6	135.
Stdev.	7.9	0.8	0.6	0.2	2.8

Table 24. **SSC campaign (Phase 2):** Solvent Composition

Sample	**Total Amine wt.%**		**CO_2 wt.%**	**TEG**	**Water**
	wet	dry	wt.%	wt. %	wt.%
Initial	45.8	57	0.69	30.3	19.8
Condition 5	45.5	57	1.14	31.2	20.2
Condition 6	47.4	58	0.87	32.2	17.9
Condition 7	45.9	59	0.37	31.2	21.9
Condition 8	45.3	59	1.3	33.6	23.4
Condition 9	48.2	59.2	1.3	33.8	18.9
Condition 10	47.2	58.3	2.2	33.7	19

4.4.2.1. 0.5 MW_e SSC Campaign (Phase 2): Solvent circulation

Effect of the amine to CO_2 stoichiometry on the fresh GAP-1_m/TEG performance was evaluated by increasing the flue gas flow rate from 2500 lb/hr (0.25 MW_e) to 5000 lb/hr (0.5 MW_e) while all the other process parameters were kept constant (Conditions 5-7). Optimization of the regenerator column was performed with fresh GAP-1 / TEG working solution. Solvent properties are listed in **Table *24***. Water content in the working solution was maintained between 18-20 wt.% by controlling liquid level in the lean storage tank (401) through automatic water addition from the water wash tank (501), and mist separator tank (602). **Figure 71** shows liquid level in the lean storage tank (401), water wash tank (501) and mist separator tank (602) for conditions 5-7.

Effect of the liquid flow rate on CO_2 capture efficiency is shown in **Figure 72**. CO_2 capture efficiency reached 100% at GAP-1_m : CO_2 molar ratios between 1.3 to 2 (Condition 5 and 6). Under CO_2 excess (GAP-1_m : CO_2 = 0.9 (molar), condition 7), CO_2 capture efficiency reached 87%, demonstrating stoichiometric capture efficiency under low-temperature desorption conditions.

Performance of the three-bed, inter-staged absorber was influenced by the amine to CO_2 stoichiometry. Maximum temperature in the absorber beds, and temperature increase in each of the beds are listed in **Table 25**. Under a large excess of solvent (Condition 5, GAP-1_m : CO_2 = 2 (molar), 100% Capture Efficiency), most of the absorption happened in the bottom, and middle beds, respectively. Little or no absorption occurred in the top bed (2 ^oC temperature increase), due to near zero CO_2 inlet concentration in this bed. Lowering the amine : CO_2 molar ratio from 2 to 1.3 and 0.9, respectively changed the reaction distribution in the absorber beds. CO_2 absorption was equally distributed among the 3 beds under condition 6, as inferred from the temperature increase in the individual sections of the absorber (42 ^oF (top) > 24 ^oF (middle) > 26 ^oF (bottom)). Under excess of CO_2 (GAP-1_m : CO_2 =0.9 (molar)), most of the absorption occurred in the top bed (temperature increase: 46 ^oF (top) > 15 ^oF (middle) > 15 ^oF (bottom).

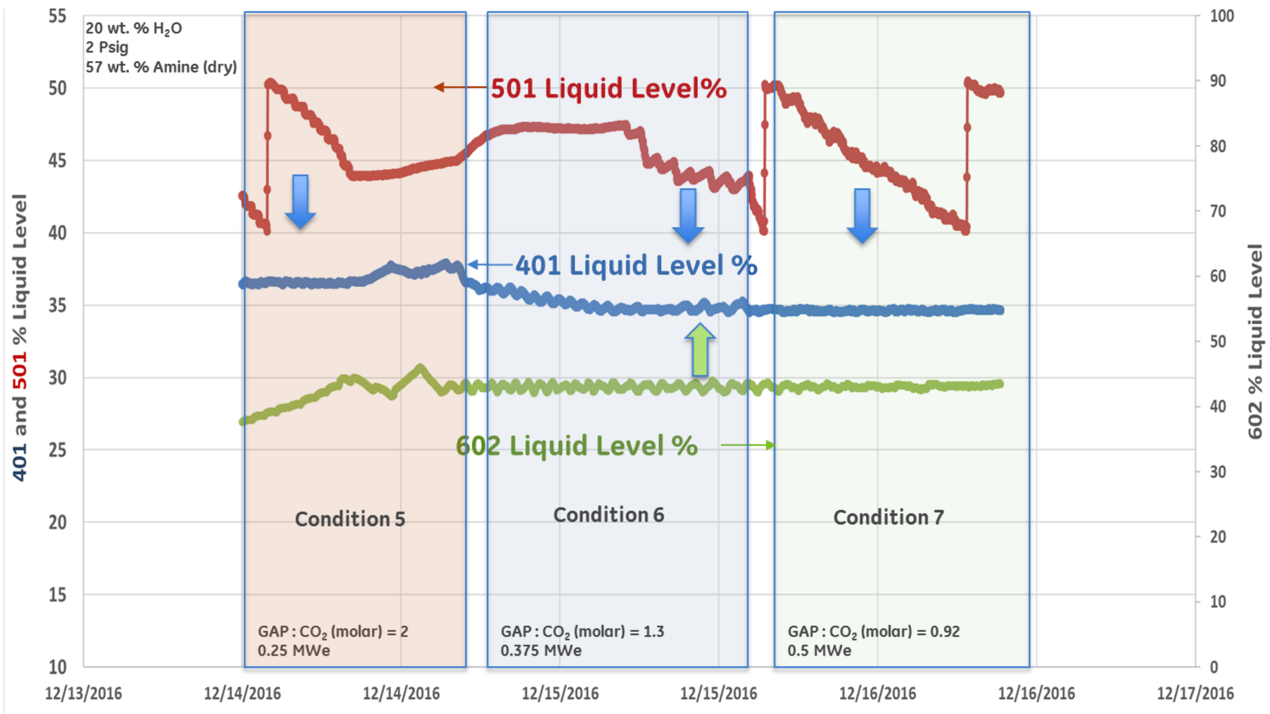

Figure 71. **SSC campaign (Phase 2 – solvent circulation):** Water management
Automatic water transfer from water wash tank (501), and mist separator tank (602) to lean storage tank (401). **Table 22** lists process conditions for Conditions 5-7.

Table 25. SCC campaign (Phase 2): Absorber performance = f (solvent circulation)

		Condition 5	Condition 6	Condition 7
P	Psig	2	2	2
T	ºF	230	235	235
GAP-1$_m$: CO$_2$	molar	2	1.3	0.9
CO$_2$ Capture	%	100	100	87
Bed 1 (top)	T$_{max}$ (F)	118	156	160
	Delta T (F)	2	42	46
Bed 2 (middle)	T$_{max}$ (F)	118	165	130
	Delta T (F)	24	24	15
Bed 3 (bottom)	T$_{max}$ (F)	141	150	115
	Delta T (F)	32	26	15

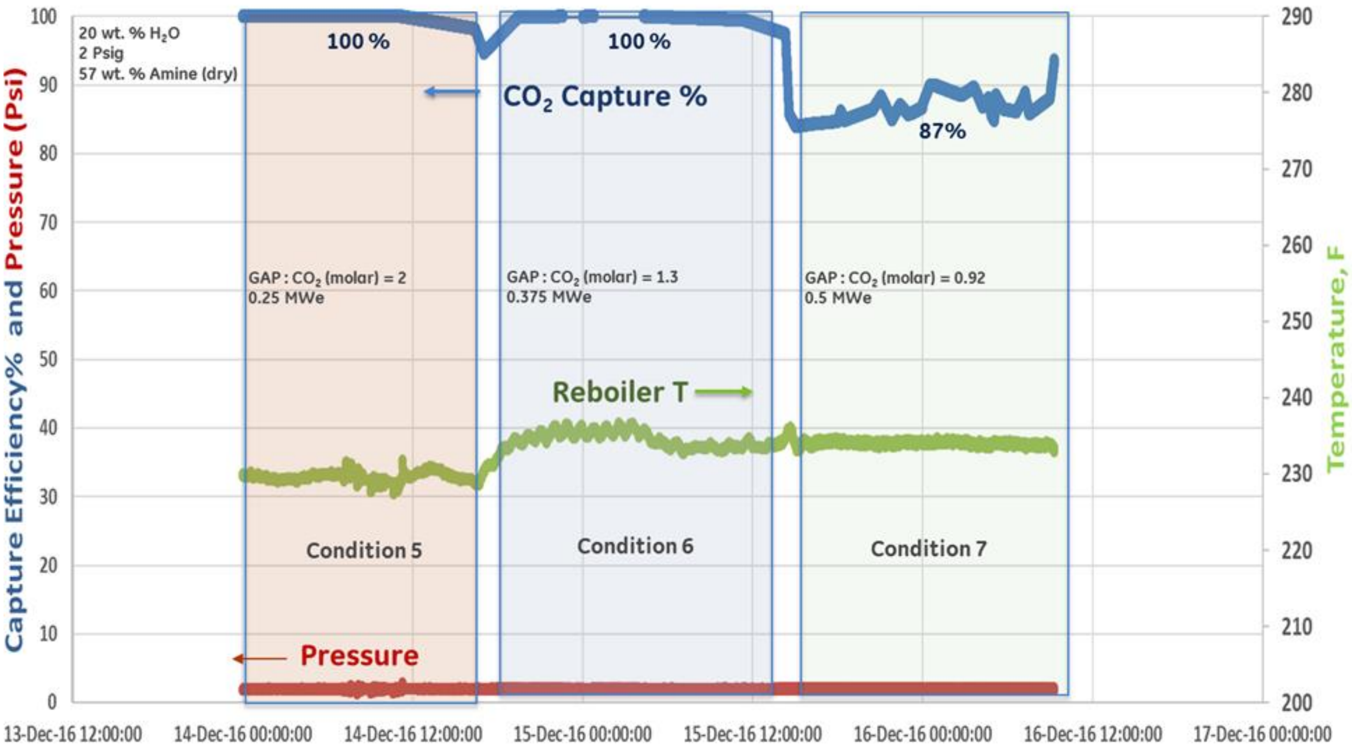

Figure 72. **SSC campaign (Phase 2 - solvent circulation):** CO_2 Capture Efficiency
Table 22 lists process conditions for Conditions 5-7.

Regenerator temperature profile for Conditions 5 is shown in **Figure 73** indicating that 90% of the regenerator column was under steam conditions. Water carry-over from the regenerator column was collected in the total condenser and/or mist separator (602). The condensate was periodically transfferend back to the lean storage tank (401) to control the liquid level in the mist separator tank (602) at 43% fill. Finally, amine to CO_2 stoichimetry had little or no effect on the specific steam utilization (0.48 - 0.5 lb CO_2/ lb steam, **Figure 74**), as long as the water content of the working solution was maintained constant (~ 20 wt.%).

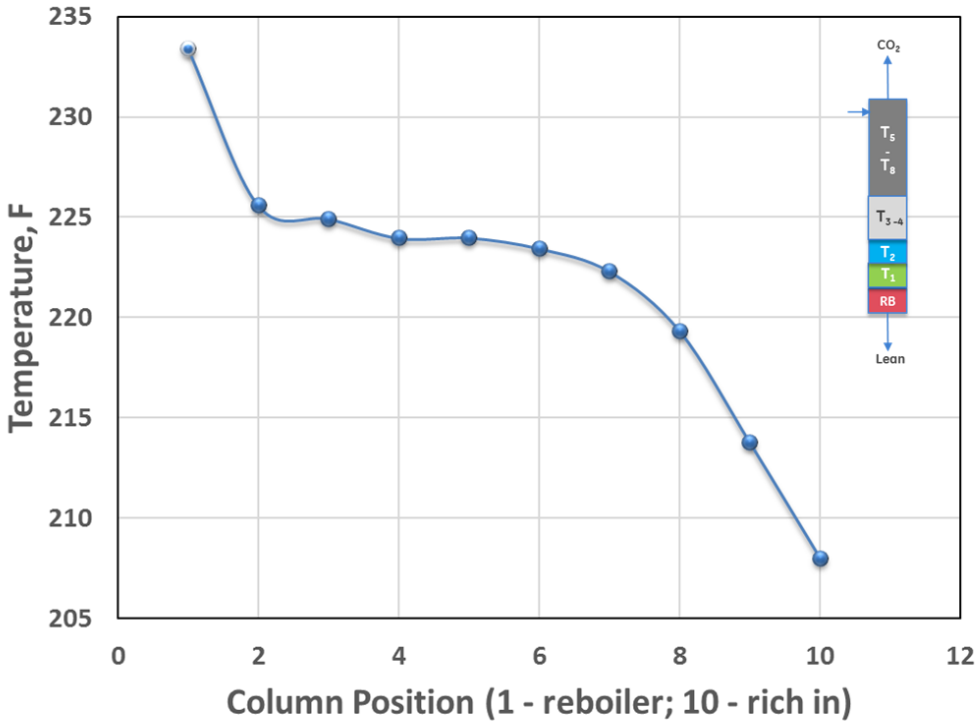

Figure 73. **SSC campaign (Phase 2– solvent circulation):** SSC temperature profile **Table 22** lists process conditions for Conditions 5.

In summary, stoichiometric capture was demonstrated with the regenerator column for the GAP-1_m/TEG working solution (20 wt. % H_2O) at 0.5 MW_e, 2 Psig and 235 ^oF desorption. Absorber operation was greatly influenced by the CO_2 to amine stoichiometry. Under amine excess, most of the absorption occurred in the bottom bed and capture efficiency reached 100%. Finally, specific steam utilization (lb. CO_2 / lb. steam) was constant (0.48 - 0.52) as a function of the amine to CO_2 stoichiometry.

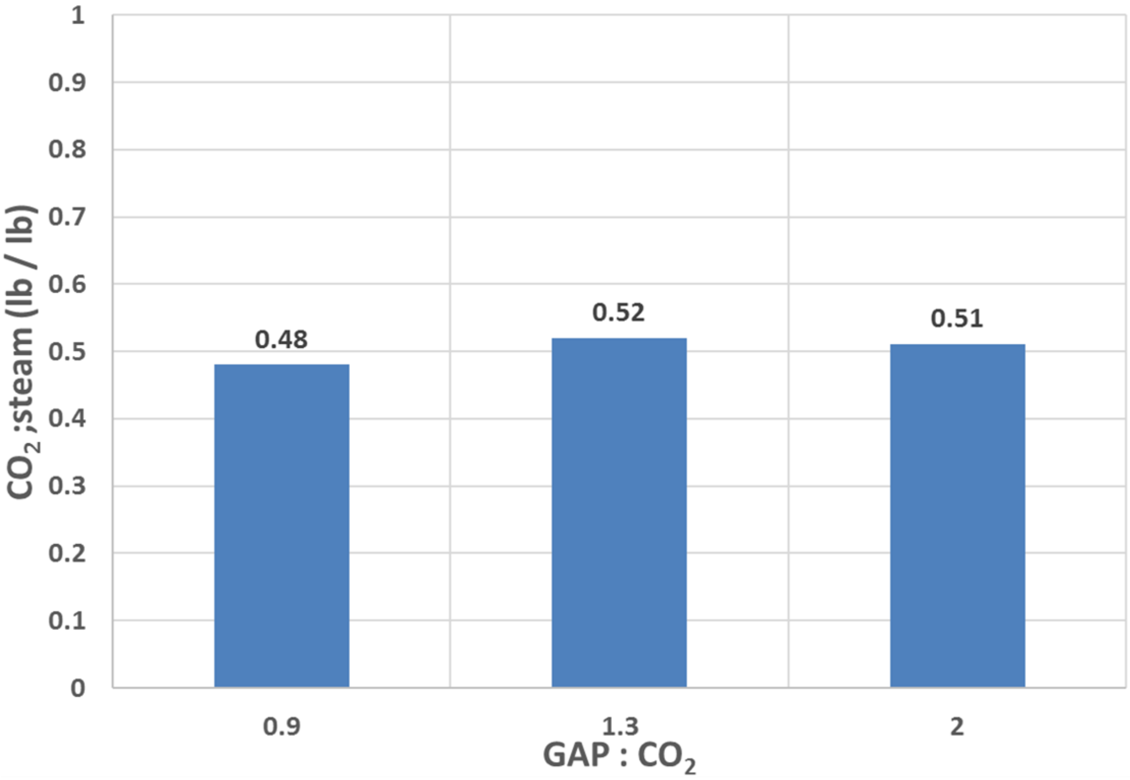

Figure 74. **SSC campaign (Phase 2– solvent circulation):** Specific steam utilization
Table 22 lists process conditions for Conditions 5-7.

4.4.2.2. 0.5 MW_e SSC Campaign (Phase 2): 0.5 MW_e Demo

Performance of the SSC with GAP-1_m/TEG solvent was demonstrated at 0.5 MW_e for 84 hours. Process conditions are listed in **Table 22** (Condition 8). GAP-1_m : CO_2 molar ratio was maintained at 1.1. Desorption conditions were kept constant at 235 ^oF and 2 Psig, respectively. Solvent composition is listed in **Table 24** (condition 8).

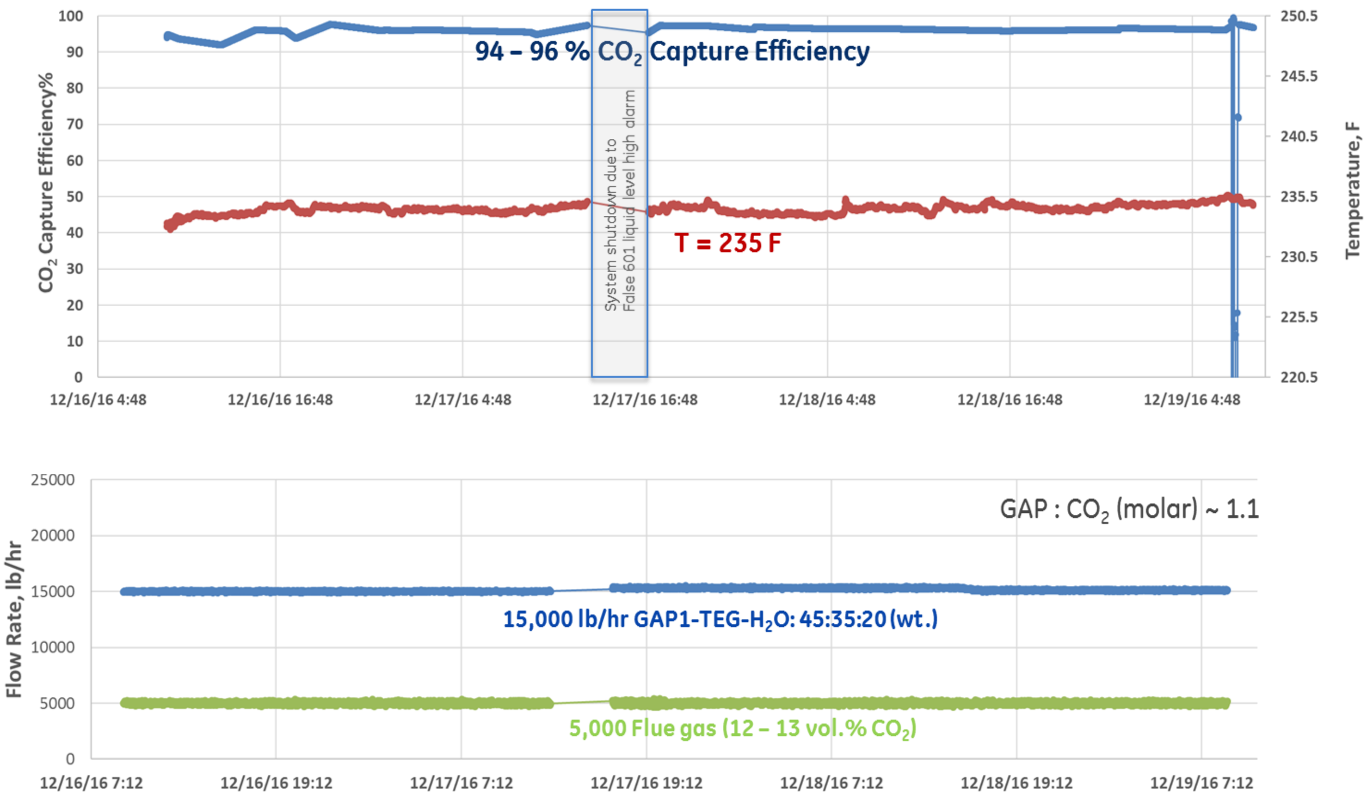

Figure 75. **SSC campaign (Phase 2 - 0.5 MW$_e$ Demo):** CO$_2$ capture efficiency

Table 22 lists process conditions for Conditions 8.

Performance of the SSC at 0.5 MW$_e$ is shown in **Figure 75**. The system was shut down for 2 hours due to a false liquid level high alarm. CO$_2$ capture efficiency reached 94 - 96 % based on the gas phase analysis.

Absorber temperature profile is shown in **Figure 76**. Temperature increase in the three absorber beds varied as following: 55 ^{o}F (top bed) > 22 ^{o}F (middle bed) > 16 ^{o}F (bottom bed). Temperature reached a maximum of 163 ^{o}F in the top bed. Most of the absorption occurred in the top bed, indicating that the size of the absorber and the location of the inter-stage cooler could be further optimized to reduce the footprint, and the maximum temperature in the absorber. Reducing absorber temperature is an effective way to minimize the oxidative degradation of the solvent, as indicated by separate bench scale experiments.

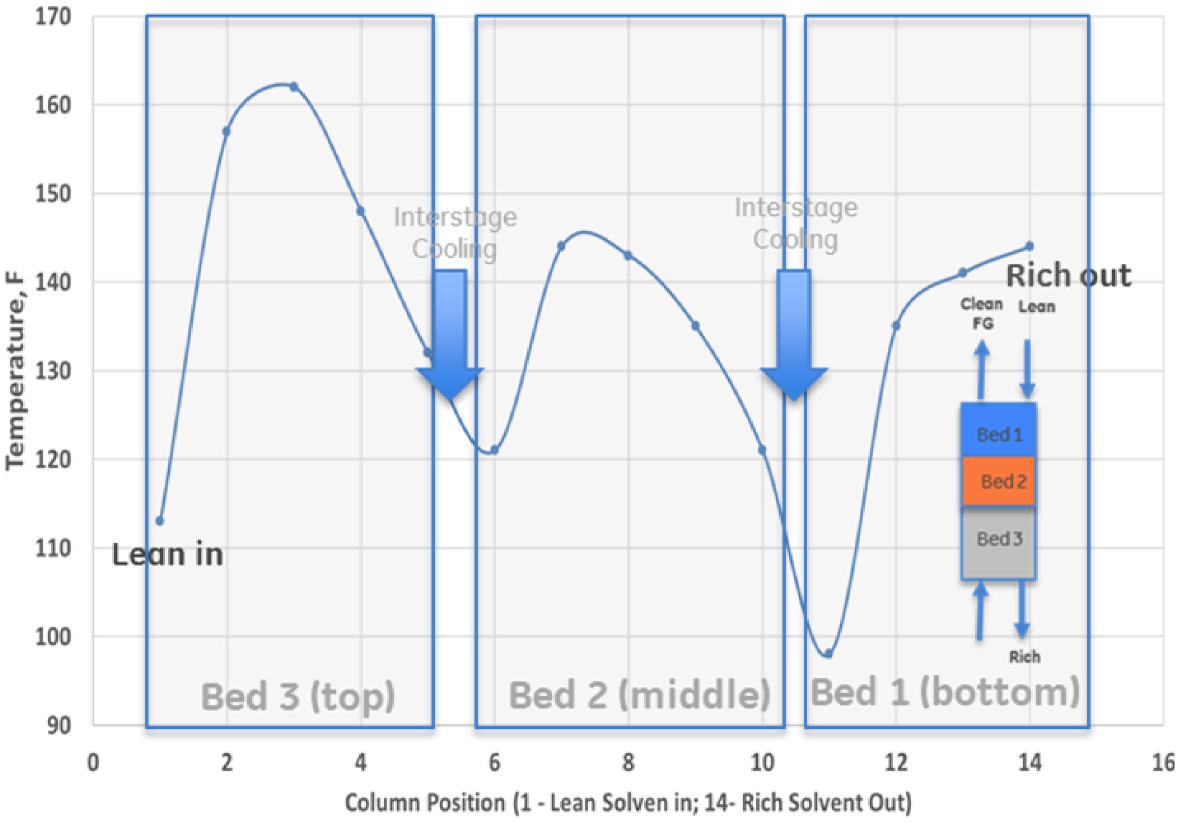

Figure 76. **SSC campaign (Phase 2 - 0.5 MW$_e$ Demo):** Absorber temperature profile **Table 22** lists process conditions for Conditions 8.

Regenerator temperature profile was similar to the one shown in **Figure 73**. 90% of the regenerator column was under steam conditions. Water content in the working solution was maintained constant at 20 wt % by utilizing the strategy highlighted for conditions 5-7. Water was continuously transferred from the water wash tank (501) and mist separator (602) to the lean storage tank (401). In the last 12 hours of the test, no condensate was transferred from the 602 to 401 tank due to a frozen valve. **(Figure 77)** This led to the increase of the liquid level in 602 tank from 43% to 58%, and water content in the working solution increased from 20.4 wt.% to 23.8 wt.%. At 23.8 wt.% water, the rich solvent sample was bi-phasic: lower phase contained mostly water and TEG (5 wt. % GAP-1$_m$ carbamate, 50 wt. % H_2O, 45 wt. % TEG, by ^{1}H NMR) while the upper phase had similar composition to the initial working solution (54 wt.% GAP-1$_m$ carbamate, 33 wt.% TEG, and 13 wt. % water, by ^{1}H NMR). The corresponding lean solvent sample containing 23.8 wt. % H_2O was homogeneous. Finally, all the other samples with lower water content (< 20 wt.%) were homogeneous regardless of the CO_2 content.

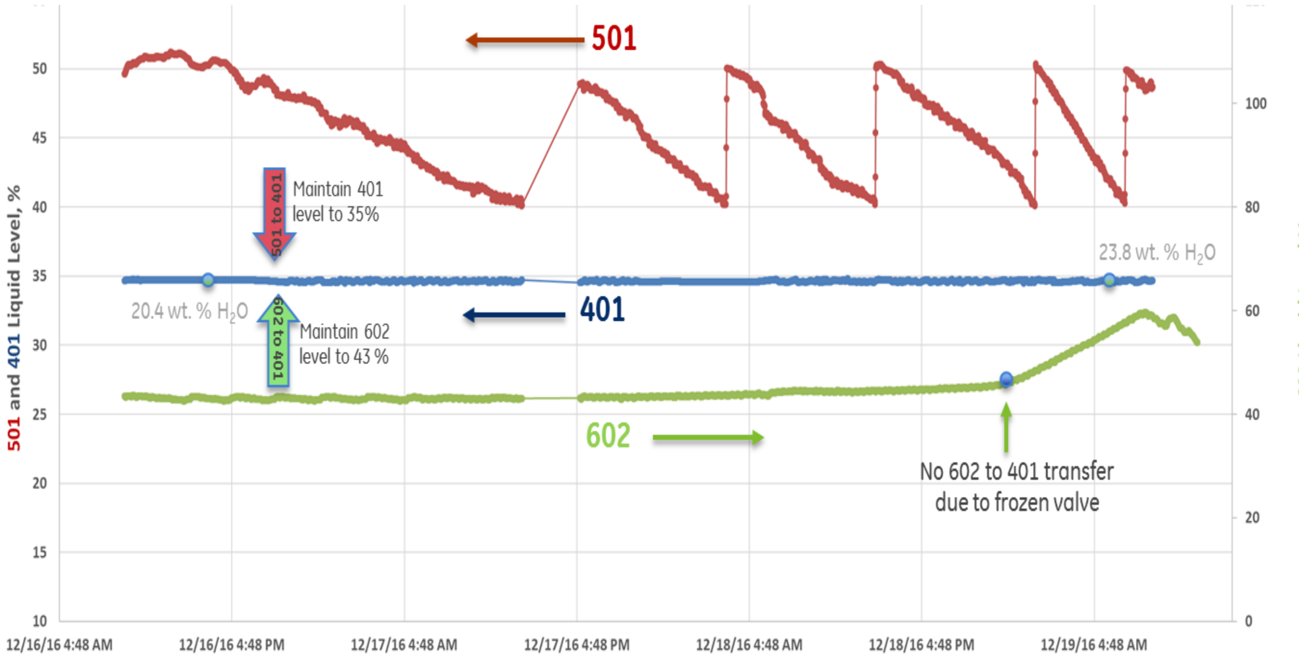

Figure 77. **SSC campaign (Phase 2 - 0.5 MW$_e$ Demo):** Water management
Table 22 lists process conditions for Conditions 8.

Specific steam utilization was between 0.45 – 0.5 (lb CO_2 / lb steam) (**Figure 78**). Steam conditions were as following: 43 Psig and 335 ^oF. CO_2 capture efficiency exceeded 95% for most of the run. Under these conditions, 90 % of the column was under steam conditions indicating that steam input can be further optimized. On the other hand, the specific steam utilization of the SSC was almost half when compared to CSTR desorber due to the increased water content in the working solution.

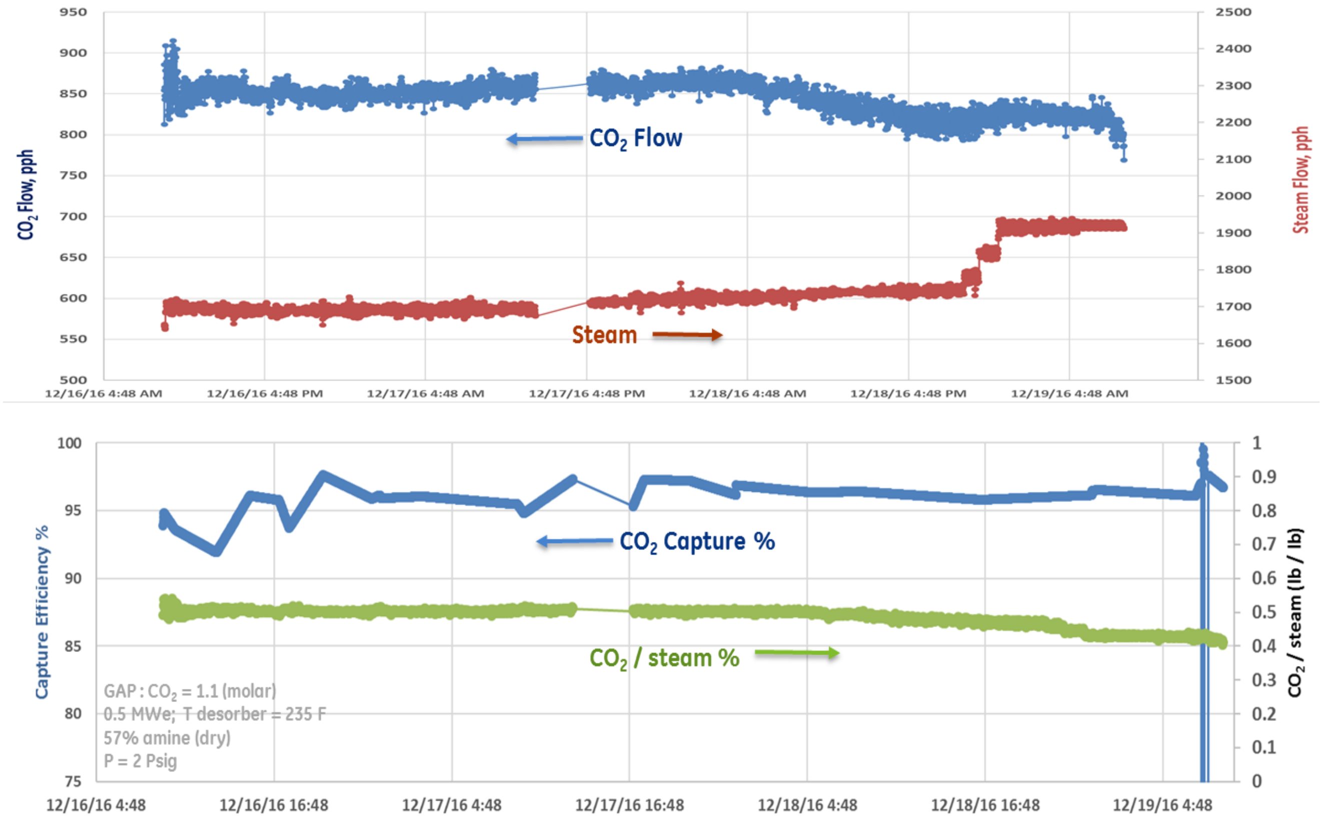

Figure 78. **SSC campaign (Phase 2 - 0.5 MW_e Demo):** Specific steam utilization
Table 22 lists process conditions for Conditions 8.

Most of the process variability during the 0.5 MW_e demo run was caused by the change in the power load of the power plant. Nominally, the plant operated at 800 MW. Under these conditions, average flue gas temperature was 127 ^oF, CO_2 concentration averaged around 12.8 % vol, average temperature in the bottom absorber bed was 124.4 ^oF, and top bed regenerator temperature was 215 ^oF **(Table 26)**. After 50 hours into the demo run, the power plant power load was downgraded to 650 MW to adjust for lower demand. The variables during this time period included an average flue gas temperature from 127 ^oF to 122 ^oF, absorber temperature (bottom bed) from 125 ^oF to 102 ^oF, regenerator temperature (upper bed) from 216 ^oF to 211 ^oF, and CO_2 concentration of 12.5 vol.%. **Figure 79** describes the time traces for all these parameters during the 0.5 MW_e SSC demo. The process was robust with respect to the variability caused by the power load, as the CO_2 capture efficiency remained above 95% for most of the run.

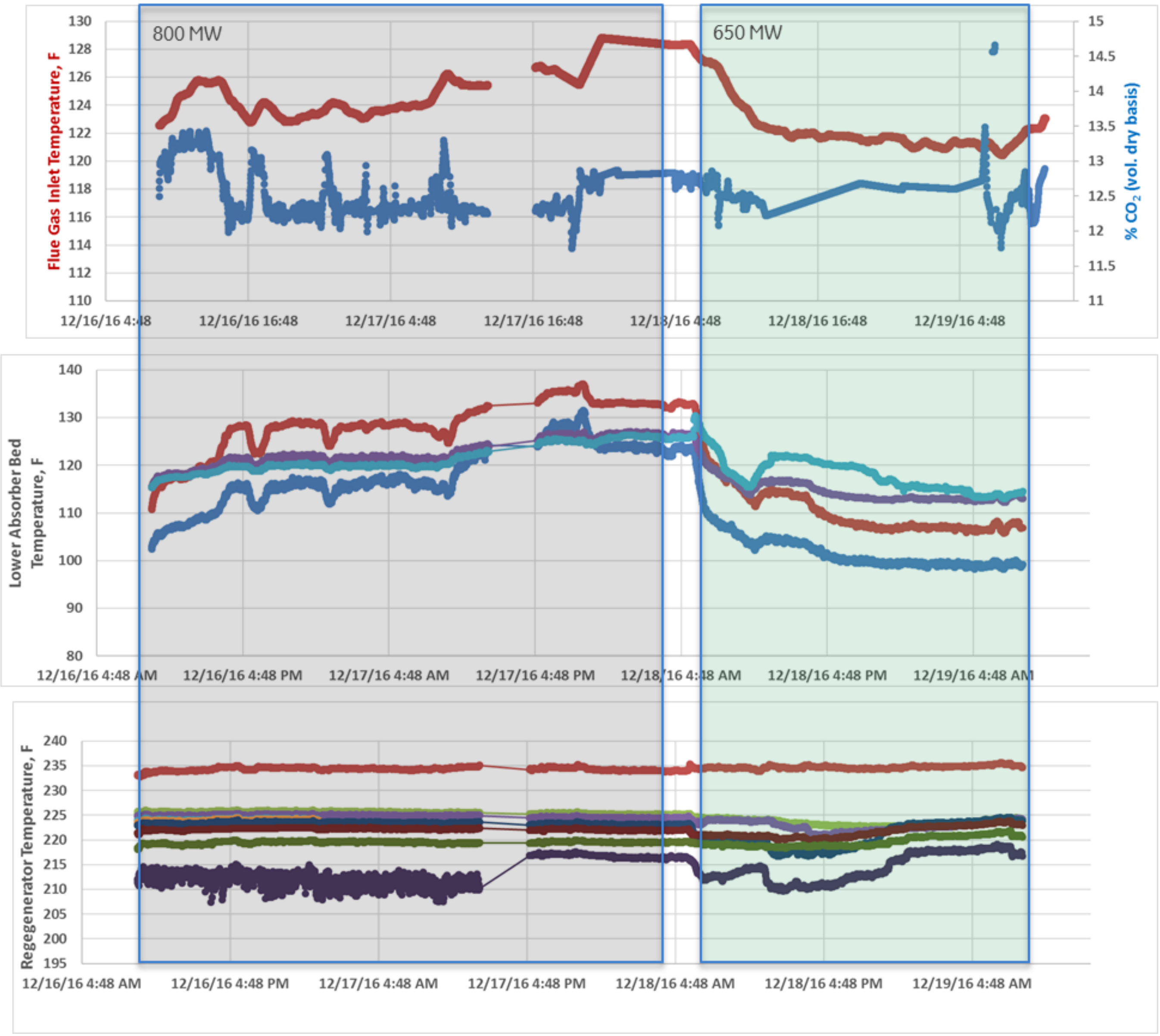

Figure 79. **SSC campaign (Phase 2 – 0.5 MW$_e$ Demo):** Input process variability

Table 22 lists process conditions for Conditions 8.

Table 26. **SCC campaign (Phase 2):** Input process variability (0.5 MW_e)

Load	**Flue Gas Temperature**		**CO_2**		**Absorber T (Lower Bed)**		**Regenerator T (Top Bed)**	
	Avg.	Stdev.	Avg.	Stdev.	Avg.	Stdev.	Avg.	Stdev.
	F	F	% vol.	% vol	F	F	F	F
800 MW	127.3	0.3	12.8	0.1	124.4	2.6	215.7	2.2
650 MW	121.9	0.2	12.5	0.0	101.7	4.0	211.0	1.6

In summary, we demonstrated sustained performance of the GAP-1_m/TEG working solution with the SSC at 0.5 MW_e for over 80 hours of operation. Under near stoichiometry (GAP-1_m : $CO_{2\ molar}$ = 1.1), CO_2 capture efficiency reached 95%. Maximum absorber temperature was 162 ^oF (top bed). Temperature increase in the absorber beds varied as following: Top (55 ^oF) > Middle (22 ^oF) > Bottom (16 ^oF). 90 % of the steam stripper column was under steam conditions. Specific steam utilization was between 0.45 – 0.5 (lb CO_2 / lb steam). Water content was kept between 20 -24 wt.% through automatic control of the liquid level in the lean storage tank (401). CO_2 capture process was robust as a function of the input variability caused by the power plant load.

4.4.2.3. 0.5 MW_e SSC Campaign (Phase 2): Steam input and Water loading

Performance of the GAP-1_m/TEG working solution with the SSC at 0.5 MW_e was evaluated with a non-optimized steam input and water content. As discussed in the previous sections, controlled amounts of water in the GAP-1_m/TEG working solution were found to be an effective way to enable steam stripping, to lower desorption temperature, and hence reduce thermal degradation. Steam stripping also increased working capacity by 30 % due to more efficient desorption. Controlled water addition had additional benefit of reducing the viscosity of the working solution, making both the absorption and desorption steps more efficient. On the other hand, increased water levels in the working solution increased the steam duty of the regeneration process. Hence, in the next set of conditions during Phase 2, we further optimized the operation of the SSC by reducing the water content and steam input while keeping the CO_2 capture efficiency at 90%.

Figure 80 describes the steps taken to reduce the water content in the working solution from 23.8 wt. % (end of Condition 8) to 18 wt.% (Condition 9). During the partial dehydration step, the water transfer from the water wash tank (501) to lean lean storage tank (401) was stopped, and the liquid level in the 401 tank was set at 30.5 %. 1% percent drop in the liquid level of the 401 tank corresponds to a 1.5 wt. % decrease in the water content. At 0.5 MW_e, the rate of partial de-hydration was 1.75 wt. % H_2O solvent/hr. Once the desired water content was reached (18 wt.%, Condition 9), liquid level control in 401 tank was switched back to automatic. During condition 9, water was automatically transferred from the water wash tank (501) and the mist separator (602) to the lean storage tank (401). Water level in the working solution was maintained at 18 wt. % while running condition 9.

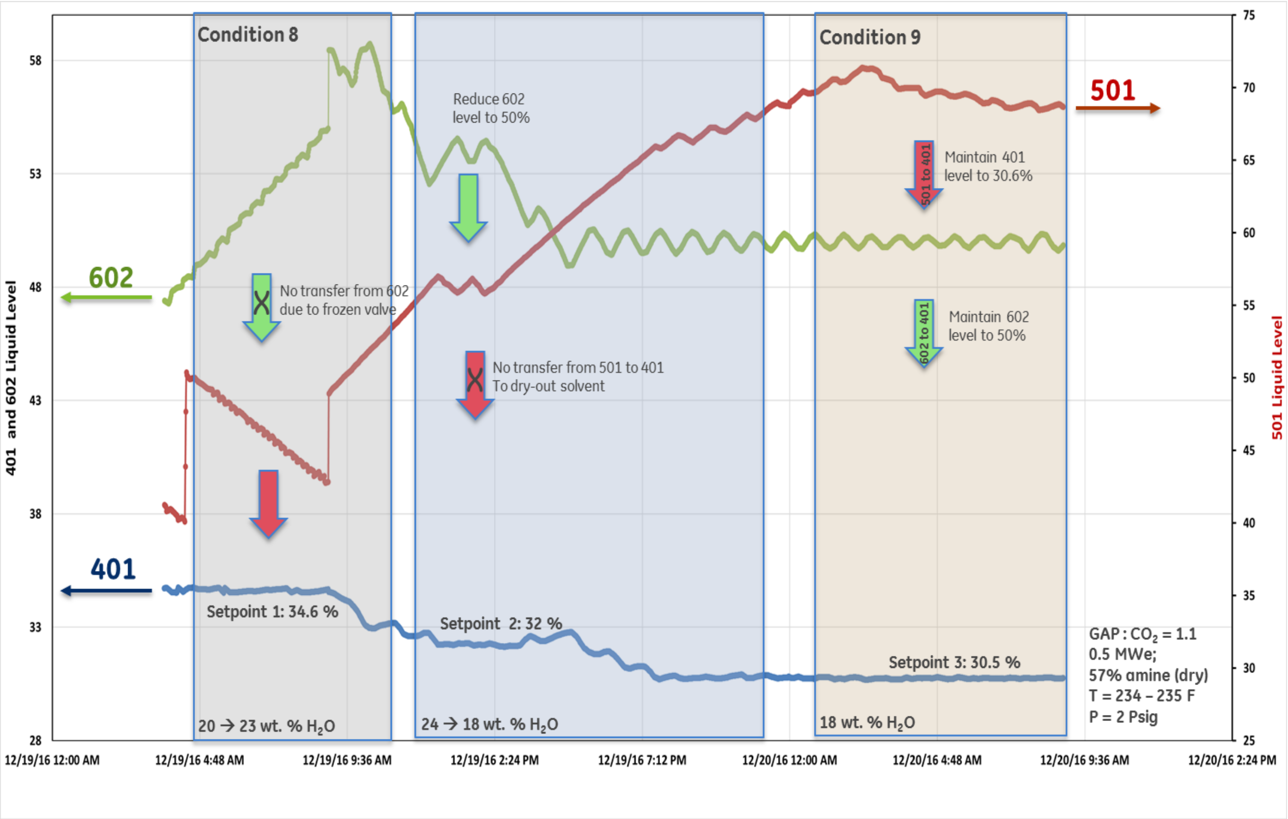

Figure 80. **SSC campaign (Phase 2 - % H_2O Optimization):** Water Management
Table 22 lists process conditions for Conditions 8 and 9.
Tank 501 - water wash tank; **Tank 602** - mist separator (602); **Tank 401** - Lean storage tank.

As part of the optimization, steam input was lowered from 1,900 lb/hr (Condition 8) to 1,300 lb/hr (Condition 9). Furthermore, water content was dropped from 23.8 wt.% (Condition 8) to 18 wt. % (Condition 9). CO_2 capture efficiency was maintained between 87 – 90%. (**Figure 81**) Reduced water content, and optimized steam input increased the specific steam utilization (CO_2/steam) from 0.45 to 0.58, while maintaining the CO_2 capture efficiency at 90%.

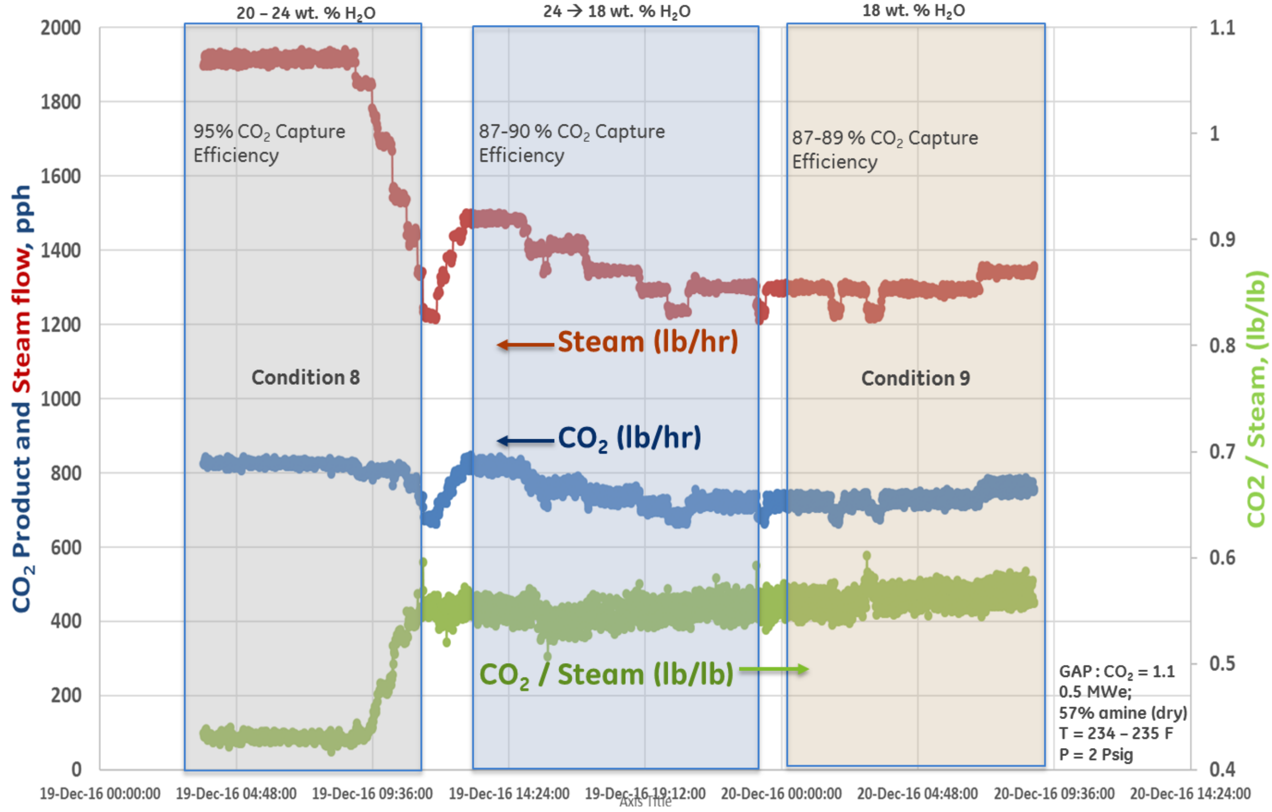

Figure 81. **SSC campaign (Phase 2 - % H_2O Optimization):** Specific steam utilization
Table 22 lists process conditions for Conditions 8 and 9.

Lower steam input and water content in the working solution decreased the steam circulation in the steam stripper column (**Figure 82**). Under Condition 9, only one-third of the regenerator column was under steam conditions, indicating the column is oversized. Optimized conditions reduced also the water carry-over in the total condenser. Most of the steam was condensed in the middle section of the column before reaching the total overhead condenser. (**Figure 83**)

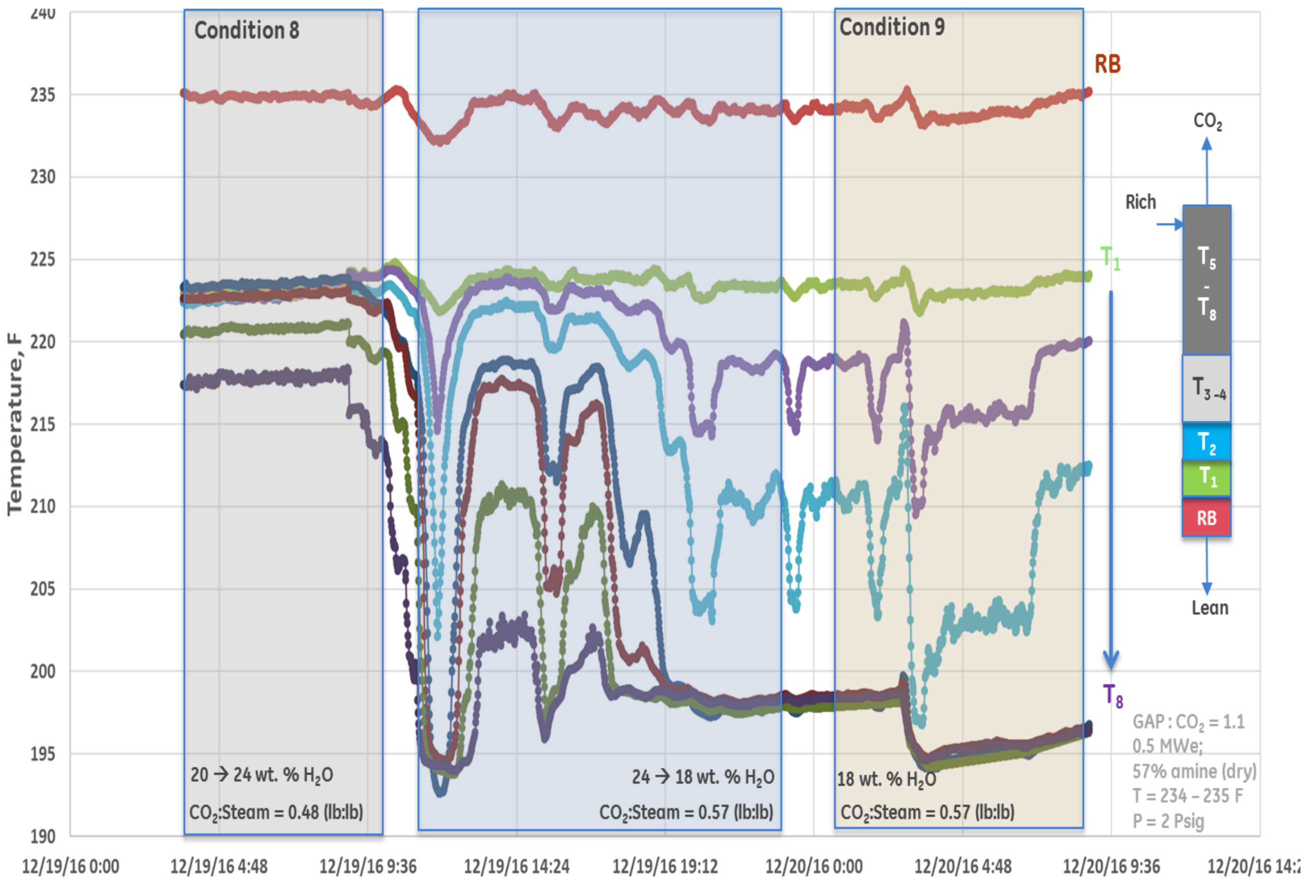

Figure 82. **SSC campaign (Phase 2 - % H_2O Optimization):** SSC temperature profile **Table 22** lists process conditions for Conditions 8 and 9.

In summary, we optimized operation of the SSC by lowering water content in the working solution (from 23 to 18 wt. %) and steam input (1900 lb./hr. to 1,300 lb./hr.) while maintaining CO_2 capture efficiency at 90%. Specific steam utilization was increased by 25 %. Limited water carry-over from the regenerator column occurred under the optimized conditions.

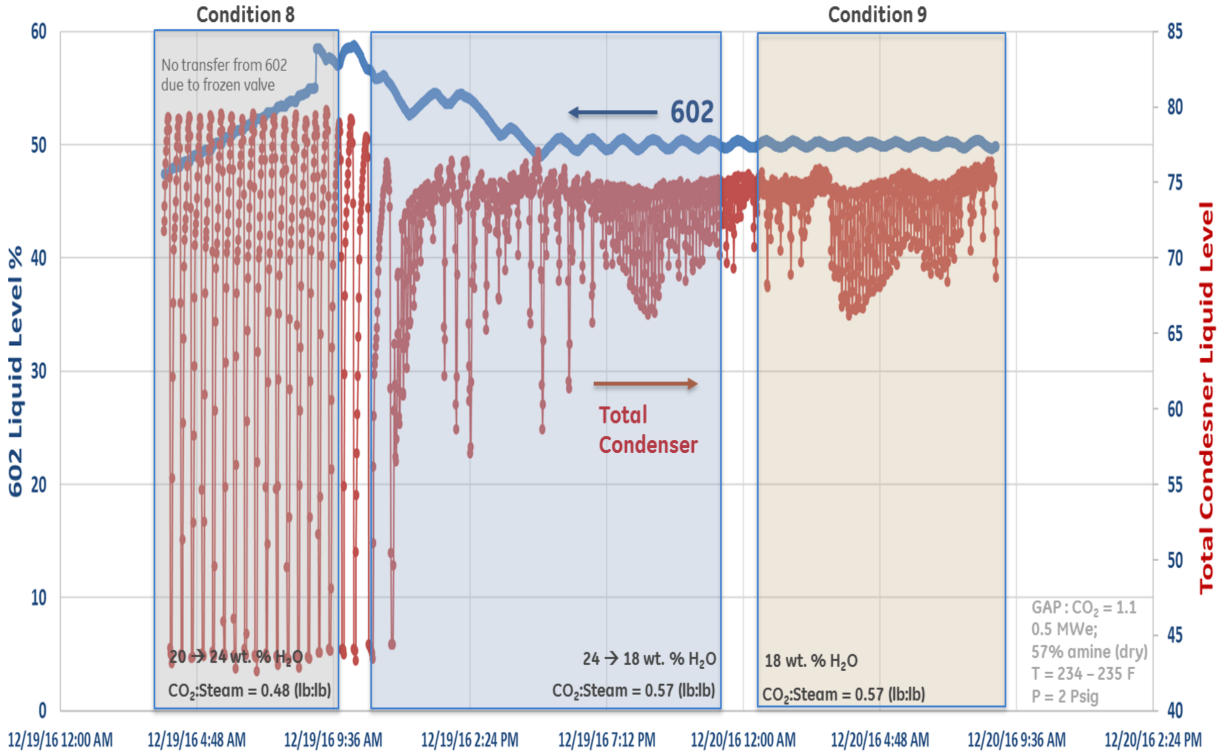

Figure 83. **SSC campaign (Phase 2 - % H_2O Optimization):** Total condenser and mist separator liquid level

Table 22 lists process conditions for Conditions 8 and 9.

4.4.2.4. 0.5 MW_e SSC Campaign (Phase 2): Desorption pressure

Increasing desorption pressure from 2 Psig to 5 Psig had a significant effect on the performance of the GAP-1_m/TEG solvent with SSC. Overall process conditions, and solvent composition are listed in **Table 22** and **Table 24**, respectively. CO_2 capture efficiency dropped from 88% (2 Psig, Condition 9) to 70% (5 Psig, Condition 10) upon pressure increase (**Figure 84**). This significant drop in capture efficiency could be traced back to the effect of pressure on the steam circulation in the steam stripper column (**Figure 85**). One third of the SSC was under steam conditions at 2 Psig desorption (T_1 – T_4 > 200 ^oF). Increased desorption pressure led to a reduced steam circulation in the column, and only 10% of the SSC was under steam conditions (i.e. T_1 > 200 ^oF, T_i < 200 ^oF, i = 2-8). Accordingly, CO_2 loading of the lean solvent leaving the SSC increased from 1.3 wt.% at 2 Psig (Condition 9) to 2.3 wt. % at 5 Psig (Condition 10). Finally, when the flue gas was shut down and solvent was leaned-out, the entire column was under steam conditions (i.e T_1 – T_8 ~ 230 ^oF) as all heat input was utilized for steam generation in the SSC.

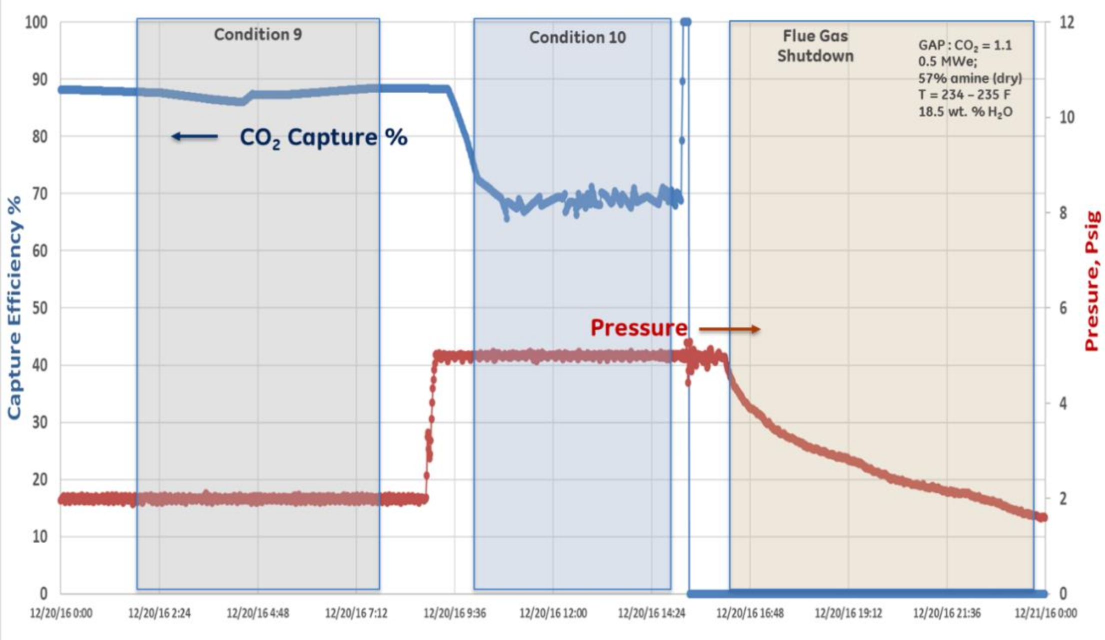

Figure 84. **SSC campaign (Phase 2 – Pressure effect):** CO_2 capture efficiency
Table 22 lists process conditions for Conditions 9 and 10.

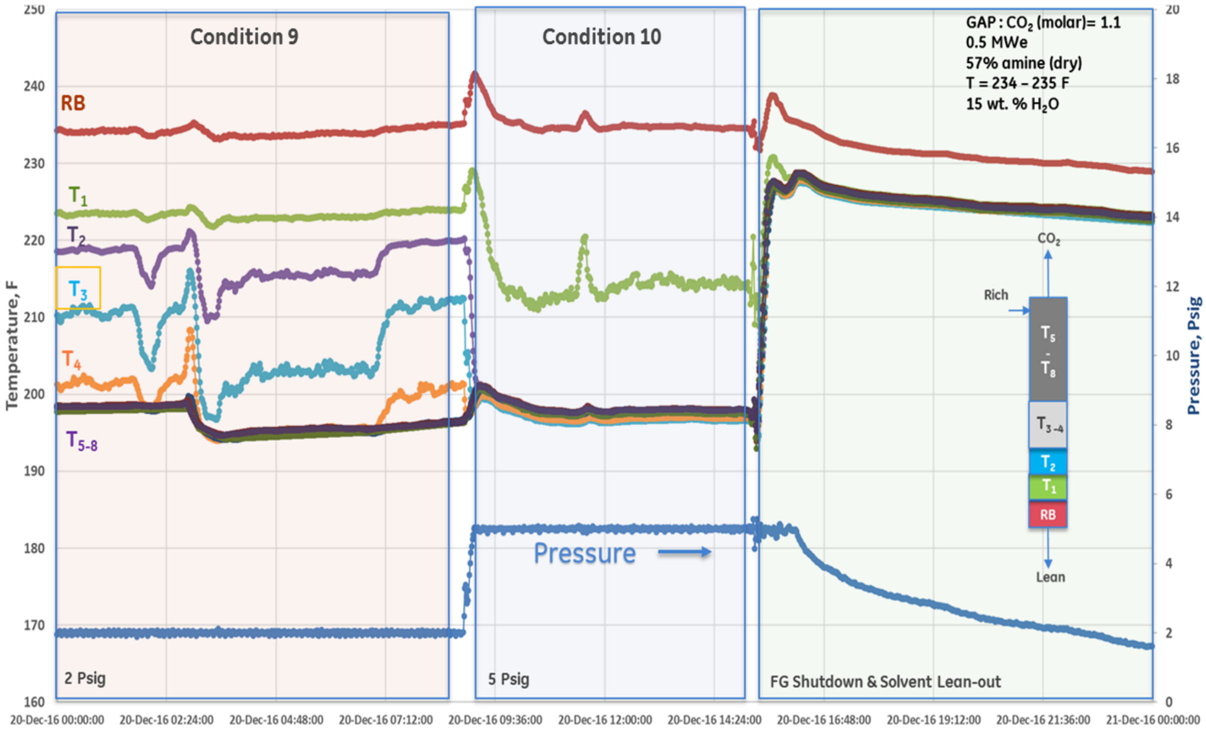

Figure 85. **SSC campaign (Phase 2 – Pressure effect):** SSC temperature profile

Table 22 lists process conditions for Conditions 9 and 10.

Increased desorber pressure lowered CO_2 product flow rate from 750 pph (2 Psig, Condition 9) to 550 pph (5 Psig, Condition 10). Steam input dropped proportionally from 1300 pph (Condition 9) to 1000 pph (Condition 10). Hence, specific steam utilization remained constant (0.55 lb. CO_2 / lb. steam) as a function of pressure, even though steam circulation in the regenerator column was lower at 5 Psig (**Figure 86**). Finally, temperature across the absorber beds was slightly lower (5 ^oF) at 5 Psig, due to overall decreased absorption efficiency (**Figure 87**).

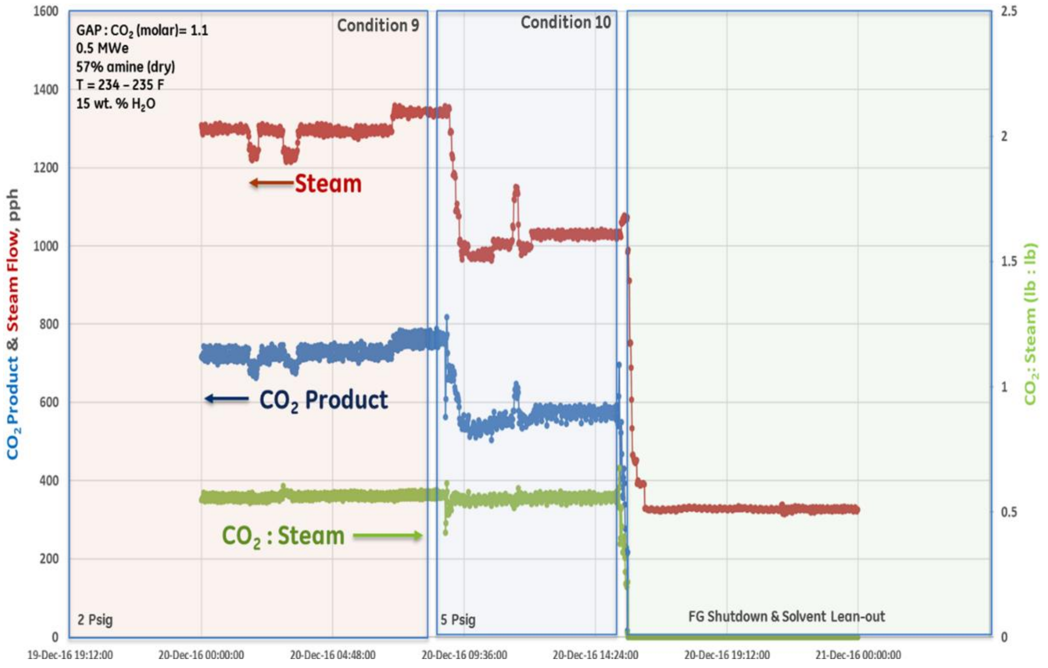

Figure 86. **SSC campaign (Phase 2 – Pressure effect):** Specific steam utilization

Table 22 lists process conditions for Conditions 9 and 10.

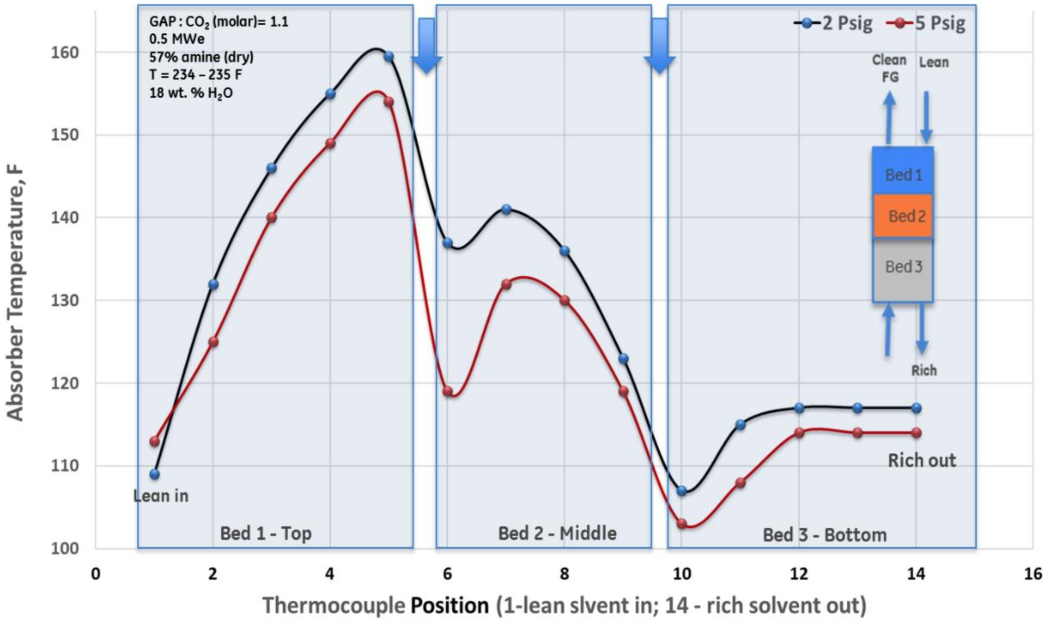

Figure 87. **SSC campaign (Phase 2 – Pressure effect):** Absorber performance

Table 22 lists process conditions for Conditions 9 and 10.

4.4.2.5. 0.5 MW_e SSC Campaign (Phase 2): Summary

Solvent Circulation Effect

Effect of solvent circulation (L : G) was evaluated at constant water content (20 wt.% H_2O), 2 Psig and 235 ^oF desorption conditions. Stoichiometric capture was demonstrated at 0.5 MW_e. Maximum working capacity was 6.1 wt. % (dry basis). Under GAP-1_m excess, most of the absorption occurred in the bottom bed of the absorber. Specific steam utilization (lb. CO_2 / lb. steam) was constant (0.48 - 0.52) as a function of the amine to CO_2 stoichiometry.

0.5 MW_e Demo

Performance of the aminosilicone solvent was demonstrated at 0.5 MW_e with the SSC for 84 hours. Capture efficiency reached 95 – 97% under stoichiometric conditions (GAP-1_m : CO_2 (molar) ~ 1.1), 235 ^oF and two Psig desorption conditions. Active working capacity was 6.1 wt.% (dry basis).

Steam / water optimization

Specific steam utilization was increased by 25 % by lowering water content to 18 wt.% at 90% capture. Under optimized conditions, only 30% of the regenerator column was under the steam conditions, with limited solvent/water carry-over in the overhead total condenser.

Pressure Effect

CO_2 capture efficiency dropped from 90% to 70% upon increasing desorption pressure from 2 to 5 Psig while maintaining amine to CO_2 stoichiometry. At elevated pressures, only 10% of the regenerator column was under steam conditions.

4.4.3. 0.5 MW_e SSC Campaign (Phase 3): Solvent Degradation

Phase 3 of the NCCC steam stripper column campaign was conducted to further optimize performance of the aminosilicone solvent at 0.5 MW_e scale and evaluate solvent degradation (**Figure 88**). First, water content in the working solution was varied between 14 wt. % and 37 wt. % while maintaining molar ratio GAP-1_m : CO_2 between 1.1 to 1.3 and steam input at 1,500 pph. Desorber pressure was kept at 2 Psig, while temperature did not exceed 235 ^oF, to minimize the solvent thermal degradation**.** **Table 27** and **Table 28** list the process conditions and flue gas composition utilized during the campaign.

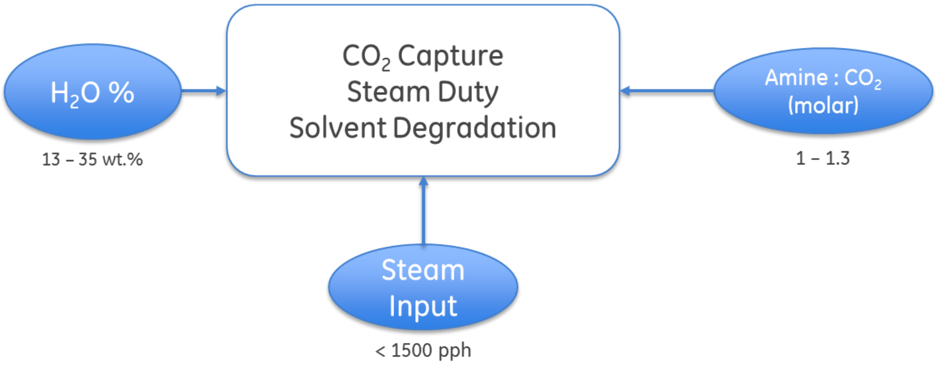

Figure 88. **SSC campaign (Phase 3):** Optimization of H_2O% and probe solvent degradation

Table 27. SSC campaign (Phase 3): Process conditions

Condition	**11**	**12**	**13**	**14**	**15**	**16**	**17**
Objective	Water content & steam optimization						Solvent Circulation
Flue Gas (FG) (lb/hr)	5000	5000	5000	5000	5000	5000	5000
Liquid (lb/hr)	15000	15000	15000	15000	15000	15000	16500
$T_{desorber}$ (F)	226	228	234	234	234	234	234
$P_{desorber}$ (Psi)	2	2	2	2	2	2	2
Water (wt.%)	37	30	23	19	14	17.5	17.5

Water Management: automatic water addition from water wash tank (501) to lean storage tank (401).

Table 28. SSC campaign (Phase 3): Flue gas conditions

	NO	**O_2**	**CO_2**	**NO_2**	**T**
	ppm	vol.%	vol.%	ppm	F
Avg	37.1	6.45	12.78	0.82	138.1
Stdev.	6.9	0.85	0.52	0.2	2.35

Table 29. SSC campaign (Phase 3): Lean solvent composition

Sample	**Total Amine wt.%**		**CO_2 wt.%**	**TEG**	**Water**
	wet	dry	wt.%	wt. %	wt.%
Initial	45.8	57	0.69	30.3	19.8
Condition 11	33	52	0.87	26.3	36.7
Condition 12	37	52	1.14	30.6	29.7
Condition 13	39.4	51	3.82	33.8	22.7
Condition 14	47.2	58.4	1.35	36.8	19.3
Condition 15	50.2	58.3	2.26	33.8	13.9
Condition 16	50.5	60.1	1.55	33	17.5
Condition 17	50.5	60.1	1.55	33	17.5

4.4.3.1. 0.5 MW_e SSC Campaign (Phase 3): Effect of water loading

Performance of the GAP-1_m/TEG working solution with SSC at 0.5 MW_e was further evaluated as a function of a wider range of water loadings in the working solution while probing longer term solvent degradation. Water content was decreased from 37 wt. % (Condition 11, **Table 27 and Table 29**) to 14 wt.% (Condition 15, **Table 27 and Table 29**) by gradually lowering the set point of the liquid level in the lean storage tank (401) while automatically transferring water from the water wash tank (501) and the mist separator tank (602) (**Figure 89**). Rich working solutions were bi-phasic for water content higher than 20 wt. %. SSC operated normally even under high level of water (30 – 35 wt.%). Solvent carry-over was minimized due to a larger disengagement volume of the regenerator. SSC design allowed more flexibility with respect to the water content in the working solution compared to the CSTR.

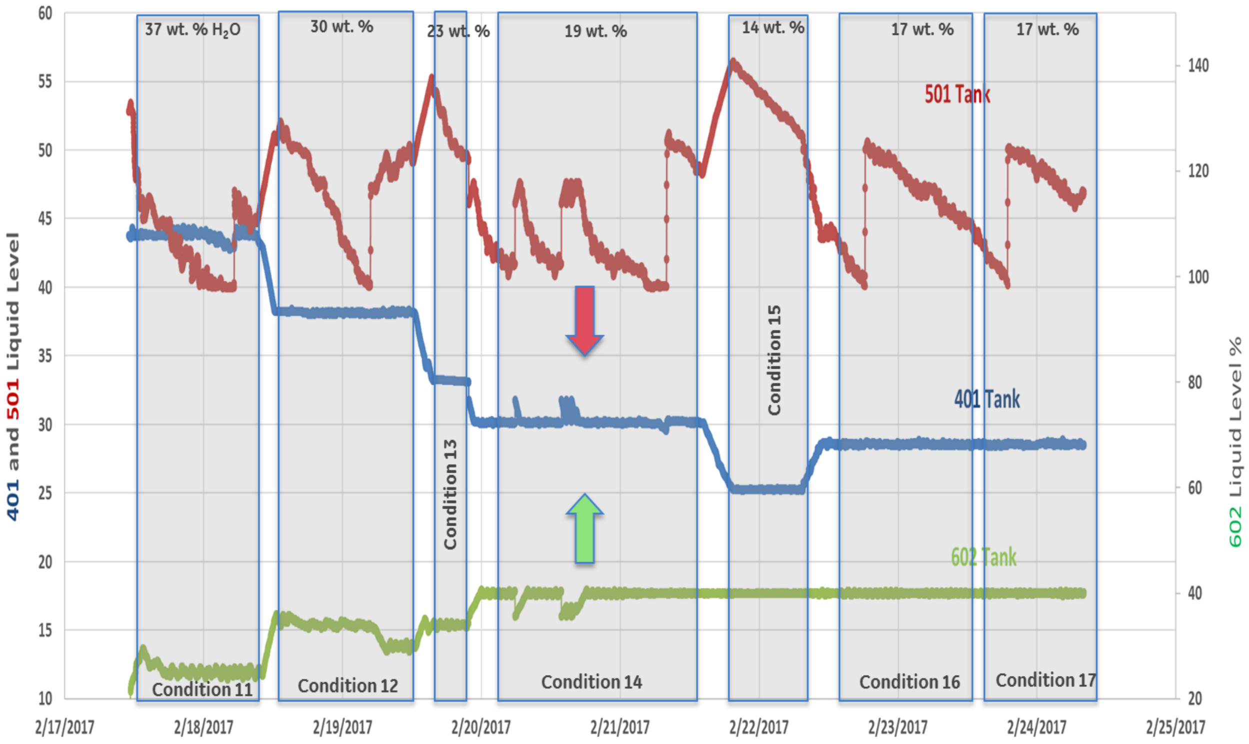

Figure 89. **SSC campaign (Phase 3 – water loading):** Water management

Table 27 lists process conditions for Conditions 11 - 17.

Figure 90 shows the CO_2 capture efficiency plot as a function of the water content in the working solution while maintaining steam input at a maximum of 1500 pph. At the high levels of water (30 wt. % and 37 wt. %), a larger portion of the steam input is utilized for boiling water, and therefore the reboiler temperature did not exceed 227 °F. CO_2 capture efficiency was 78% and 84%, respectively. Upon drying the solvent, reboiler temperature increased to 235 °F, and CO_2 capture efficiency reached a maximum of 88-89% for 17 – 19 wt. % H_2O. At the lowest water content (14 wt.%, Condition 15), CO_2 capture efficiency did not exceed 70%.

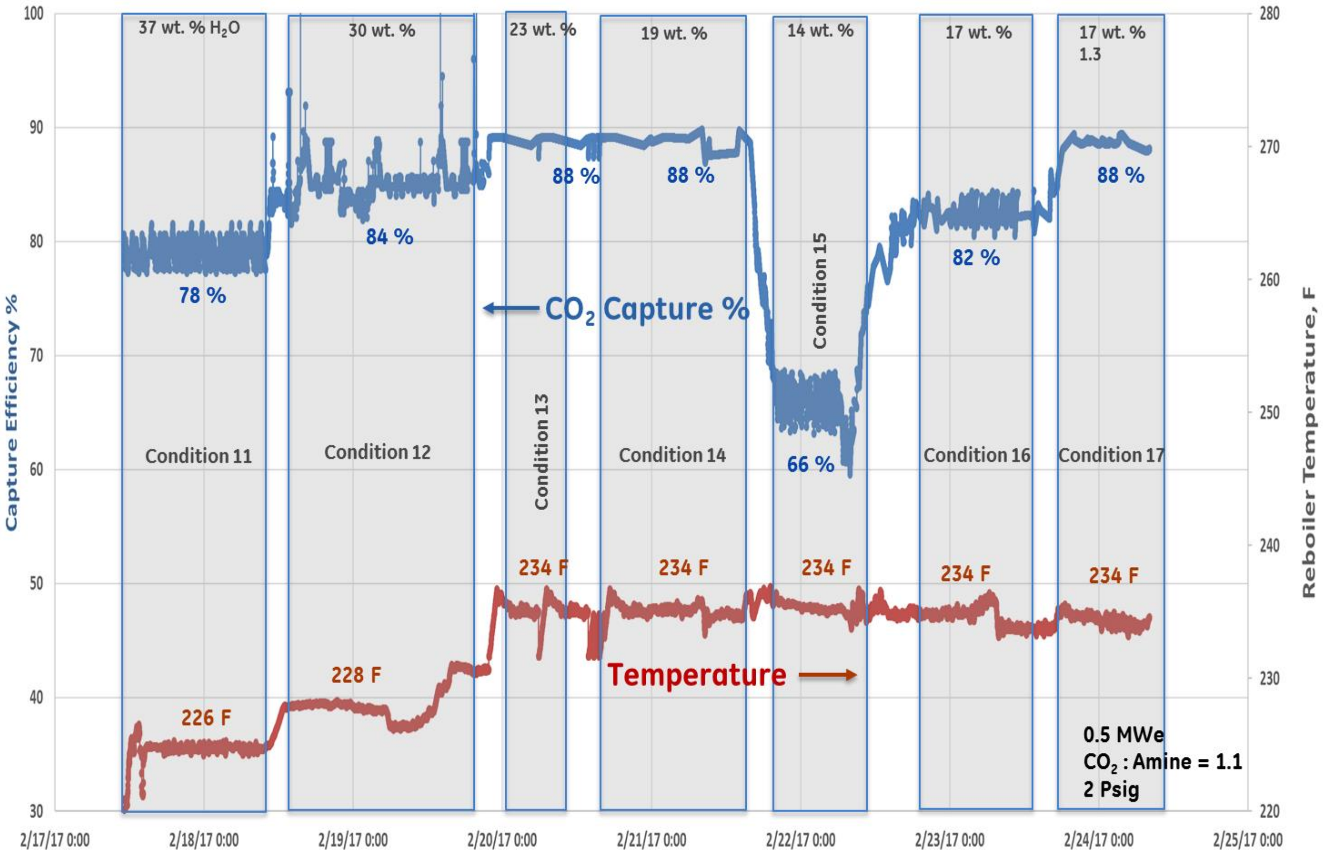

Figure 90. **SCC campaign (Phase 3):** CO_2 Capture efficiency
Table 27 lists process conditions for Conditions 11 - 17

The effects of water loading on the CO_2 capture efficiency can be rationalized based on the performance of both the absorber and steam stripper columns. **Figure 91** shows the temperature profile in the SSC. Upon decreasing water content, only a fraction of the regenerator column is under the steam conditions. Only the first stage from the bottom is under the steam conditions at lower water content, leading to a non-ideal desorption process and lower CO_2 capture efficiency. The optimum conditions are reached at 18-20 % wt. H_2O, when 30% of the column (stages 1-4) is under the steam conditions, and water / solvent carry-over in the overhead is minimized.

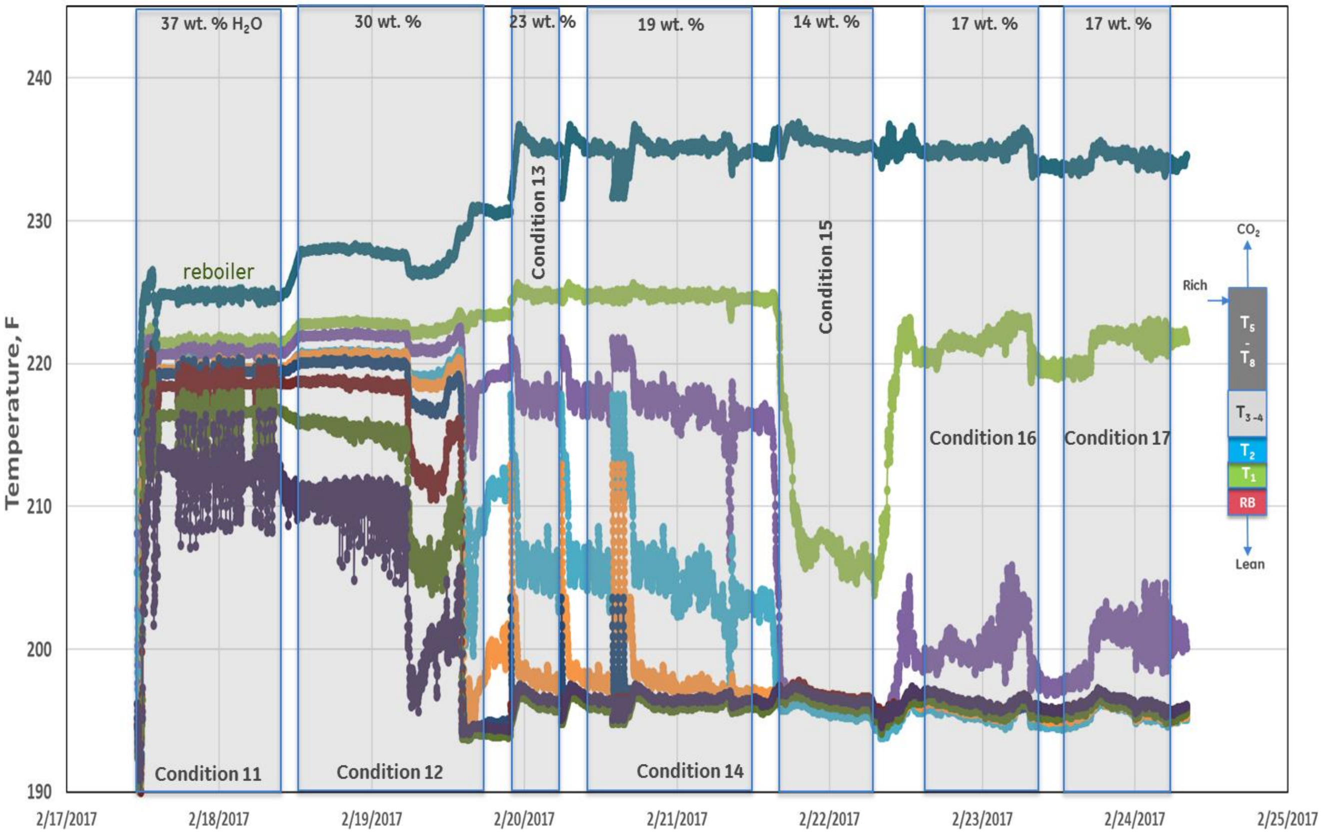

Figure 91. **SCC campaign (Phase 3):** SSC performance
Table 27 lists process conditions for Conditions 11 - 17

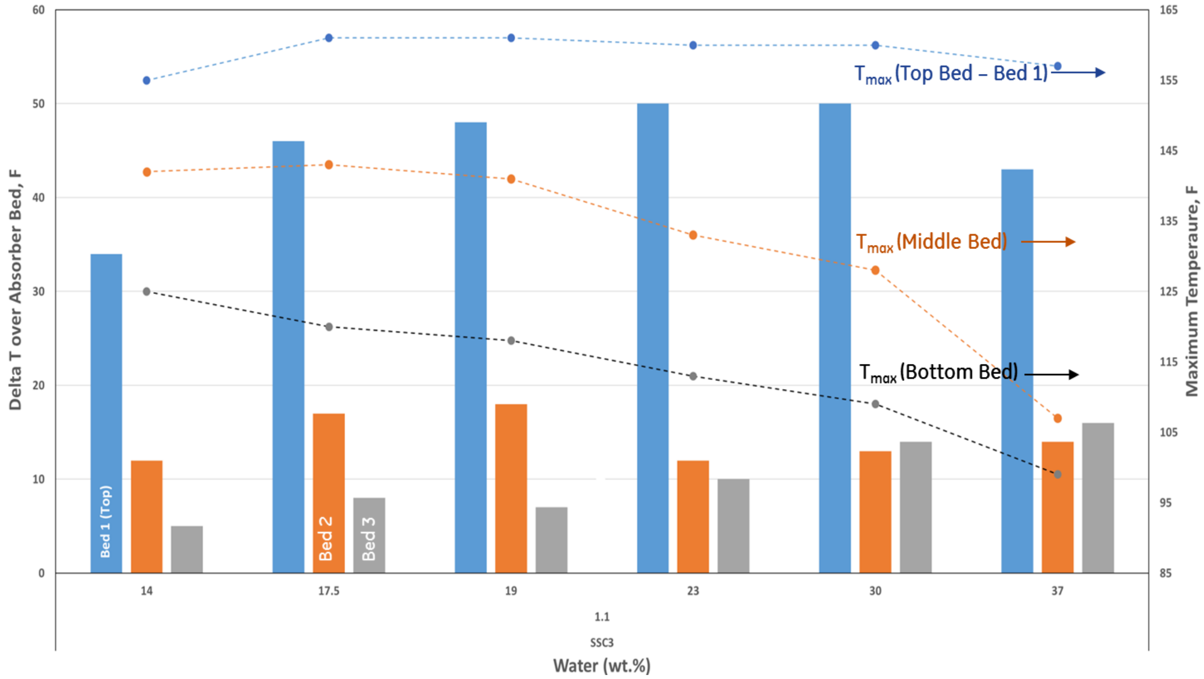

Figure 92. **SCC campaign (Phase 3):** Absorber performance
Table 27 lists process conditions for Conditions 11 - 17

Temperature increase and the maximum temperature in the absorber beds as a function of water loading are shown in **Figure 92**. Maximum absorber temperature in the bottom and middle beds decreased while water content was increased from 14 to 37 wt.%. In the lower bed, the maximum temperature decreased from 125 ^oF (14 wt. % H_2O) to 97 ^oF (37 wt.% H_2O) due to evaporative cooling of water from the liquid to gas phase. At the same time, the top bed was the hottest part of the column (155 – 160 ^oF) indicating that this was the location where most of the absorption occurred.

Finally, **Figure 93** shows the effect of water loading on the specific steam utilization and CO_2 capture efficiency. At 30+ wt.% H_2O, steam utilization is the lowest (CO_2 : Steam = 0.45), as a large extent of steam input is utilized to vaporize the excess water carried-over in the total condenser and mist separator tank. At the lowest water content (14 wt.%), the CO_2 capture efficiency is below 70% due to the insufficient steam circulation in the regenerator column. The water loading for which both the specific steam utilization and CO_2 capture are optimized is reached at 18-20 wt.%. Under these conditions, the regenerator column is operated efficiently with a minimum water / solvent carry-over.

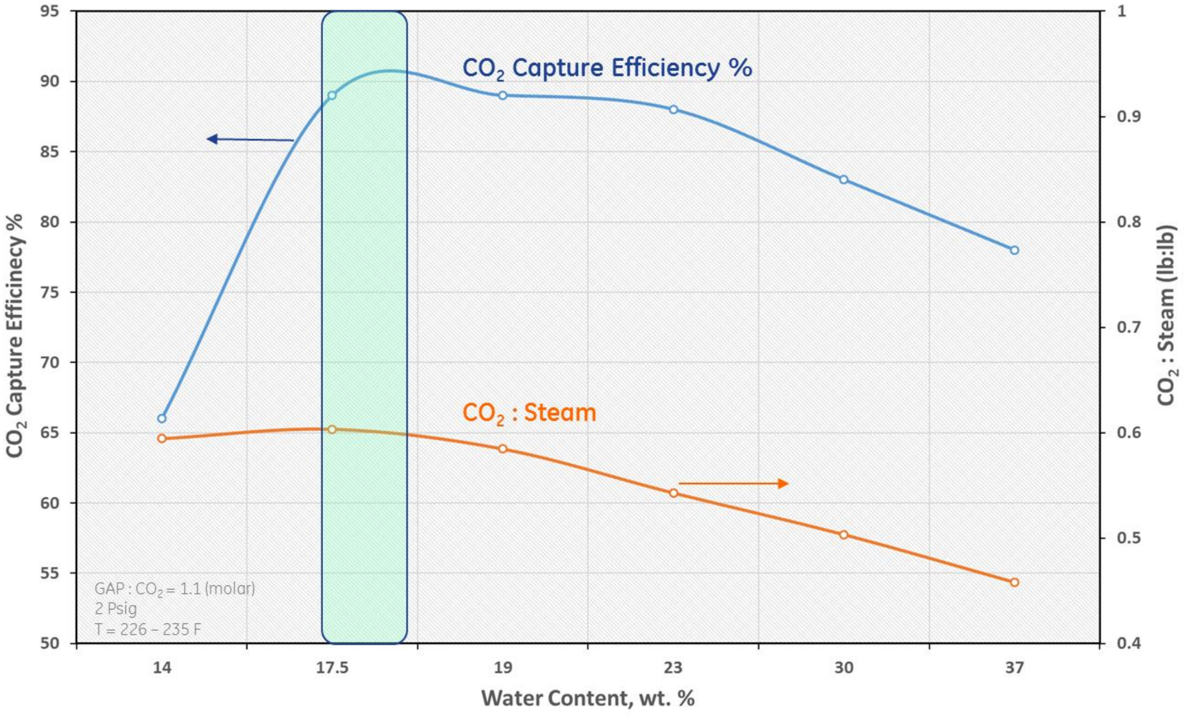

Figure 93. **SCC campaign (Phase 3):** Steam utilization and CO_2 capture efficiency
Table 27 lists process conditions for Conditions 11 - 17

4.4.3.2. 0.5 MW_e SSC Campaign (Phase 3): Solvent degradation

A variety of analyses were conducted to determine how GAP-1_m/TEG solvent mixture performed and changed during both CSTR and SSC campaigns. Solvent performance and degradation during the SSC campaign was monitored based on the following measurements: (i) amine content of the working solution, (ii) ^{1}H NMR and (iii) CO_2 uptake experiments. They provided information on the GAP # of the aminosilicone, mass balance of the components, and urea formation.

Figure 94 shows the absorber samples taken during the SSC campaign. The initial solvent was dark amber because a substantial amount of solvent mixture from the previous CSTR campaign was still in the system. Not enough fresh solvent was available to completely refill the system so a mixture of old and new was used for the SSC campaign. However, the color did not change over time.

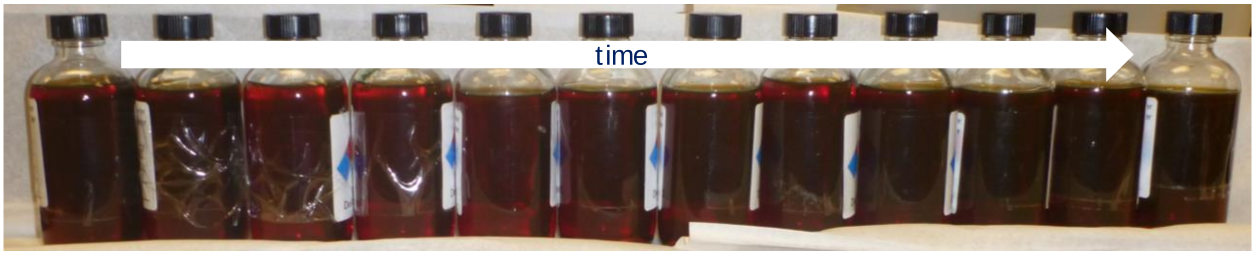

Figure 94. **Solvent Degradation (SSC Campaign):** Absorber samples = f (time)
The dark amber initial color is indicating that the starting solvent of the SSC campaign had been slightly contaminated with used solvent from the CSTR campaign.

Active amine functionality in the GAP-1_m/TEG working solution was monitored during both the CSTR and SSC campaigns. For the CSTR campaign, reboiler temperature varied between 230 °F to 265 °F to maintain CO_2 capture efficiency between 70% - 90%. Water loading was less than 5 wt.%, and desorber pressure was kept at 7 Psig to avoid solvent carry-over. Total run time was more than 360 hours at temperature, before a make-up solvent was added. For the SSC campaign, temperature of the desorber was maintained below 235 °F, while water content varied between 14 to 37 wt.%, and desorption pressure varied between 2 – 5 Psig. Under these conditions, CO_2 capture efficiency varied between 66% – 95%. Total run time for the SSC campaign was 360 hours.

Figure 95 describes the amine content (dry basis) of the GAP-1_m / TEG working solution as a function of time, and desorber temperature for both CSTR and SSC desorbers. The rate of amine degradation strongly depends on the desorption temperature for the CSTR. The rate of degradation was 0.45 wt.% amine / day at temperatures below 240 ^oF, and accelerated to 1.65 wt.% amine / day upon increasing desorption temperature to 265 ^oF. In the case of SSC, amine content oscillated between 57.5 – 60 wt.% for over 350 hours of operation, with the amine degradation measured below 0.05 wt.% / day. This result agrees with our previous accelerated degradation studies indicating that a water loading of more than 10 wt.%, and desorption temperatures lower than 240 ^oF decreased the rate of degradation of the rich solvent by two orders of magnitude.

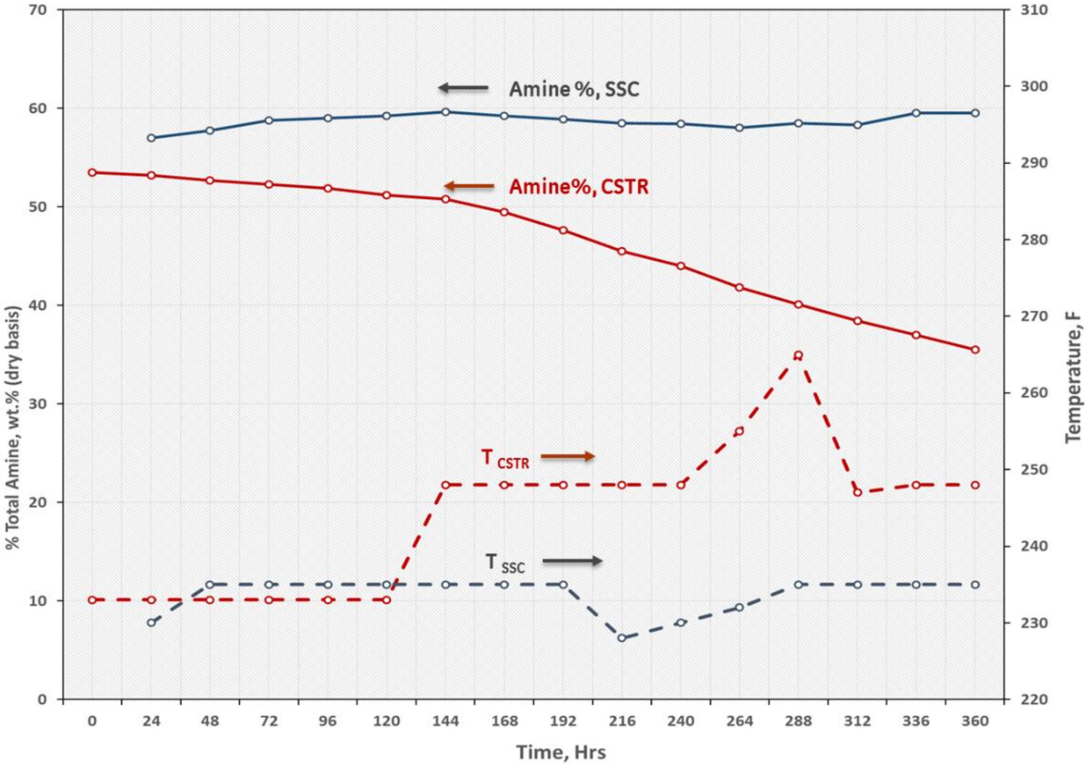

Figure 95. **Solvent Degradation**: CSTR vs. SSC

SSC: $T_{desorber}$ = 230–235 ^oF; P = 2 Psig; 0.25–0.5 MWe, 14-35 wt.% H_2O

CSTR: $T_{desorber}$ = 230 – 248 ^oF; P = 7 Psig; 0.25 – 0.5 MWe, 3-5 wt. % H_2O

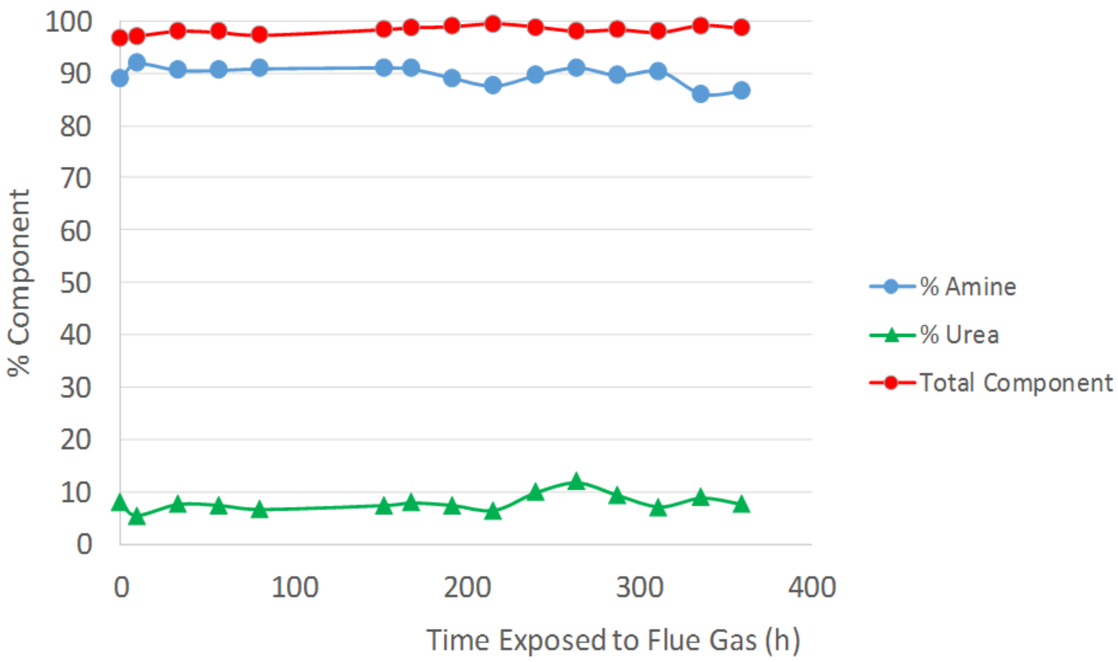

Figure 96. **Solvent Degradation (SSC Campaign):** Urea content by ^{1}H NMR
Process conditions listed in **Table 18**, **Table 22**, and **Table 27**. The non-zero initial value for urea % is indicating that the starting solvent of the SSC campaign had been slightly contaminated with used solvent from the CSTR campaign.

^{1}H NMR analysis of the aged samples allowed the quantification of both active amine and urea content of the solvent. As **Figure 96** shows, there was very little change in the amine content of the solvent and that the urea level also remained low. An average of ~8-9% urea was maintained during operation, and it is likely that very little formed during the SSC campaign because there was ~ 9% present in the starting solvent left from the CSTR campaign as noted above. Greater than 98% of the mass was accounted for from the sum of both the amine and the urea components of the solvent. This indicated that there were no significant side-reactions or losses of material that were unaccounted for.

Hydrothermal equilibration process was also evaluated based on the ^{1}H NMR analysis. GAP-# was calculated based on the ratio of the methylene group adjacent to the Si atom relative to the total number of methyl groups on silicon. The original GAP-1_m/TEG solvent started with a GAP-# of 0.96 indicating that it was very close to the desired starting # of 1. **Figure 97** shows that this value steadily decreased with time. This was expected as a re-equilibration reaction can occur under basic conditions and with heat and water present. This re-equilibration reaction not only generates an aminosilicone with a smaller average GAP-# but also results in the formation of cyclic silicones such as D_4 and D_5. The largest change was in the first 200 hours of operation with the GAP # dropping from 0.96 to 0.41. This is in marked contrast to that seen with the CSTR which showed a GAP # of 0.62 after the same time. The SSC was anticipated to give a higher rate of re-equilibration than the CSTR because of the greater abundance of water present in the system. It appeared that a steady state was being approached with regard to the GAP # after ~ 300 hours with a value of 0.3 being reached.

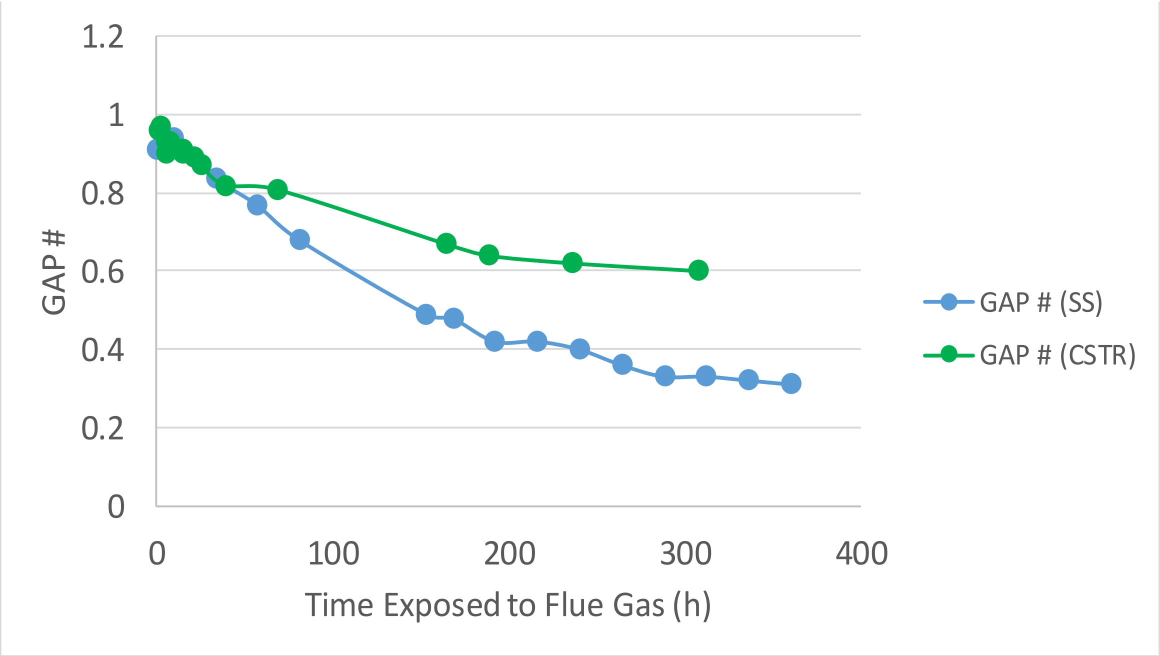

Figure 97. **Solvent Degradation (SSC / CSTR Campaigns):** Hydrothermal equilibration Process conditions listed in **Table 18**, **Table 22**, and **Table 27**. GAP# calculated based on ^{1}H NMR.

While not as large a contributor to the loss of activity as urea formation, undoubtedly, some oxidation of GAP-1_m was likely occurring. The myriad of anticipated decomposition products formed at low levels precluded any identification by NMR and the silicon-containing materials did not provide useful data via GC/MS analysis. An alternate method employed to look for low levels of decomposition products was HPLC Electro Spray Q-ToF MS (high performance liquid chromatography electro spray quadripolar-time of flight mass spectrometry). An absorber sample that had seen significant thermal history was examined by this method and many of the expected compounds like carbamates, amines, ureas and silanols were seen. In addition to those, identification of oxidation products were also sought. These included olefins from ammonia loss, hydroxylamines, nitroso and N-nitroso compounds, nitrates and sulfonic amides shown below.

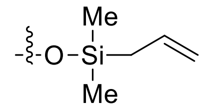

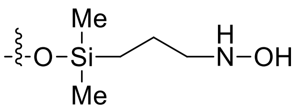

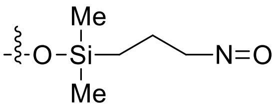

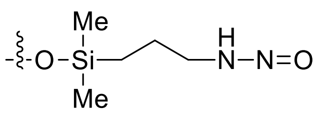

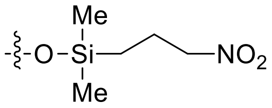

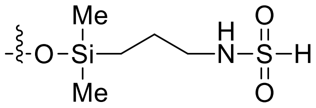

Surprisingly, none of these species were detected, indicating that, if any of these products were produced, they were at very low levels. Both positive and negative ionization techniques were employed. The positive mode showed substantial levels of GAP and silanols homologs as noted above (**Figure 98** / **Figure 99**).

Finally, metals analyses were performed on the sample of solvent from the CSTR campaign. It was thought that, given the harsher conditions in the CSTR than the SSC, that any metal contamination would be greater in these samples than those from the SSC campaign. **Table 30** shows that, except for low levels of iron, little metal contamination was present.

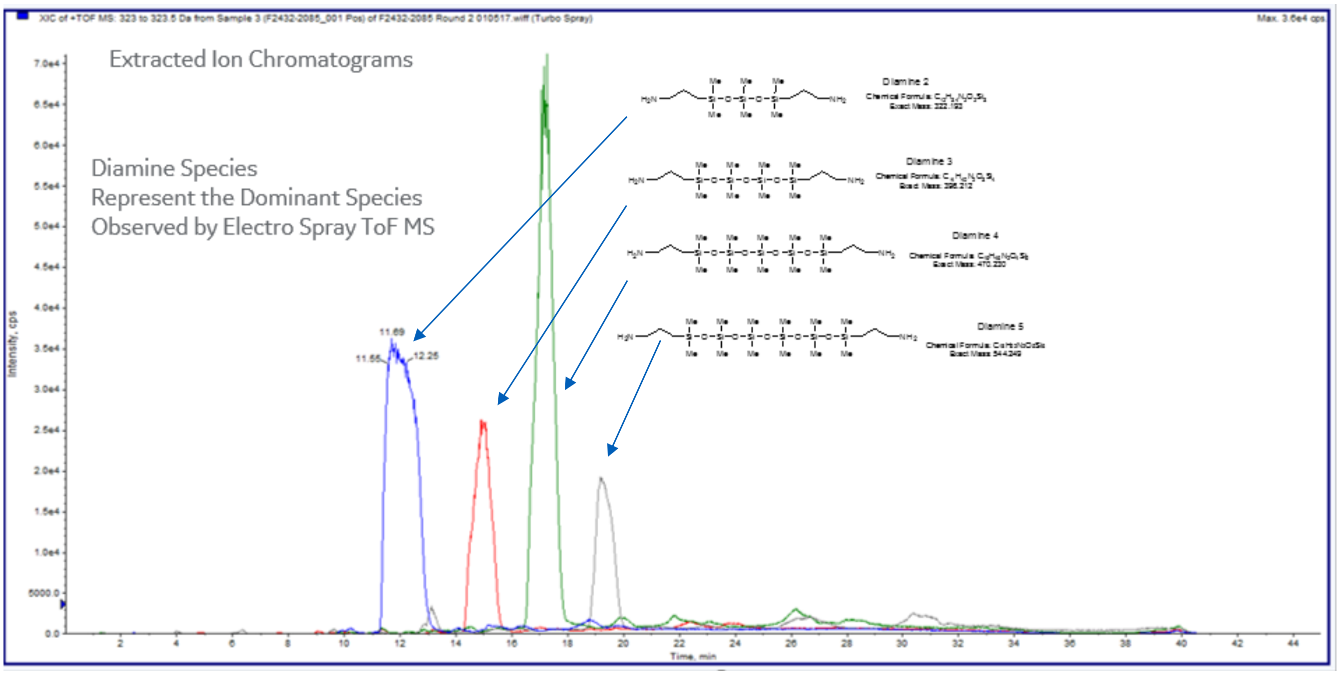

Figure 98. **Solvent Degradation (SSC Campaign):** GAP-X species
Species detected by HPLC Electro Spray Q-ToF MS

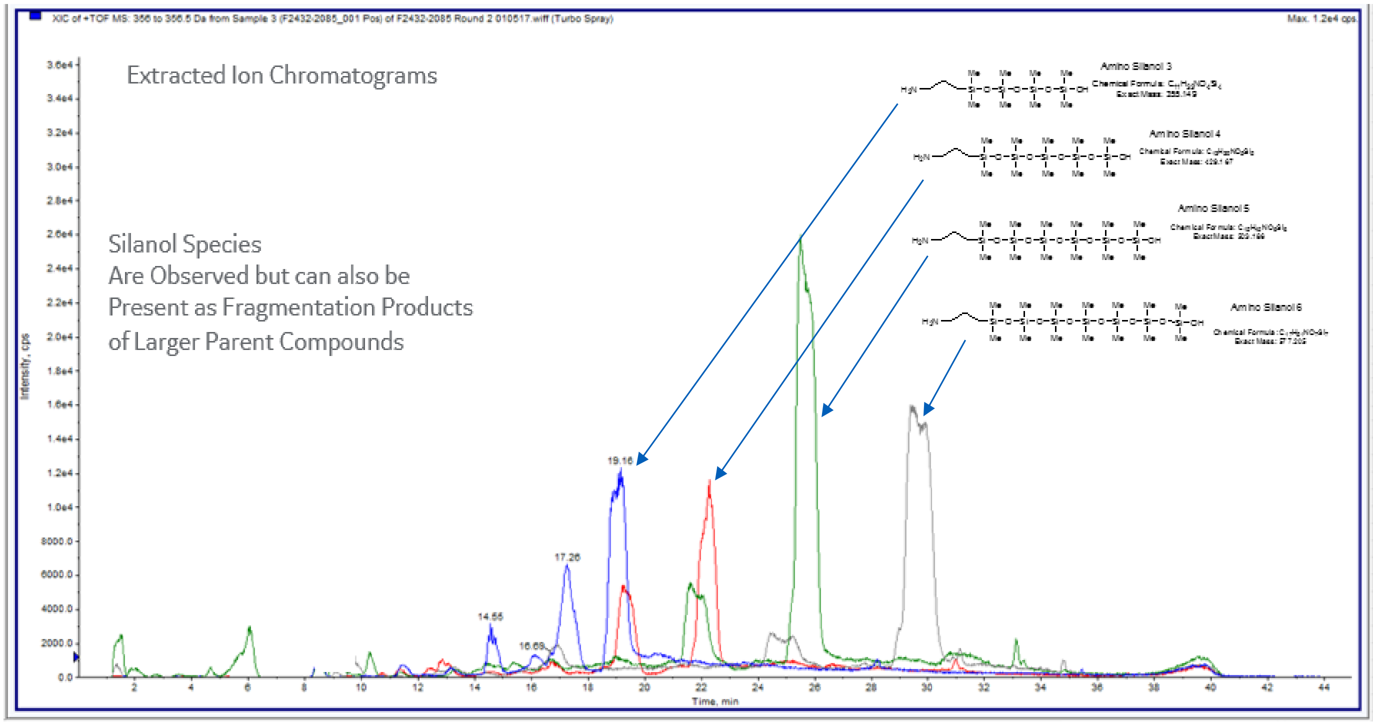

Figure 99. **Solvent Degradation (SSC Campaign):** GAP-silanol species
Species detected by HPLC Electro Spray Q-ToF MS

Table 30. **Solvent Degradation (SCR Campaign):** Metal Analysis

nple ID	LIMS ID	Rep	Al µg/g	Ba µg/g	Be µg/g	Ca µg/g	±95% CI [†]	Cd µg/g	Co µg/g	Cr µg/g	±95% CI [†]	Cu µg/g	Fe µg/g	±95% CI [†]
32-94-1628	S17-00850	A	1<x<3	<0.5	<0.9	3	±1	<0.5	<0.5	0.6	±0.2	<1	4.9	±0.3
		B	1<x<3	<0.5	<0.9	3	±1	<0.5	<0.5	0.6	±0.2	<1	4.9	±0.3
		C	1<x<3	<0.5	<0.9	3	±1	<0.5	<0.5	0.6	±0.2	<1	5.2	±0.3
		Mean[a]	**1<x<3**	**<0.5**	**<0.9**	**3**		**<0.5**	**<0.5**	**0.6**		**<1**	**5.0**	
		SD				0.4				0.02			0.2	
32-94-1925	S17-00851	A	1<x<3	<0.5	<0.9	4	±1	<0.5	<0.5	0.9	±0.2	<1	12.5	±0.3
		B	1<x<3	<0.5	<0.9	3	±1	<0.5	<0.5	0.9	±0.2	<1	12.6	±0.3
		C	1<x<3	<0.5	<0.9	3	±1	<0.5	<0.5	0.9	±0.2	<1	12.5	±0.3
		Mean[a]	**1<x<3**	**<0.5**	**<0.9**	**4**		**<0.5**	**<0.5**	**0.9**		**<1**	**12.5**	
		SD				0.8				0.01			0.1	
32-94-2103	S17-00852	A	1<x<3	<0.5	<0.9	4	±1	<0.5	<0.5	<0.2		<1	0.3<x<0.9	
		B	1<x<3	<0.5	<0.9	<1		<0.5	<0.5	<0.2		<1	0.3<x<0.9	
		C	1<x<3	<0.5	<0.9	<1		<0.5	<0.5	<0.2		<1	0.3<x<0.9	
		Mean[a]	**1<x<3**	**<0.5**	**<0.9**	**1<x<3**		**<0.5**	**<0.5**	**<0.2**		**<1**	**0.3<x<0.9**	
		SD												

nple ID	LIMS ID	Rep	K µg/g	Li µg/g	Mg µg/g	±95% CI [†]	Mn µg/g	Na µg/g	±95% CI [†]	Ni µg/g	Sr µg/g	V µg/g	Zn µg/g
32-94-1628	S17-00850	A	<3	<0.5	2.4	±0.5	<0.5	0.5<x<1.5		<0.9	<0.5	<0.5	<0.9
		B	<3	<0.5	2.4	±0.5	<0.5	0.5<x<1.5		<0.9	<0.5	<0.5	<0.9
		C	<3	<0.5	2.4	±0.5	<0.5	0.5<x<1.5		<0.9	<0.5	<0.5	<0.9
		Mean[a]	**<3**	**<0.5**	**2.4**		**<0.5**	**0.5<x<1.5**		**<0.9**	**<0.5**	**<0.5**	**<0.9**
		SD			0.02								
32-94-1925	S17-00851	A	<3	<0.5	3.0	±0.5	<0.5	2.2	±0.5	<0.9	<0.5	<0.5	<0.9
		B	<3	<0.5	3.3	±0.5	<0.5	2.2	±0.5	<0.9	<0.5	<0.5	<0.9
		C	<3	<0.5	3.2	±0.5	<0.5	2.0	±0.5	<0.9	<0.5	<0.5	<0.9
		Mean[a]	**<3**	**<0.5**	**3.2**		**<0.5**	**2.1**		**<0.9**	**<0.5**	**<0.5**	**<0.9**
		SD			0.1			0.1					
32-94-2103	S17-00852	A	<3	<0.5	<1		<0.5	4.8	±0.5	<0.9	<0.5	<0.5	<0.9
		B	<3	<0.5	<1		<0.5	4.9	±0.5	<0.9	<0.5	<0.5	<0.9
		C	<3	<0.5	<1		<0.5	4.9	±0.5	<0.9	<0.5	<0.5	<0.9
		Mean[a]	**<3**	**<0.5**	**<1**		**<0.5**	**4.9**		**<0.9**	**<0.5**	**<0.5**	**<0.9**
		SD						0.04					

4.4.3.3. 0.5 MW_e SSC Campaign (Phase 3): Gas Analysis

Gas adsorption samples were collected downstream from the water wash tower (Condition 14, **Table 27**) by passing the vapor effluent through a condensing system. The condensate was collected, and the vapor slip from the condenser was captured on gas adsorption tubes. Details of the gas adsorption tubes are shown in **Table 31**. At each sampling interval, two tubes of each type were sampled, and all tubes were shipped to GE for analysis.

Table 31. **Gas Analysis (SSC Campaign):** Adsorbent tubes for water wash vapor sampling

Adsorbent type	Tube size (mm)	Vendor	Analysis Company	Analytes of interest
226-10-06	6x70	SKC, Inc.	Analytics Corp.	Ammonia
226-30-18	6x70	SKC, Inc.	Analytics Corp.	Methyl amine, Ethyl amine
226-119	6x100	SKC, Inc.	Analytics Corp.	Formaldehyde, Acetaldehyde
226-01	6x70	SKC, Inc.	Analytics Corp.	Ketones (Acetone)
32010001	N/A	Ellutia, Inc.	RJ Lee	Nitrosodimethylamine, Nitrosodiethylamine, Nitromethylethylamine, Nitrosodi-n-propylamine
Carbotrap 300 (GE-supplied)	6x178	Gerstel	GE	Aminosilicone, Carbamate, TEG, D4, D5, D6, Ethylene oxide, Ethylene glycol, Dimethyl aminopropyl silanol

The results of gas adsorption analysis are shown in **Table 32**. Nitrosamines not listed were not detected above the limit of quantification of 0.011ug/tube in any samples. The analysis for ethylene glycol, D4, D5, and D6 was not quantitative. These species were detected in all samples for CSTR and SSC samples. Ammonia formation was reduced by 75% in the SSC due to a lower absorber temperature. This is also reflected in the lower amine degradation during the SSC campaign.

Table 33 lists the composition of the CO_2 stream measured for two of the conditions ran during the CSTR and SSC campaign, respectively. In both cases the CO_2 purity was above 99%. The CO_2 stream obtained during the SSC run had lower oxidation / contamination by-products. These results can be attributed to the lower desorption temperature of the SSC.

Table 32. **Gas Analysis (SSC and CSTR):** Clean flue gas composition

Analyte	units	10/21/2016	2/21/2017
		CSTR	SSC
Formaldehyde	ppm	0.00383	< 0.003
Ammonia	ppm	42.1	10
Acetaldehyde	ppm	Not Analyzed	0.682
Acetone	ppm	8.51	< 0.351
Ethylamine	ppm	< 0.181	< .181
Methylamine	ppm	< 0.262	< . 262
N-nitrosodi-n-propylamine	ug /tube	< 0.0011	< 0.0011
N-nitrosomethylamine	ug/tube	0.018	0.0193
EG	Presence	Present	Present
D4	Presence	Present	Present
D5	Presence	Present	Present
D6	Presence	Present	Present

SSC: $T_{desorber}$ = 235 °F; P = 2 Psig; 0.5 MWe, 18 wt.% H_2O, GAP-1 : CO_2 ~ 1.1
CSTR: $T_{desorber}$ = 262 °F; P = 7 Psig; 0.5 MWe, 3-7 wt. % H_2O, GAP-1 : CO_2 ~ 1.5

Table 33. **Gas Analysis (SSC and CSTR):** CO_2 steam

Desorber			**CSTR**	**Steam Stripper**
Test Date			**10/11/2016***	**Conditon 14**
		LOQ		
CO2 purity	vol%	5	99.4+	99+
H2	ppmv	10	ND	
O2 + Ar	ppmv	10	98	180
N2	ppmv	10	3200	1600
CO	ppmv	2	2.4	ND
Ammonia	ppmv	0.5	1	ND
NOx	ppmv	0.5	1.5	ND
NO	ppmv	0.5	na	ND
NO2	ppmv	0.5	na	ND
Total HCs	ppmv as CH4	0.1	1700	700
Total non-methane HCs	ppmv as CH4	0.1	1700	700
Methane	ppmv	0.1	0.9	0.2
Acetaldehyde	ppmv	0.05	27	6.6
Aromatic HCs	ppb as C6H6	2	ND	ND
Total Sulfur content	ppmv	0.05	trace	ND
SO2	ppmv	0.05	ND	ND
HCN	ppmv	0.2	ND	ND
Ethane	ppmv	0.1	0.1	ND
Propylene	ppmv	0.1	78	3.3
Hexanes +	ppmv	0.1	240	110
H2S	ppmv	0.01	trace	ND
Propionaldehyde	ppmv	0.1	54	15
Acetone	ppmv	0.1	27	2.1
Methanol	ppmv	0.1	17	ND
t-butanol	ppmv	0.1	ND	ND
Ethanol	ppmv	0.1	0.1	0.2
Methyl Ethyl Ketone	ppmv	0.1	0.7	ND
2-Butanol	ppmv	0.1	150	84
Isoamyl Acetate	ppmv	0.1	trace	1.4
Unknown VOX	ppmv	0.1	210	ND
Decamethylcyclopentasiloxane (D5)	ppmv	0.02	not analyzed	1.6
Hexamethylcyclotrisiloxane (D3)	ppmv	0.02	not analyzed	ND
Octamethylcyclotetrasiloxand (D4)	ppmv	0.02	not analyzed	ND
Trimethyl silanol	ppmv	0.02	not analyzed	ND

SSC: $T_{desorber}$ = 235 °F; P = 2 Psig; 0.5 MWe, 18 wt.% H_2O, GAP-1 : CO_2 ~ 1.1
CSTR: $T_{desorber}$ = 262 °F; P = 7 Psig; 0.5 MWe, 3-7 wt. % H_2O, GAP-1 : CO_2 ~ 1.5

4.4.3.4. 0.5 MW$_e$ SSC Campaign (Phase 3): Corrosion studies

Prior results established that under the most aggressive process conditions examined (CSTR desorber conditions: 140 °C, 1 bar air/CO_2, 3 wt% H_2O) CS1018 carbon steel coupons exhibited a high corrosion rate of approximately 2.2 mm/year. Under similar conditions, 304L stainless steel coupons exhibited corrosion rates that were indistinguishable from the control condition.

A series of 304L stainless steel (1.25" ID) and C1018 carbon steel coupons was placed in multiple locations of the PSTU (absorber tower, wash tower, rich lean heat exchanger, CSTR desorber and SSC desorber) at the beginning of the CSTR campaign. All coupons were collected at the end of the SSC campaign. The time accumulated for the absorber and rich/lean HX coupons was 900 hours, including both the CSTR and SSC campaigns. CSTR coupons accumulated 500 hours while SSC coupons accumulated 400 hours. The coupons were then cleaned according to the procedure listed in ASTM G1-03. Specifically, the coupons were exposed to the cleaning solution for 10 minutes, rinsed with deionized water, dried in a vacuum oven at 100 °C for 30 minutes, and weighed. The cleaning procedure was repeated until the slope of the weight loss vs. cleaning cycle curve matched that of control samples. (**Figure 100 and Figure 101).**

Figure 102 shows the corrosion rates for 304L SS and CS1018 coupons placed in various locations of the PSTU. 304L stainless steel was corrosion resistant under all the conditions tested, while CS1018 coupons showed a differentiation in corrosion rates as a function of location. Corrosion rates under CSTR and SSC conditions were similar. It is conceivable that higher CSTR temperatures and CO_2 loading of the lean solvent are being balanced out by the higher water content in the working solution for the SSC. The highest rate of corrosion was recorded under the absorber conditions, due to higher oxygen content. Minimal corrosion rates were measured under the rich lean HX conditions (lean side). For both absorber and rich/lean HX, the corrosion rates were averaged over both CSTR and SSC campaigns. However, corrosion rates for CS1018 are 50 – 75 %

lower than the values reported for a typical MEA plant. (HYDROCARBON PROCESSING, April 1993, pages 75-80 and May 1993 issue, pages 89-94.)

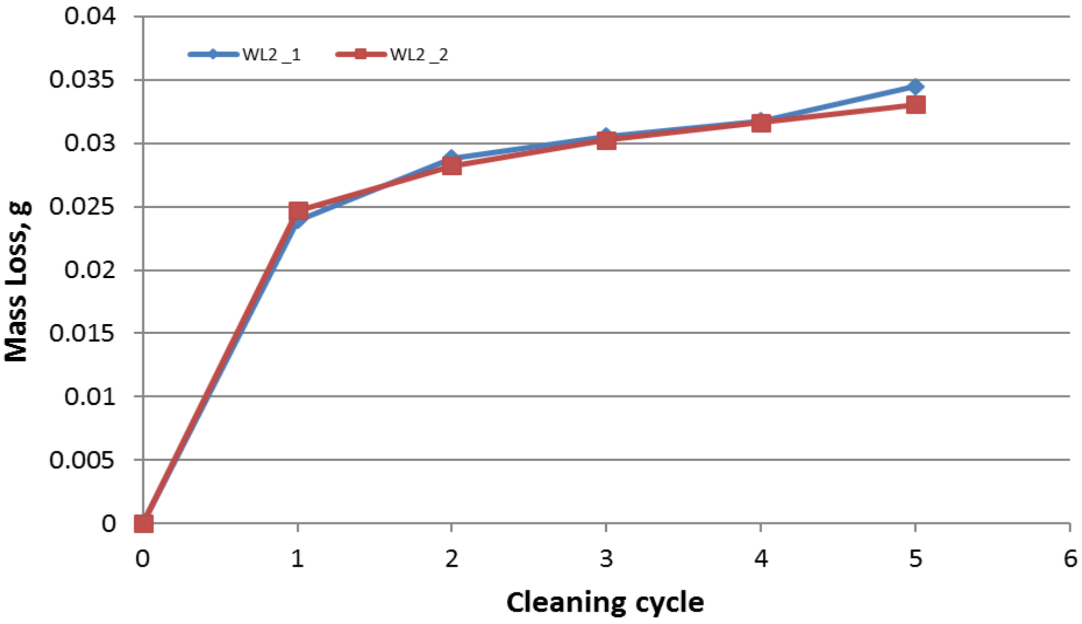

Figure 100. **Corrosion studies (SSC and CSTR):** Mass loss vs. cleaning cycle for CS1018 Absorber coupons / ASTM G1-03 Cleaning Procedure

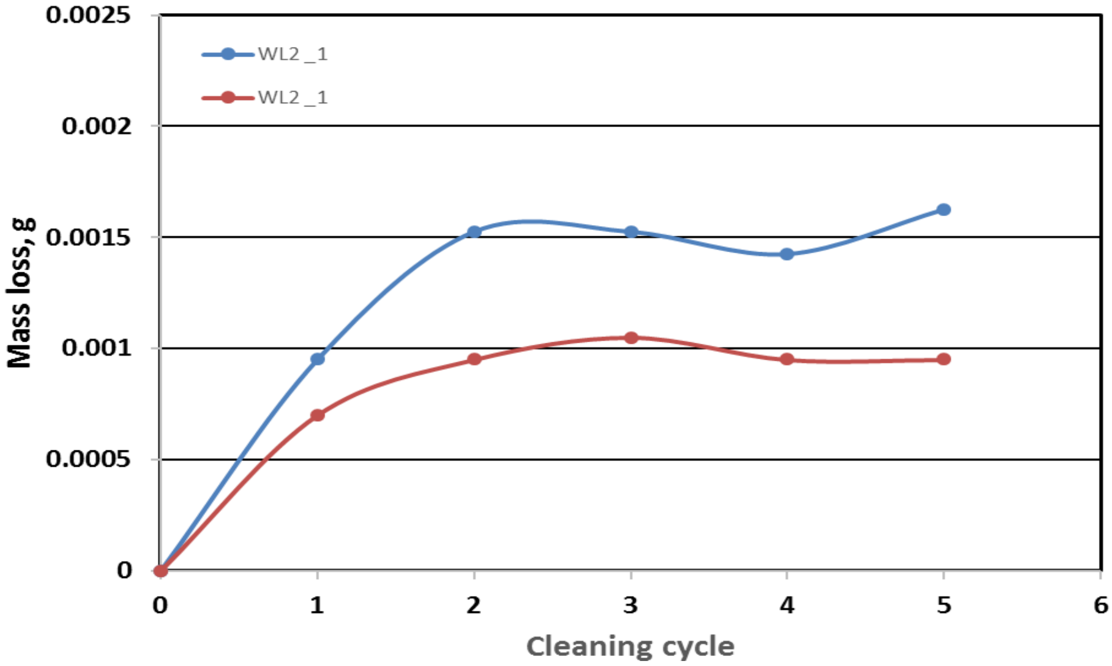

Figure 101. **Corrosion studies (SSC and CSTR): Mass loss vs. cleaning cycle for 304L SS**

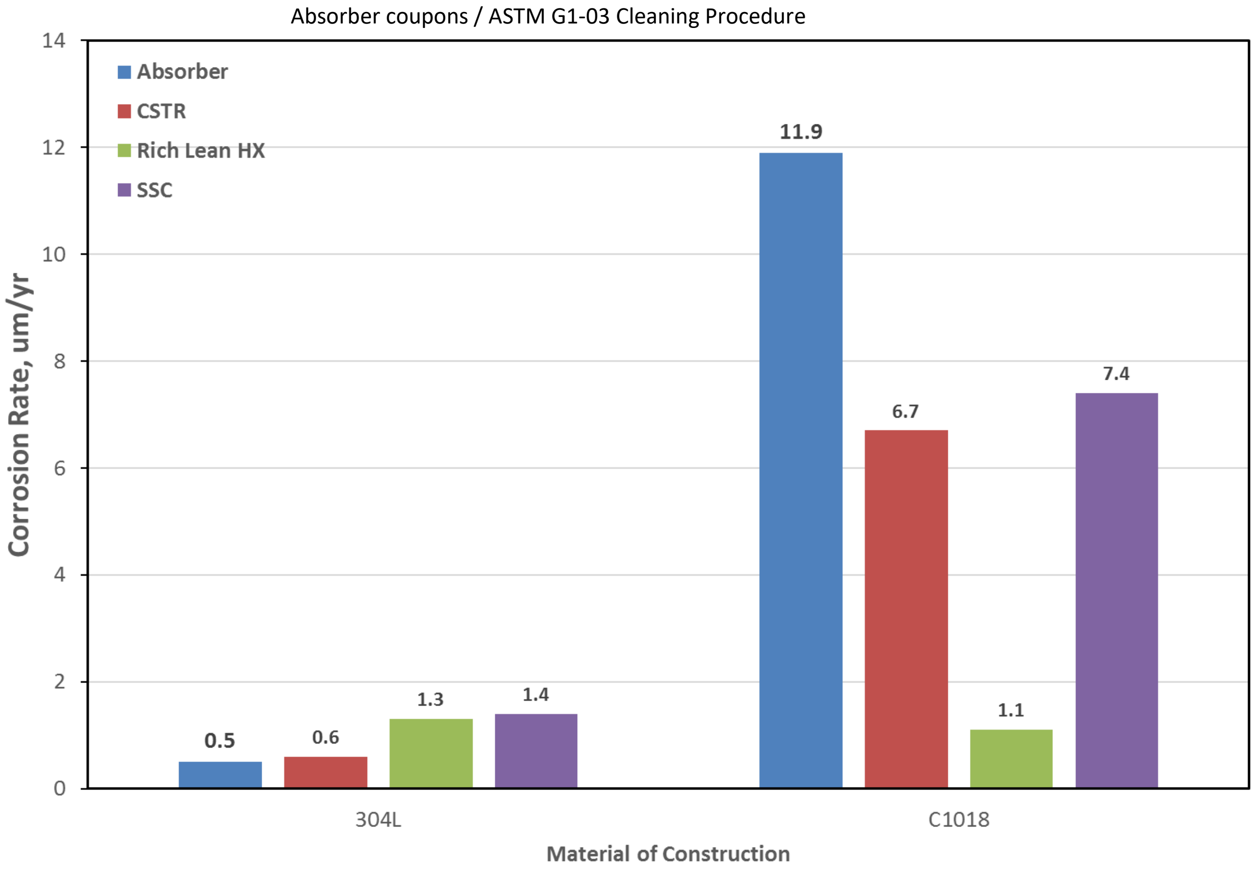

Figure 102. Corrosion rates (SSC and CSTR): 304L SS vs. C1018 at different positions in PSTU

4.4.3.5. MEA vs. Aminosilicone (CSTR and SSC) at 0.5 MW_e

GAP-1_m/TEG solvent was compared to the benchmark MEA based on the performance measured at 0.5 MW_e at NCCC. Both CSTR and SSC desorber systems were considered for the comparison, and the performance is listed in **Table 34.**

CSTR vs. SSC for GAP-1_m/TEG

Water content was four times lower in the CSTR (4 wt.%) vs. SSC (17 wt.%) to avoid solvent entrainment. We were able to achieve 90% capture at almost stoichiometric ratio with the SSC. CO_2 capture efficiency reached only 65% for CSTR even though solvent circulation was 25% higher. Amine degradation rate was 0.45% / day for temperatures lower than 248 ^oF for the CSTR. Less than 0.05 wt.% amine degradation was measured during the SSC campaign. Specific steam utilization was 50% higher with CSTR than SSC due to low water content.

GAP-1_m/TEG vs. MEA with SSC

Comparison of the GAP-1_m/TEG vs. MEA was conducted at 0.5 MW_e scale with the SSC. There are several process conditions that differentiate the two technologies. Water content in the working solution was almost five times lower in the case GAP-1_m/TEG (18 wt.% vs. 69 wt.%). This led to a 25% decrease in solvent recirculation to treat 5000 pph flue gas and achieve 90 % CO_2 capture efficiency. Desorption temperature was 9 ^oF lower for GAP-1_m/TEG at 2 Psig desorption pressure. Specific steam utilization (lb CO_2 / lb steam) increased by 10% for the GAP-1_m/TEG. As highlighted before, little amine degradation (< 0.05 wt. %/ day) was recorded for the GAP-1_m/TEG solvent.

Table 34. **GAP-1_m/TEG vs. MEA:** Performance comparison at 0.5 MW_e (NCCC)

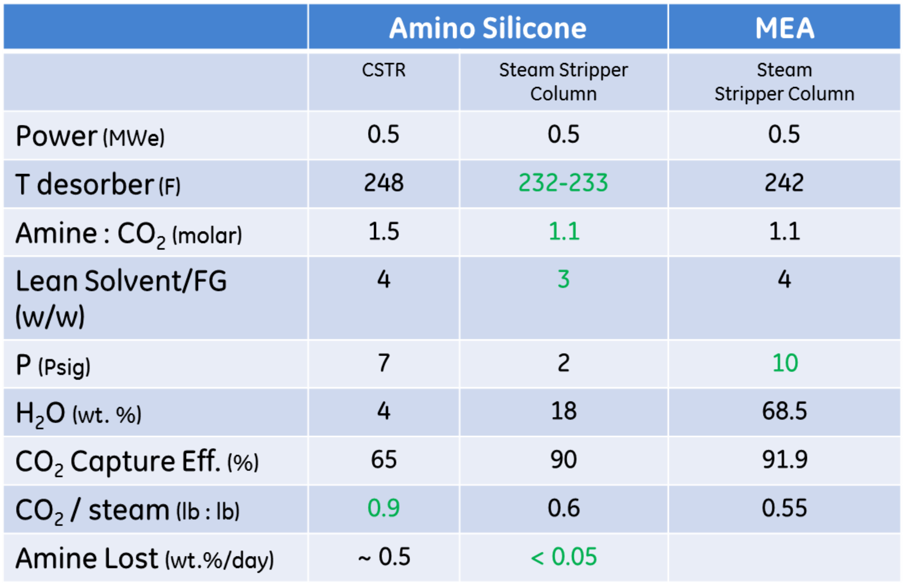

	Amino Silicone		MEA
	CSTR	Steam Stripper Column	Steam Stripper Column
Power (MWe)	0.5	0.5	0.5
T desorber (F)	248	232-233	242
Amine : CO_2 (molar)	1.5	1.1	1.1
Lean Solvent/FG (w/w)	4	3	4
P (Psig)	7	2	10
H_2O (wt. %)	4	18	68.5
CO_2 Capture Eff. (%)	65	90	91.9
CO_2 / steam (lb : lb)	0.9	0.6	0.55
Amine Lost (wt.%/day)	~ 0.5	< 0.05	

4.5. SSC Campaign: Summary

- Controlled water addition to GAP-1_m/TEG and steam stripping desorption were first tested in a glass stripping column (GE GRC), optimized in a continuous bench scale system (2 kW_e, GE GRC), and demonstrated in a 0.5 MW_e pilot (NCCC).

- Bench-Scale (2 kW_e): Small amounts of water in the working solution were found to be an effective way to enable steam stripping, lower desorption temperature, and hence reduce thermal degradation. Steam stripping also increased working capacity by 30% due to a more efficient desorption.

- Pilot-Scale (0.5 MW_e):
  No special system modifications were required to the PSTU to accommodate the testing of the non-aqueous GAP-1_m solvent with the regenerator column.

90 – 95% CO_2 capture efficiency was achieved under stoichiometric conditions at 0.5 MW_e (235 ^oF desorption, 2 psig and 19 wt. % H_2O). Both CO_2 capture efficiency and specific duty reached optimum conditions at 18 wt.% H_2O.

Low amine degradation (< 0.05 wt.%/day) was recorded over 350 hours of operation.

GAP-1_m/TEG solvent exhibited a 25% increased working capacity, and 10% reduction in specific steam duty vs. MEA, at 10 ^oF lower desorption temperature.

5. Techno-Economic Analysis

An ASPEN Plus model was developed for the CO_2 capture process with the GAP-1_m/TEG solvent and CSTR desorber. The overview of the model is presented in **Figure 103**. Next, it was scaled-up for a 550-MW supercritical coal-fired power plant. The base case chosen was similar to Case 11 in the DOE-NETL study.[1] Sensitivity cases were then developed for a number of different CO_2-capture process configurations with varying absorber and desorber operating conditions. The flue gas flow rate was fixed to match the Case 11 from the DOE NETL study which produces 550 MW net power without CO_2 capture. The best case was then scaled up to 550 MW net power with CO_2 capture.

Table 35 lists the sensitivity cases obtained by exercising this process model for CSTR. An additional sensitivity case was developed to incorporate the performance of the SSC (Case L). Case L was built based on the optimized case ran at NCCC (Condition 14, 0.5 MW_e) that demonstrated a 30% increase in the working capacity and a 20% increase in steam duty vs CSTR.

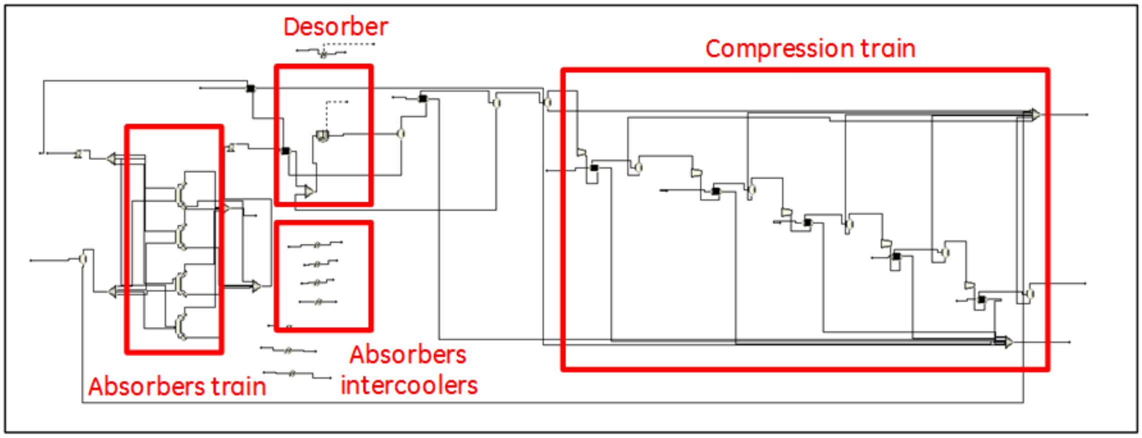

Figure 103. Techno-economic Analysis: Aspen Plus model for CO_2 separation sub-system

---

[1] "Cost and Performance Baseline for Fossil Energy Plants - Volume 1: Bituminous Coal and Natural Gas to Electricity (Rev 2, November 2010)", DOE/2010/1397.

Table 35. Techno-economic Analysis: Sensitivity Analysis

MEA	Base MEA (DOE Case 11 w CC and, Case 12)
GAP-1_m/TEG Cases	
Case A	140 C, 63 psia
Case B	Added Absorber Intercoolers
Case C	Increased Intercooling
Case D	Structured Packing
Scaled Up GAP-1_m/TEG Cases	
Case E	Scaled to 550 MW_e
Case F	Flue Gas and Cooling Water Integration
Case G	Reduced Absorber Height
Case H	Reduced desorber T to 130 ^oC
Case I	Optimized number of absorbers
Case J	Heat rejection from flue gas
Case K	Low pressure & low T desorption / CSTR
Case L	Low pressure desorption / SSC

First year COE was calculated (with and without TS&M) as shown in **Figure 104** and **Figure 105**. When TS&M is included in the analysis, then Case L COE is 12.8 vs. 14.73 cents/kWh for the MEA-based system.

The first year removal cost of CO_2 for Case K (CSTR, low P) is \$47.78 \$/ton of CO_2 as compared to \$60.25/ton of CO_2 when MEA is used. For the SSC, the first year removal cost of CO_2 for case L (SSC, low P) is 42.4\$/ton of CO_2. This shows a significant reduction in removal cost when aminosilicone solvent is used for carbon capture. (**Figure 106**)

Based on the 0.5 MW_e Demo performed at NCCC, the solvent make-up rate was 15% / yr. for SSC, and 120 % / yr. for CSTR, respectively. **Figure 107** and **Figure 108** show the predicted values for CO_2 cost assuming the measured make-up solvent degradation rates. For CSTR desorber, the high solvent degradation rate renders a cost of CO_2 over \$100/ ton CO_2. On the other hand, lower solvent make-up rate and improved performance for the SSC led to a cost of CO_2 of \$48 / ton of CO_2. This shows a significant reduction in removal cost vs MEA when aminosilicone solvent is used for carbon capture.

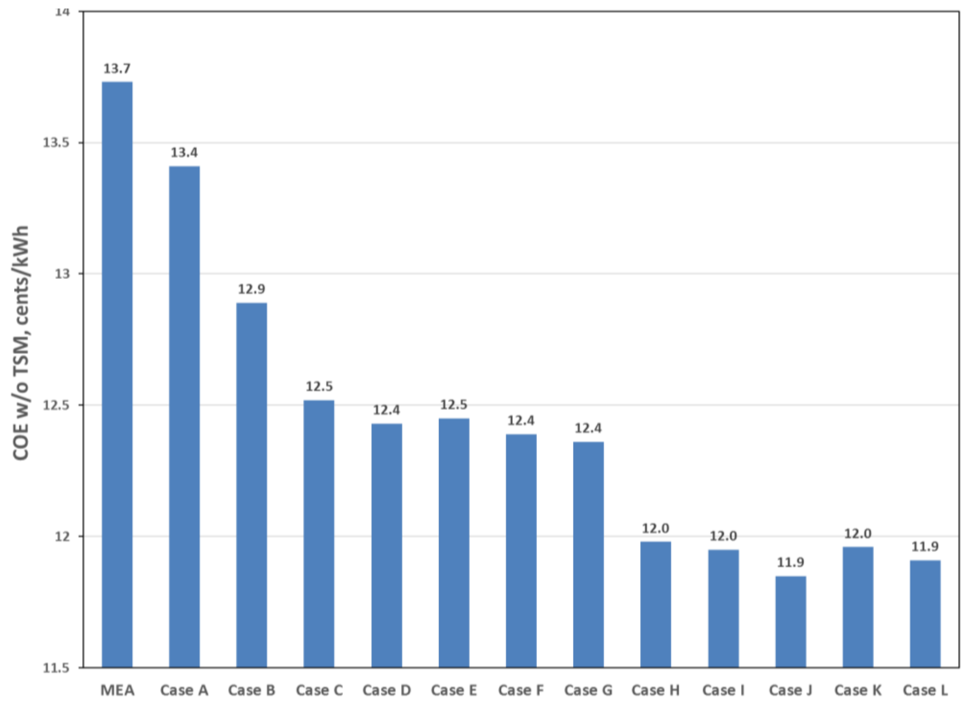

Figure 104. **Techno-economic Analysis:** Cost of electricity without TS&M

Design basis as described in Case 12 DOE/NETL[1]

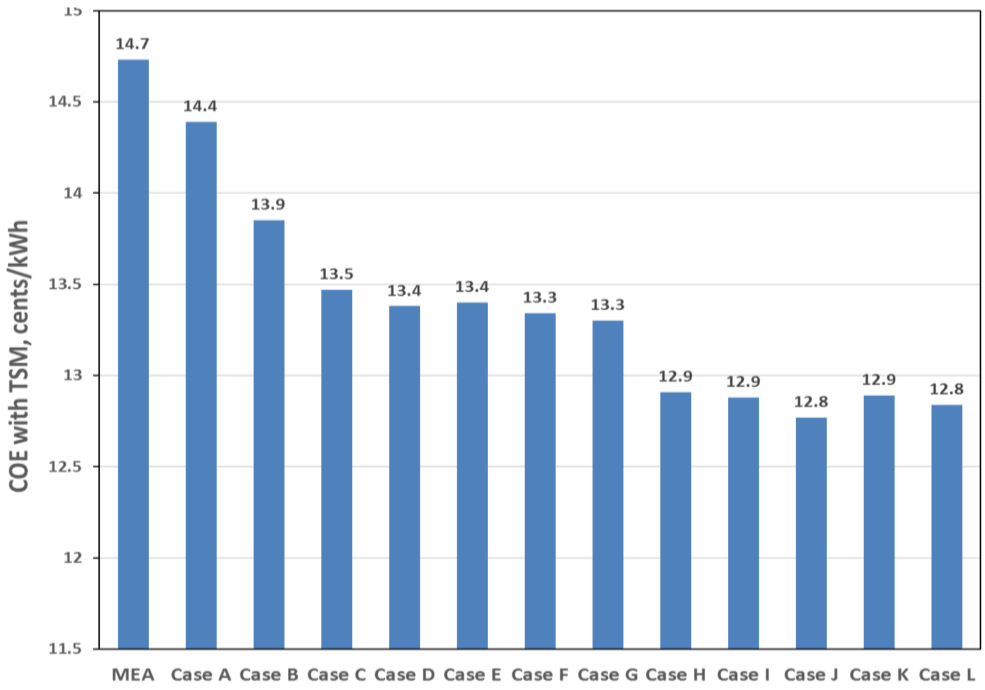

Figure 105. **Techno-economic Analysis:** Cost of electricity with TS&M
Design basis as described in Case 12 DOE/NETL report[1]

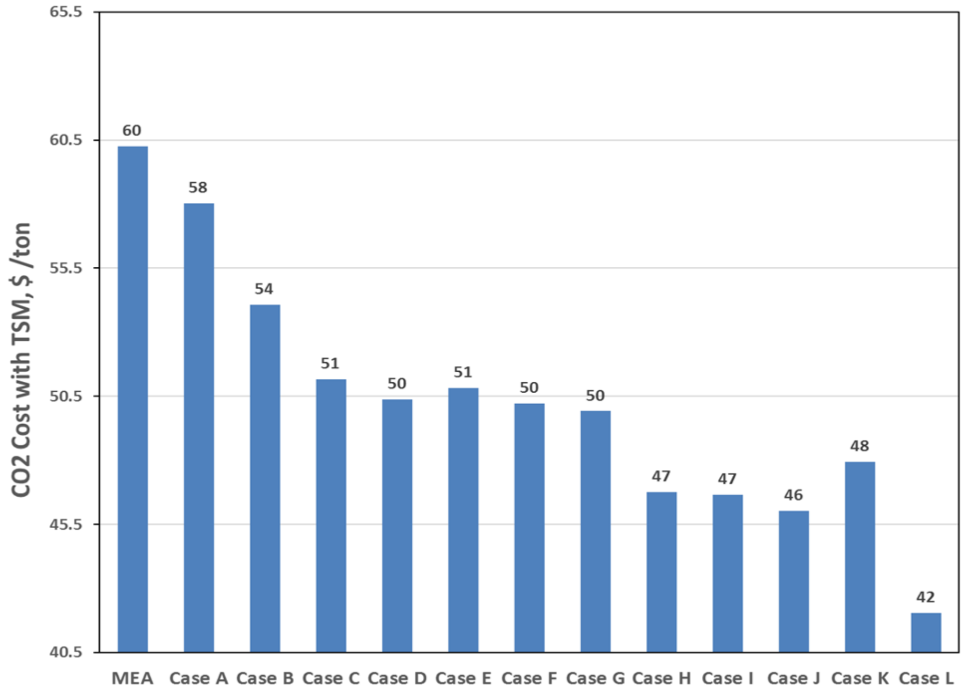

Figure 106. **Techno-economic Analysis:** 1st removal cost of CO_2
Design basis as described in Case 12 DOE/NETL report[1]

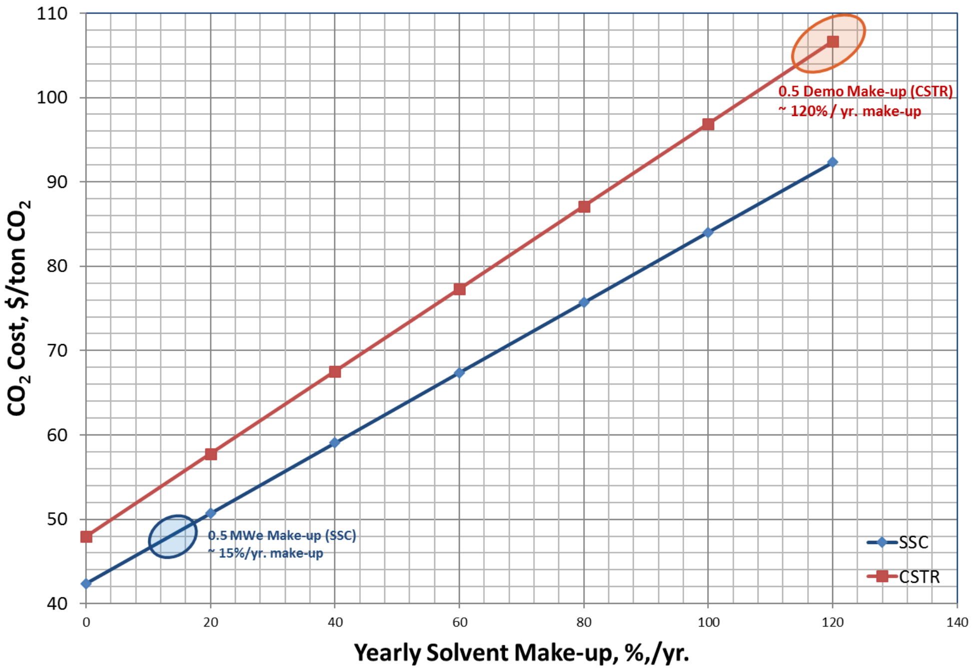

Figure 107. **Techno-economic Analysis:** Effect of solvent make-up rate SSC vs. CSTR

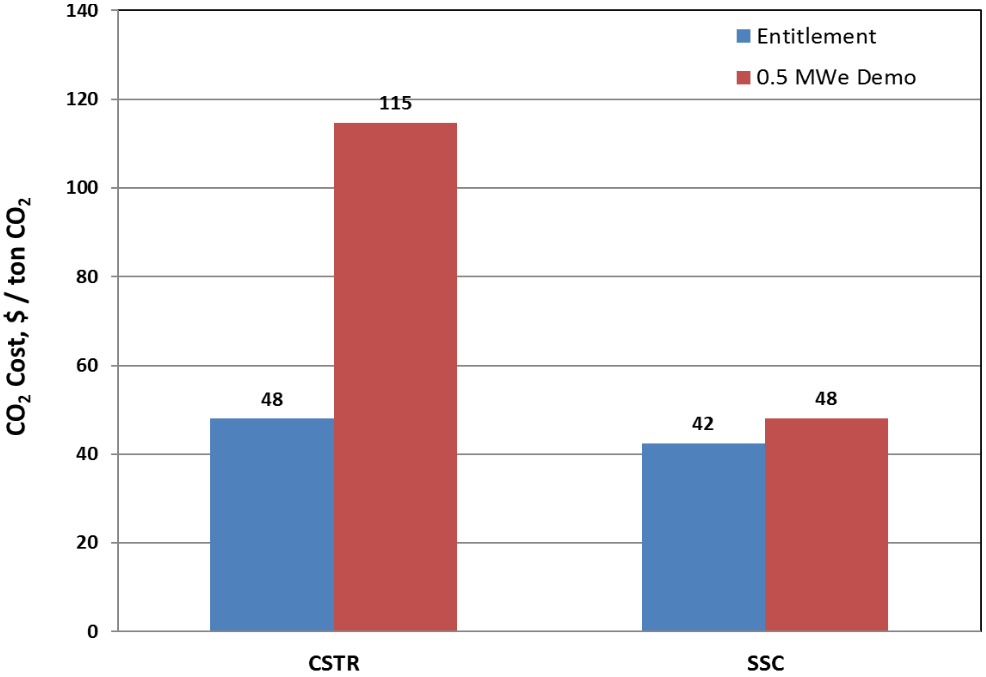

Figure 108. **Techno-economic Analysis:** Entitlement vs. Prediction based on measured yearly solvent make-up rates at 0.5 MW_e pilot (NCCC)

6. Summary

Performance of the GAP-1_m/TEG non-aqueous solvent was demonstrated at 0.5 MW_e at NCCC for over 900 hours using two desorber technologies: continuous stirred reactor (CSTR) and steam stripper column (SSC).

GAP-1_m/TEG

GAP-1_m/TEG is a non-aqueous post-combustion CO_2 capture system with lower vapor pressure, lower corrosity and improved working capacity vs. aqueous amines solvents. Formation of urea under desorber conditions and hydrothermal equilibration are major pathways in thermal degradation. Solvent management can be improved by implementing low-temperature desorption processes and/or by developing Gen 2 solvent systems with reduced thermal degradation.

CSTR Campaign

A CSTR desorber system was designed, fabricated and integrated with the PSTU at NCCC. The CSTR is a one-stage separation unit with reduced space requirements, and capital cost. GAP-1_m/TEG performance with CSTR was tested for over 500 hours. Solvent carry-over in the CSTR overhead was controlled by limiting the water content to less than 5 wt.%. 65 % CO_2 capture efficiency was achieved at 0.5 MWe with the CSTR desorber. Solvent degradation was dominated by the thermal formation of urea under desorber conditions. To take advantage of the low capital cost / low reduced space requirement of the CSTR, one needs to develop and scale-up the Gen 2 aminosilicone solvents with improved thermal stability.

Steam Stripping Column Campaign

Controlled water addition to GAP-1_m/TEG and steam stripping desorption were developed to mitigate thermal degradation. The concepts were first tested in a glass stripping column (GE GRC), optimized in a continuous bench-scale system (2 kW_e, GE GRC), and demonstrated in a 0.5

MW_e pilot (NCCC). Small amounts of water in the working solution were found to be an effective way to enable steam stripping, lower desorption temperature, and hence reduce thermal degradation. Steam stripping also increased working capacity by 30% due to a more efficient desorption. No special system modifications were required to the PSTU to accommodate the testing of the non-aqueous GAP-1_m solvent with the regenerator column. 90 – 95% CO_2 capture efficiency was achieved under stoichiometric conditions at 0.5 MW_e (235 ^oF desorption, 2 psig and 19 wt. % H_2O). Both CO_2 capture efficiency and specific duty reached optimum conditions at 18 wt.% H_2O. Low amine degradation (< 0.05 wt.%/day) was recorded over 350 hours of operation. GAP-1_m/TEG solvent exhibited a 25% increased working capacity, and 10% reduction in specific steam duty vs. MEA, at 10 ^oF lower desorption temperature. Further improvements in specific steam utilization can be achieved by optimizing water loading and implementing an advanced process scheme with staged steam injection.

Techno-economic Analysis

An ASPEN process model was developed for the GAP-1_m/TEG solvent. Techno-economical analysis developed for a 550-MW supercritical coal plant[1] showed a 20 – 30 % improvements in both CAPEX and CO_2 removal cost vs. aqueous amine systems. The first-year CO_2 removal cost for the aminosilicone-based carbon-capture process was evaluated at \$48/ton CO_2 using the steam stripper column. CO_2 cost using the CSTR desorber is dominated by the economics of the solvent make-up. The steam stripper desorber is the preferred unit operation due to a more efficient desorption, and reduced solvent make-up rate. Improved economics can be achieved by implementing Gen 2 aminosilicone solvents and advanced process schemes.

Acknowledgment: This material is based upon work supported by the Department of Energy under Award Number DE-FE0013755.